

## INFORMATION TO USERS

This manuscript has been reproduced from the microfilm master. UMI films the text directly from the original or copy submitted. Thus, some thesis and dissertation copies are in typewriter face, while others may be from any type of computer printer.

**The quality of this reproduction is dependent upon the quality of the copy submitted.** Broken or indistinct print, colored or poor quality illustrations and photographs, print bleedthrough, substandard margins, and improper alignment can adversely affect reproduction.

In the unlikely event that the author did not send UMI a complete manuscript and there are missing pages, these will be noted. Also, if unauthorized copyright material had to be removed, a note will indicate the deletion.

Oversize materials (e.g., maps, drawings, charts) are reproduced by sectioning the original, beginning at the upper left-hand corner and continuing from left to right in equal sections with small overlaps.

ProQuest Information and Learning  
300 North Zeeb Road, Ann Arbor, MI 48106-1346 USA  
800-521-0600

UMI<sup>®</sup>



# **Genetic Approaches to Characterize the Role of the Yeast Niemann-Pick C-Related Gene, *NCR1***

by

**Anathea S. Flaman**

Submitted in partial fulfillment of the requirements  
for the degree of Doctor of Philosophy

at

Dalhousie University  
Halifax, Nova Scotia  
August, 2005

© Copyright by Anathea S. Flaman, 2005



Library and  
Archives Canada

Bibliothèque et  
Archives Canada

0-494-08411-1

Published Heritage  
Branch

Direction du  
Patrimoine de l'édition

395 Wellington Street  
Ottawa ON K1A 0N4  
Canada

395, rue Wellington  
Ottawa ON K1A 0N4  
Canada

*Your file* *Votre référence*

*ISBN:*

*Our file* *Notre référence*

*ISBN:*

#### NOTICE:

The author has granted a non-exclusive license allowing Library and Archives Canada to reproduce, publish, archive, preserve, conserve, communicate to the public by telecommunication or on the Internet, loan, distribute and sell theses worldwide, for commercial or non-commercial purposes, in microform, paper, electronic and/or any other formats.

The author retains copyright ownership and moral rights in this thesis. Neither the thesis nor substantial extracts from it may be printed or otherwise reproduced without the author's permission.

#### AVIS:

L'auteur a accordé une licence non exclusive permettant à la Bibliothèque et Archives Canada de reproduire, publier, archiver, sauvegarder, conserver, transmettre au public par télécommunication ou par l'Internet, prêter, distribuer et vendre des thèses partout dans le monde, à des fins commerciales ou autres, sur support microforme, papier, électronique et/ou autres formats.

L'auteur conserve la propriété du droit d'auteur et des droits moraux qui protègent cette thèse. Ni la thèse ni des extraits substantiels de celle-ci ne doivent être imprimés ou autrement reproduits sans son autorisation.

---

In compliance with the Canadian Privacy Act some supporting forms may have been removed from this thesis.

Conformément à la loi canadienne sur la protection de la vie privée, quelques formulaires secondaires ont été enlevés de cette thèse.

While these forms may be included in the document page count, their removal does not represent any loss of content from the thesis.

Bien que ces formulaires aient inclus dans la pagination, il n'y aura aucun contenu manquant.

  
**Canada**

DALHOUSIE UNIVERSITY

To comply with the Canadian Privacy Act the National Library of Canada has requested that the following pages be removed from this copy of the thesis:

Preliminary Pages

Examiners Signature Page (pii)

Dalhousie Library Copyright Agreement (piii)

Appendices

Copyright Releases (if applicable)

## TABLE OF CONTENTS

	page
Table of Contents	iv
List of Figures	ix
List of Tables	xii
Abstract	xiii
List of Abbreviations	xiv
Acknowledgements	xix
1. Introduction	1
1.1. Niemann-Pick Type C disease	1
1.2. Intracellular cholesterol trafficking	2
1.3. The NPC1 protein	6
1.4. The yeast homologue of NPC1, <i>NCR1</i>	10
1.5. My research	13

2. Materials and Methods	14
2.1. Yeast and bacterial strains	14
2.2. Media and growth conditions	14
2.3. DNA isolation and analysis	21
2.4. PCR	22
2.5. Plasmids	26
2.6. Transformation of yeast and <i>E. coli</i>	31
2.7. Plasmid Loss	33
2.8. Extraction of proteins from yeast	33
2.9. Extraction of proteins from <i>E. coli</i>	34
2.10. Purification of His <sub>6</sub> -tagged insoluble proteins	34
2.11. SDS-PAGE analysis	36
2.12. Western analysis	36
2.13. Yeast two-hybrid and $\beta$ -galactosidase assays	37
2.14. Plating assays	37
2.15. Recovery from deep stationary phase	38
2.16. Heat stress viability assay	38
2.17. Generation of petites	38
2.18. Hygromycin assays	39

2.19. Secretion of invertase	39
2.20. Radiolabeling and immunoprecipitation of Gas1	40
2.21. Lipid labeling	42
2.22. Secretion of carboxypeptidase Y	43
2.23. Thin section electron microscopy	44
2.24. Screen for mutants that are synthetic lethal with <i>ncr1Δ</i>	44
2.25. Synthetic genetic array (SGA) analysis	45
2.26. Digital analysis of SGA plates	46
 3. Results	 48
3.1. <i>NCR1</i> is not an essential gene	48
3.2. Loss of <i>NCR1</i> does not affect lipid metabolism	48
3.3. <i>NCR1</i> is not required for secretion of invertase	50
3.4. Ncr1 is not required for sorting of GPI-anchored proteins	52
3.5. Effects of drugs or inhibitors	55
3.6. <i>NCR1</i> expression is not induced by elevated temperature	59
3.7. <i>NCR1</i> and <i>ncr1Δ</i> yeast have similar survival at high temperature, but <i>ncr1Δ</i> yeast produce fewer petites	60



3.8. Loss of <i>NCR1</i> does not inhibit petite production in response to exposure to ethidium bromide	62
3.9. Screen for mutants that are synthetic lethal with <i>ncr1Δ</i>	63
3.9.1. Characterization of synthetic lethal mutant 33-13	68
3.9.2. Characterization of synthetic lethal mutant 45-6b	71
3.10. Overexpression of wild type <i>NCR1</i> is toxic	75
3.11. $\text{CaCl}_2$ and sorbitol partially alleviate toxicity of <i>NCR1</i> overexpression	81
3.12. Screen for high-copy suppressors of <i>NCR1</i> -overexpression toxicity	84
3.13. Synthetic Genetic Array analysis to identify <i>NCR1</i> genetic interactions	87
3.13.1. SGA screen for suppressors of <i>NCR1</i> overexpression toxicity	88
3.13.2. SGA analysis to reveal genes that contribute to survival when <i>NCR1</i> is overexpressed	93
3.14. Loss of <i>NHX1</i> impairs cells overexpressing <i>NCR1</i>	103
3.15. As with <i>NHX1</i> deletion, <i>NCR1</i> overexpression results in hygromycin B sensitivity	106

3.16. The Nhx1 C-terminal tail and Ncr1 cysteine-rich loop do not interact by yeast two-hybrid analysis	108
3.17. Excess <i>NCRI</i> does not cause cells to mis-sort carboxypeptidase Y	110
3.18. <i>NCRI</i> contributes to pH homeostasis in the absence of V-ATPase	114
4. Discussion	117
References	145

## LIST OF FIGURES

	page
Figure 1. Intracellular cholesterol trafficking in mammalian cells	3
Figure 2. Schematic model showing the structure and topology of the NPC1 protein	8
Figure 3. Comparison of the predicted secondary structure of human NPC1 and yeast Ncr1	12
Figure 4. Loss of <i>NCR1</i> has no effect on viability of yeast cells	49
Figure 5. Loss of <i>NCR1</i> does not affect metabolic or steady-state lipid metabolism at 30°C or 37°C	51
Figure 6. Maturation of Gas1 is indistinguishable in <i>NCR1</i> and <i>ncr1Δ</i> yeast	54
Figure 7. Yeast lacking <i>NCR1</i> are more sensitive to thermal stress due to lower petite production	61
Figure 8. Deletion of <i>NCR1</i> does not prevent production of petites in response to ethidium bromide	64
Figure 9. The <i>ncr1Δ</i> and <i>yg1250wΔ</i> mutations are not synthetically lethal	70

Figure 10. Viability of presumptive <i>gfa1-45</i> spores is improved with plasmid encoding <i>NCR1</i> and <i>URA3</i>	73
Figure 11. Ncr1 is overexpressed from plasmid pEMBL-NCR1 on galactose	77
Figure 12. Overexpression of <i>NCR1</i> is deleterious, but degree of toxicity is dependent on growth medium	79
Figure 13. Overexpression of <i>NCR1</i> does not affect cell ultrastructure	82
Figure 14. CaCl <sub>2</sub> and sorbitol partially suppress, while CdCl <sub>2</sub> enhances, toxicity of <i>NCR1</i> overexpression	83
Figure 15. Yeast gene deletions suppress the toxicity of <i>NCR1</i> overexpression	90
Figure 16. Digital modification of SGA robot plates facilitates screening	95
Figure 17. Deletion mutations render cells hypersensitive to overexpression of <i>NCR1</i>	97
Figure 18. <i>slt2Δ</i> cells are hypersensitive to excess <i>NCR1</i>	101
Figure 19. <i>ncr1Δ</i> cells are not hypersensitive to excess <i>BCK1-20</i>	102
Figure 20. Yeast lacking <i>NHX1</i> are hypersensitive to overexpression of <i>NCR1</i>	104
Figure 21. Hygromycin B is toxic to cells overexpressing <i>NCR1</i> , while deletion of <i>NCR1</i> confers hygromycin resistance	107
Figure 22. The Nhx1 C-terminal tail and Ncr1 cysteine-rich loop do not interact in a two-hybrid assay	109

Figure 23. Effect of <i>NCR1</i> overexpression on CPY secretion	113
Figure 24. Yeast cells lacking both <i>VMA6</i> and <i>NCR1</i> are sensitive to acidic and alkaline pH	116
Figure 25. Deletion suppressors of <i>NCR1</i> overexpression	128
Figure 26. Genetic interaction network representing the synthetic lethal/sick interactions	130
Figure 27. Synthetic lethality of overexpressed <i>NCR1</i> in cell-polarity mutants suggests Ncr1 participates in recycling from sites of polarized growth	134

## LIST OF TABLES

	page
Table 1. Yeast strains used in this study	15
Table 2. Chemical additions to media to assess growth phenotypes	19
Table 3. Primers used in this study	23
Table 4. Plasmids used in this study	27
Table 5. Cellular processes affected by chemical additions	57
Table 6. Deletion suppressors of <i>NCRI</i> overexpression toxicity	91
Table 7. Genes that contribute to survival when <i>NCRI</i> is overexpressed	98

## Abstract

Niemann-Pick Type C (NPC) disease is a fatal neurodegenerative disorder characterized by endosomal and lysosomal lipid accumulation. Most cases of NPC disease result from mutations in the NPC1 gene. To investigate NPC1 function, the single NPC1-related gene, *NCR1* in the yeast *Saccharomyces cerevisiae* was deleted or overexpressed. Loss of *NCR1* did not influence cell proliferation, lipid metabolism, protein secretion, or cell response to chemical agents, suggesting Ncr1 is not required or other proteins can compensate for *NCR1* deficiency under the conditions examined.

Overexpression of *NCR1* was found to be deleterious. All nonessential yeast gene deletion mutants that rendered cells hypersensitive or resistant to *NCR1* overexpression toxicity were identified by synthetic genetic array screens. Cell polarity genes were found to contribute to survival when *NCR1* was overexpressed, implying a role for *NCR1* in recycling materials from sites of polarized growth. Deletion of several genes encoding transporters alleviated *NCR1*-overexpression toxicity while loss of the *NHX1*-encoded sodium-proton antiporter enhanced *NCR1* overexpression toxicity. These genetic interactions imply Ncr1 may participate in an opposing process or negatively regulate Nhx1 activity. Yeast lacking *NHX1* (*nhx1Δ*) display defects in retrograde vesicular trafficking from the late endosomal prevacuolar compartment (PVC). In contrast, *NCR1* overexpression did not impair delivery of carboxypeptidase Y to the vacuole, the yeast hydrolytic compartment, suggesting Ncr1 does not negatively regulate Nhx1 or mediate Golgi-to-PVC trafficking. However, like deletion of *NHX1*, *NCR1* overexpression increased sensitivity to a small, positively charged aminoglycoside antibiotic, hygromycin B, a phenotype associated with hyperpolarization of the plasma membrane or defective vacuolar sequestration of the drug. Deletion of *NCR1* increased resistance to hygromycin B, suggesting Ncr1 might regulate cation or proton uptake or efflux from the PVC. A role for Ncr1 in intracellular ion homeostasis was further implied by finding *NCR1* was essential when cells lacking the vacuolar H<sup>+</sup>-ATPase, a major contributor to pH homeostasis, were grown on media buffered to extremes in pH. If the human NPC1 protein participates in regulating the pH of intracellular compartments, as suggested by the findings with the yeast Ncr1 protein, defective pH homeostasis may be the primary cellular defect in NPC disease.

## LIST OF ABBREVIATIONS AND SYMBOLS USED

A	adenine
ACAT	acyl-CoA cholesterol acyltransferase
AIR	P-ribosylaminoimidazole
APG	arginine phosphoric acid glucose medium
bp	base pairs
C	cytosine
CAIR	P-ribosylaminoimidazolecarboxylate
CE	cholesterol ester
CHO	Chinese hamster ovary
CPY	carboxypeptidase Y
CRL	cysteine-rich loop
CRL-His <sub>6</sub>	cysteine-rich loop-thioredoxin-His <sub>6</sub> fusion protein
CTP	cytosine triphosphate
DAG	diacylglycerol
DNA	deoxyribonucleic acid
DTT	dithiothreitol
EDTA	ethylene diamine-N,N,N',N''-tetraacetic acid
EMS	ethylmethanesulphonate



ER	endoplasmic reticulum
EtBr	ethidium bromide
FA	fatty acids
FOA	5-fluoroorotic acid
G	guanine
GAP	GTPase-Activating Protein
GFP	green fluorescent protein
GPI	glycosylphosphatidylinositol
GRID	General repository for interaction datasets
HRP	Horseradish peroxidase
HygB	Hygromycin B
IPTG	isopropyl- $\beta$ -D-thiogalactoside
kV	kilovolts
kbp	kilobase pairs
LAMP2	lysosomal associated membrane protein 2
LAMP3	lysosomal associated membrane protein 3
LB	Luria-Bertani medium
LDL	low density lipoprotein
LIMP1	lysosomal integral membrane protein 1

MAPK	mitogen activated protein kinase
M(IP) <sub>2</sub> C	mannosyl-diinositolphosphorylceramide
MOPS	3-N-[morpholino]propanesulfonic acid
NPC	Niemann-Pick Type C
ORF	open reading frame
PAGE	polyacrylamide gel electrophoresis
PA/PE	phosphatidic acid/phosphatidylethanolamine
PBS	phosphate-buffered saline
PBST	phosphate-buffered saline-Tween-20
PC	phosphatidylcholine
PCR	polymerase chain reaction
PEG	polyethylene glycol
PI/PS	phosphatidylinositol/phosphatidylserine
PKC	protein kinase C
PM	plasma membrane
PMSF	phenyl methyl sulfonyl fluoride
PVC	prevacuolar compartment

PVDF	polyvinylidene difluoride
SC	synthetic complete medium
SCAP	sterol regulatory element binding protein cleavage activating protein
SD	synthetic defined medium
SE	sterol esters
SGA	sythetic genetic array
SREBP	sterol regulatory element binding protein
SSD	sterol sensing domain
ss-DNA	single-stranded DNA
STRE	stress-responsive element
T	thymine
TAG	triacylglycerols
TAPS	N-tris-[hydroxymethyl] methyl 3-aminopropane-sulfonic acid
TBS	Tris-buffered saline
TGN	trans Golgi network
TLC	thin layer chromatography
TM	transmembrane
U	units
UV	ultraviolet

V-ATPase	vacuolar ATPase
X-gal	5-bromo-4-chloro-3-indolyl- $\beta$ -D-galactopyranoside
YEPD	Yeast extract peptone dextrose medium
YNB	Yeast nitrogen base medium
YT	Yeast extract-tryptone medium

## ACKNOWLEDGEMENTS

I am indebted to my supervisor, Dr. Melanie Dobson for her guidance, support and limitless optimism. Her enthusiasm for discovery is contagious, and she has always encouraged me to pursue the avenues I found most interesting. I would like to thank Joyce Chew for her extraordinary amount of meticulous technical assistance. Thank you to Lois Murray and the past and present members of the Dobson lab for making our workplace a relaxed and fun atmosphere. In particular, I would like to thank Lindsay MacDonald and Wendy McCaul for their technical help and Jeremy Benjamin for his friendship- he brought a smile to my face every day.

I would like to thank the Dalhousie University Yeast Group for their critical insight, especially Charlene Hubbards for carrying out my SGA screens, Greg Fairn for his impressive knowledge of the literature, Dr. Pak Poon for enlightening discussions and Dr. Vanina Zaremborg for her academic and personal guidance. Thank you to Paul Briggs for his computer expertise while I was preparing this thesis.

I would like to thank my supervisory committee: Dr. Doug Hogue, Dr. Neale Ridgway, Dr. Cathy Too and Dr. Chris McMaster for their advice and constructive criticism. I would also like to thank my examining committee: Dr. Laura Liscum, Dr. David Byers, Dr. Chris McMaster and Dr. Rick Singer for their challenging, thought-provoking questions and for reviewing this thesis.

I am grateful to everyone who supplied me with reagents (Howard Reizman, Mike Hall, Rajini Rao, Wei Xiao and Chris McMaster) and to the National Niemann-Pick Disease Foundation, the Canadian Institute of Health Research and the Nova Scotia Health Research Foundation for financial support.

I would like to thank Gerald and Joan Chaisson for their outstanding hospitality while I prepared my thesis. To my family and my friends, who have given me great strength during the course of this degree and in my life in general- words cannot express my appreciation! I owe my deepest gratitude to my husband, Rodney Breau, who buoys me up after disappointments, celebrates my successes with joy and contended with two years of separation so I could complete my degree, I dedicate this thesis to you, with love.

# 1. Introduction

## 1.1. Niemann-Pick Type C disease

Niemann-Pick Type C (NPC) disease is a rare autosomal recessive, progressive neurodegenerative disorder (123) affecting 1 in 150,000 individuals (94). The most common finding in NPC patients is progressive neurodegeneration that affects mainly the thalamus and Purkinje cells in the cerebellum (153, 162). These defects give rise to the classic signs of NPC including vertical supranuclear gaze palsy, ataxia, dystonia and dementia (123). NPC is ultimately fatal, with death typically occurring in adolescence (123). A study of NPC is particularly relevant in Nova Scotia because the French Acadian population of Yarmouth County has an extremely high NPC carrier frequency, estimated at ~1 in 50 (W. Greer, personal communication). My approach has been to use yeast as a model system to investigate the underlying basis of NPC disease, with the hypothesis that a defect in a conserved cellular process is responsible for the pathophysiology of the disease.

NPC was initially classified as a lipid storage disorder because several organ systems in NPC patients accumulate abnormal lipid levels (123). The liver and spleen accumulate unesterified cholesterol, sphingomyelin, phospholipids, glycolipids (123) and lysobisphosphatidic acid (81). Cholesterol levels are normal in NPC brains (163), but sphingolipids accumulate with a tissue-specific profile (123, 163). NPC

neurons accumulate GM1, GM2 and GM3 gangliosides (58, 153). Although the amount of cholesterol is normal in neurons, its distribution is abnormal (77). Neural cell bodies accumulate cholesterol while distal axons are deficient (77). NPC fibroblasts sequester GM1 ganglioside in the early endosome (150). The most prominent biochemical abnormality of non-neural NPC cells is the accumulation of unesterified exogenous cholesterol (85, 122) in the lysosomes and, to a minor extent, in the Golgi (15). More recent studies indicate that endogenous cholesterol accumulates in these cells as well (39). The sequestration of cholesterol in these compartments has led to the hypothesis that the primary defect in NPC disease is a defect in intracellular trafficking of sterol (93) or sphingolipids (82, 91, 150).

## **1.2. Intracellular cholesterol trafficking**

To understand abnormal intracellular cholesterol transport in NPC, it is important to review normal cholesterol trafficking. Cholesterol is a dynamic component of membranes that is continually cycled between the interior and exterior of the cell (Fig. 1) (92). Cellular membranes contain varying concentrations of cholesterol, with the highest levels in the plasma membrane (PM) and the lowest in the endoplasmic reticulum (ER) (92, 130, 146). The ER is the site of *de novo* synthesis and acylation of excess cholesterol that becomes stored in cytosolic lipid

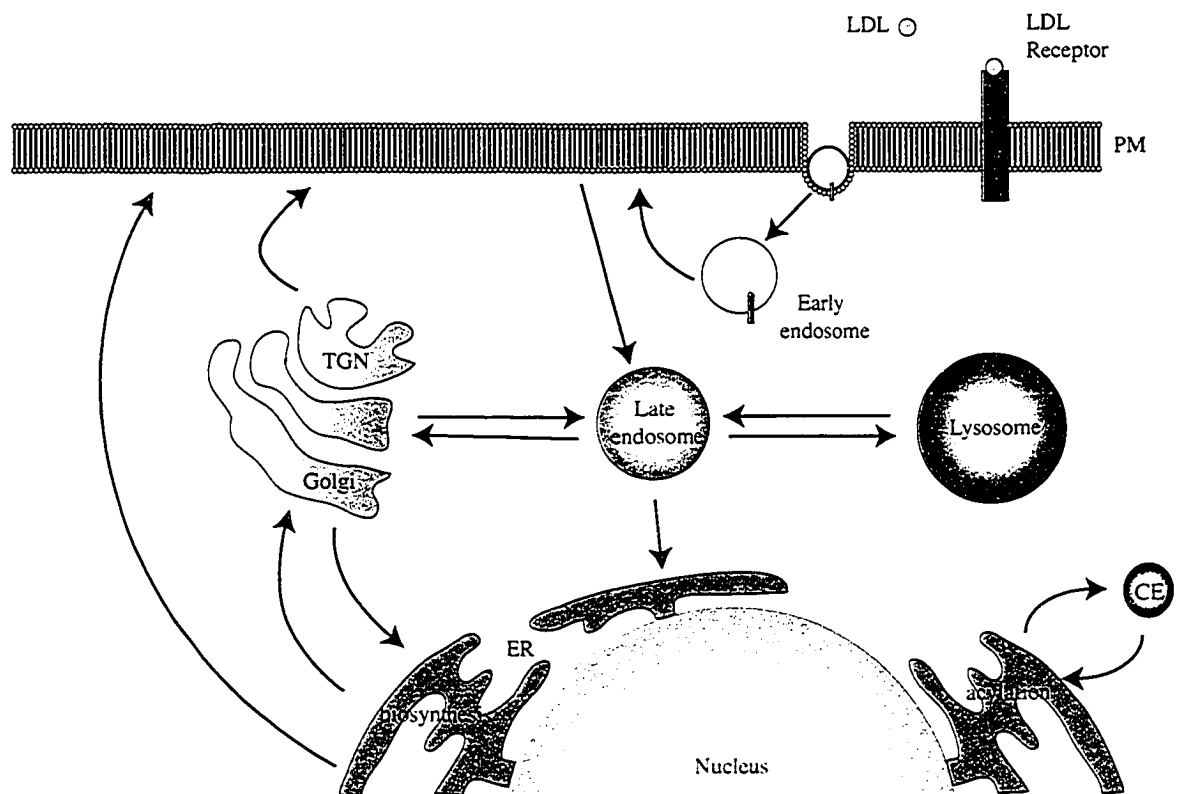


**Figure 1. Intracellular cholesterol trafficking in mammalian cells.** Cholesterol is synthesized *de novo* in the endoplasmic reticulum (ER) and is transported to the plasma membrane (PM) by a Golgi-dependent or independent route. Exogenous cholesterol is obtained from circulating low density lipoprotein (LDL) by receptor-mediated endocytosis. LDL is released from the LDL receptor and cholesterol is released in the early endosome. Cholesterol is delivered to the PM, then becomes reinternalized in the late endosome. Cholesterol may be transported to the lysosome or back to the ER, either directly or *via* the Golgi. Excess cholesterol can be esterified in the ER and stored as cholesterol ester (CE) in cytosolic lipid droplets. Adapted from (71, 145).



droplets (92, 145). The majority of mammalian cells obtain cholesterol from exogenous sources by receptor-mediated endocytosis of low density lipoprotein (LDL) circulating in plasma (92, 145). LDL binds to the LDL receptor on the cell surface and the complex is internalized into an early endosome (145). Within this compartment, the receptor releases LDL and is recycled to the cell surface (145). The LDL-cholesterol ester is hydrolyzed to free cholesterol, which is directed to the PM (145). When cholesterol levels rise at the PM, excess cholesterol is reinternalized to a cholesterol sorting compartment (40) and is then transported to the Golgi, lysosome or ER where proteins maintain appropriate cholesterol levels by regulating biosynthesis, uptake, storage and efflux of cholesterol (130, 145, 149).

Two proteins involved in maintaining cholesterol balance are the cholesterol biosynthetic enzyme HMG-CoA reductase and a sterol-regulated transcription factor, sterol-response element binding protein (SREBP), that interacts with a regulatory protein, SREBP cleavage activating protein (SCAP) (51, 86). Both HMG-CoA reductase and SCAP contain a sterol-sensing domain, the conformation of which is altered by fluctuations in the cellular sterol content (86). When sterol levels are high, the degradation of HMG-CoA reductase is triggered, while the SCAP/SREBP complex is retained in the ER (51, 86). When sterols are depleted, a conformational change in SCAP promotes delivery of SREBP to the Golgi (51, 86). In the Golgi,

proteases liberate SREBP from its membrane domains, allowing it to translocate to the nucleus and activate transcription of sterol biosynthetic genes (51, 86).

NPC cells are impaired in these cholesterol homeostatic responses. LDL receptor-mediated endocytosis and LDL hydrolysis proceed normally in NPC cells (90, 120), but the egress of cholesterol from the late endosomal/lysosomal compartment is impaired (93). Since cholesterol does not reach the ER, homeostasis is not achieved. NPC cells exhibit delays in activation of cholesterol esterification (90, 121), and in downregulation of both the LDL receptor and *de novo* cholesterol synthesis (90, 120). Excessive uptake of cholesterol and unimpeded biosynthesis contribute to the elevated total cholesterol levels in NPC cells (90).

In membranes, sterols associate with sphingolipids, forming specialized domains called rafts (144). Cholesterol metabolism is tightly linked to sphingolipid concentrations: when cellular sphingomyelin levels increase, cholesterol levels correspondingly rise (141). Conversely, when PM sphingomyelin is depleted, cholesterol synthesis is downregulated and storage is upregulated (141). This coordinate regulation of sterol and sphingolipid content is evident in NPC, where cells accumulate both sterol and sphingolipids.

The transport defects observed in NPC cells are not restricted to lipids. NPC cells exhibit delayed efflux of endocytosed [<sup>14</sup>C]sucrose from lysosomes (110) and inappropriately retain the mannose-6-phosphate receptor in late endosomes rather

than recycling it to the trans-Golgi network (TGN) (81). These defects have prompted the hypothesis that impaired vesicular trafficking from late endosomes is the primary defect in NPC cells (110). Further evidence for NPC arising from a general trafficking defect is the finding that overexpression of Rab7 or Rab9, GTPases that regulate trafficking between intracellular compartments, can correct the cholesterol accumulation defect of NPC cells (31). Rab7 mediates transport between the late endosome and the early endosome or lysosome, while Rab9 mediates transport from the late endosome to the TGN (31, 126). If the ability of overexpressed Rab7 or Rab9 to relieve the lipid storage phenotype of NPC cells is due to increased flux through these pathways, the primary defect in NPC may be a reduction in all trafficking from late endosomes.

### **1.3. The NPC1 Protein**

The majority of NPC cases result from mutations in the NPC1 gene, but approximately 5% are due to mutations in the NPC2 gene (108, 164). NPC2 encodes a soluble cholesterol-binding lysosomal protein (108). The NPC1 protein consists of 1,278 amino acids and has an estimated molecular mass of 142 kDa (25). The Nova Scotia variant of NPC disease, originally called Niemann-Pick Type D (37) was identified as a G992W point mutation in the NPC1 gene (60).

Orthologues of the NPC1 protein exist in diverse eukaryotic organisms, including mammals, fruitflies, nematodes, plants and the yeast *Saccharomyces cerevisiae* (25). A second NPC1 in humans, called NPC1L1 (43) has been found in most of these organisms, with the exception of *S. cerevisiae*, which has only a single NPC1-related gene, *NCR1*.

A signal sequence at the amino terminus of NPC1 is believed to target the protein to the ER during synthesis (25). The NPC1 protein resides in unique late endosomes that are characterized by containing LAMP2 (110, 181, 182), Rab7, LAMP3, LIMP (182) and lysobisphosphatidic acid (81). A dileucine motif (LLNF) at the carboxy terminus of mammalian NPC1 has been shown to be necessary for its normal localization in late endosomes (168). However, NPC1 has a dynamic itinerary and has been shown to localize transiently in both lysosomes and the TGN (66). In response to increased intracellular cholesterol, NPC1 is retained in the late endosomes (182).

Topological analysis of NPC1 has revealed the existence of 13 transmembrane (TM) spans (Fig. 2) (42). NPC1 contains a sterol-sensing domain (SSD) homologous to that identified in SCAP, in HMG-CoA reductase, and also in the morphogen receptor Patched (Ptc) (25), where it appears to regulate Ptc by controlling its vesicular trafficking (100). The presence of this sterol-responsive domain in NPC1 suggests it may regulate trafficking of NPC1 or that NPC1 activity is sensitive to

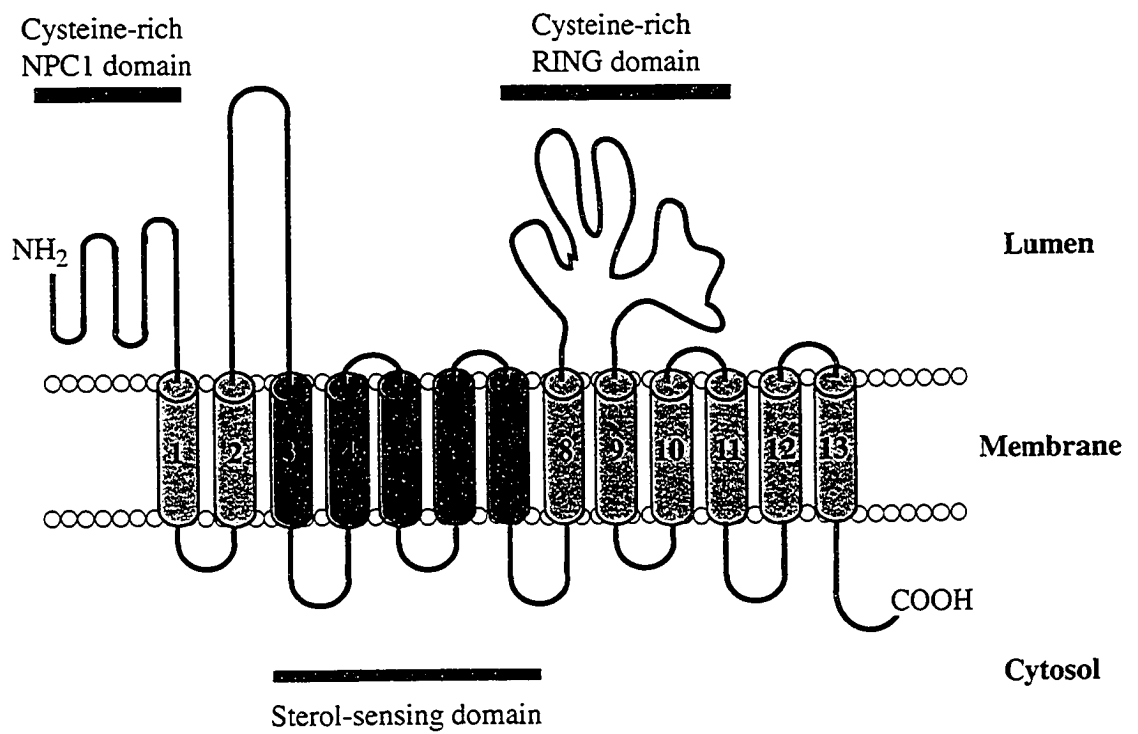


**Figure 2. Schematic model showing the structure and topology of the NPC1 protein.**  
 Predicted transmembrane spans are numbered.

membrane sterol content. Indeed, using photolabile cholesterol analogs, the NPC1 SSD has been shown to bind cholesterol (116). Mutations in the SSD render the protein incapable of clearing cholesterol from lysosomes (170), demonstrating that this domain is important for NPC1 function.

The NPC1 protein contains three large luminal domains, the first of which has been referred to as the NPC1 domain and contains a putative leucine zipper and numerous cysteine residues conserved in other NPC1 orthologues (25). The cysteine residues within this domain are crucial for protein function, since their mutation abolishes the ability of NPC1 to correct cholesterol sorting defects when expressed in NPC mutant cells (168). The third luminal domain, also rich in cysteine residues, was proposed to be a RING domain (59) and has been shown to bind zinc (169) suggesting that, like other RING domains, it may mediate protein or lipid interactions (52). A significant proportion of the missense mutations associated with NPC, including the Nova Scotia G992W mutation, are clustered in this domain (59).

While the NPC1 protein is glycosylated (42, 66, 170), removal of these carbohydrate moieties from the amino terminal luminal domain does not affect protein function or localization (170). The significance of the glycosylation is unknown.

Although much has been learned regarding the structure of the NPC1 protein and its localization within the cell, the precise function of NPC1 has remained

unclear. A bioinformatic analysis of the NPC1 protein sequence suggested a distant relationship to members of the resistance-nodulation-division family of prokaryotic permeases (41). This similarity and the trafficking defects of NPC cells both suggest the NPC1 protein may be a transporter. Delayed efflux of a cationic fluorescent dye, acriflavine, from the endosomal/lysosomal system in NPC1-deficient cells has been reported and supports this hypothesis (41). Additionally, mutant *E. coli* cells expressing NPC1 were found to import oleic acid, but not cholesterol (41). A recent study has revealed, however, that delayed clearance of acriflavine is not specific to NPC cells (118). Other sphingolipid storage disorders also result in cells that sequester acriflavine, suggesting this is a secondary effect of the accumulated lipids (118). Furthermore, the same study also found that fatty acid flux through lysosomes of NPC cells was normal. While NPC1 may function as a transporter, the endogenous substrate of NPC1 remains to be discovered.

#### **1.4. The yeast homologue of NPC1, *NCR1***

The *S. cerevisiae* *NCR1* (for Niemann Pick Type C Related) gene encodes a protein (hereafter referred to as Ncr1) that is 34% identical and 57% similar to human NPC1 (25). The yeast Ncr1 protein is localized to the limiting membrane of the vacuole and prevacuolar compartment (PVC) (98, 161, 183), the yeast equivalent of mammalian lysosomes and late endosomes, respectively. Like NPC1, Ncr1 is a

glycosylated protein (98) that contains all of the domains found in the NPC1 protein, with the exception of the dileucine motif (Fig. 3). Removal of the last 11 amino acids of Ncr1 did not disrupt its vacuolar localization, suggesting a terminal localization motif is not present or required (183). Expression of the yeast Ncr1 protein in NPC1 mutant mammalian cells was found to correct cholesterol and ganglioside accumulation, suggesting that NPC1 function is conserved in Ncr1 (98). Despite this apparent conservation of function, deletion of the *NCR1* gene has not been reported to produce any effect on sterol or sphingolipid levels in yeast (98, 183). A dominant mutation in the sterol-sensing domain of Ncr1 was reported to lead to increased levels of complex sphingolipids in the vacuole, suggesting that Ncr1 can influence sphingolipid metabolism in yeast (98). This may imply a role for the yeast Ncr1 protein in trafficking of sphingolipids but could reflect a secondary response to the dominant mutant form of *NCR1*. Previous work in our lab has revealed that loss of *NCR1* impairs the efficiency of endocytosis and causes subtle defects in polarized secretion at the elevated temperature of 37°C but not under standard growth conditions (161).



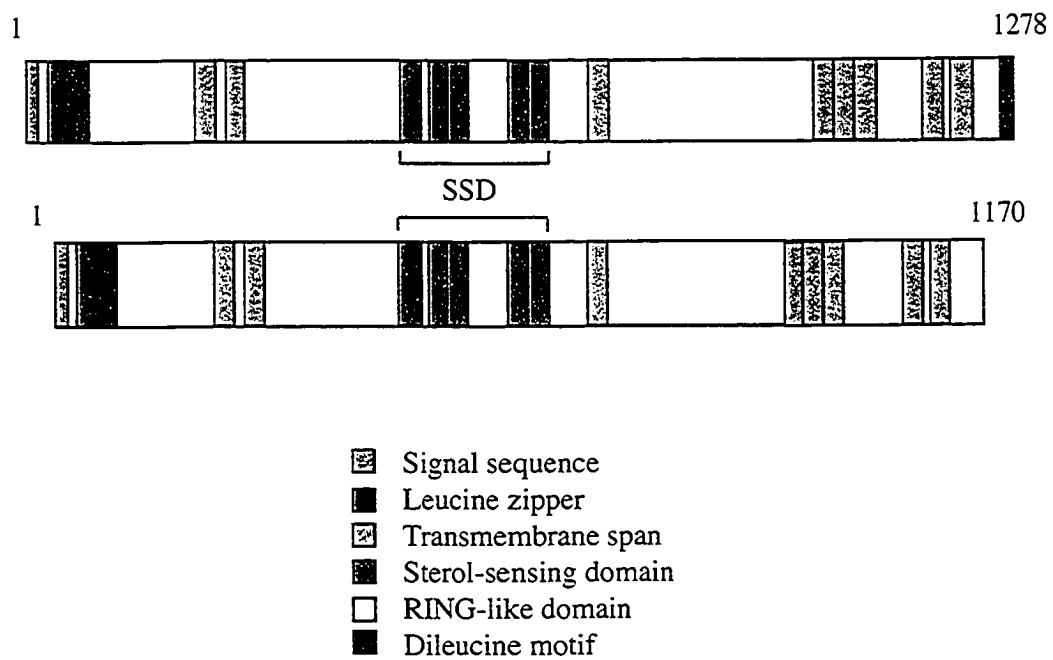


**Figure 3. Comparison of the predicted secondary structure of human NPC1 (top) and yeast Ncr1 (bottom).**

## 1.5. My research

My research was based on the hypothesis that human NPC1 and yeast Ncr1 proteins share a conserved function that is required for intracellular trafficking. My study has involved two distinct approaches aimed at dissecting the function of the yeast Ncr1 protein. The first approach has involved studying the effects of Ncr1 deficiency in yeast. Upon commencing this research, nothing was known regarding the yeast Ncr1 protein. I have found that yeast lacking *NCRI* are viable and are indistinguishable from their wild-type counterpart with respect to lipid metabolism, protein secretion and trafficking through lipid rafts, and in their response to chemical or thermal stresses. The second approach has concentrated on the effects of *NCRI* overexpression in yeast. I have discovered that overexpression of *NCRI* is deleterious, and the degree of toxicity is dependent on the abundance of Ncr1 as well as the medium in which cells are grown. To understand the mechanism by which overexpression impairs yeast, I have identified growth conditions and genes that allow cells to cope with excess Ncr1. An understanding of the cellular role of the yeast *NCRI* gene revealed by the identity of these genes is anticipated to provide insight into the primary cellular defect responsible for human NPC disease.

## 2. Materials and Methods

### 2.1. Yeast and bacterial strains

*Saccharomyces cerevisiae* strains used in this study are listed in Table 1.

Most strains were derivatives of the W303 or S288c backgrounds. The Euroscarf gene deletion collection was a derivative of the S288c background and was used for synthetic genetic array screens. *Escherichia coli* strains DH5 $\alpha$ F' or MC1066 (F-delta (*lac*) X74 *hsdR rpsL trpC9830 leuB6 pyrF::Tn5 galU galK*) were used to amplify plasmids. The *E. coli* strain BL21 DE3 was used to express proteins. Yeast were grown and genetically manipulated by standard procedures (135). Unless otherwise indicated, *E. coli* cultures were incubated at 37°C and yeast at 30°C. Cell concentrations were determined using a haemocytometer, a Coulter Counter or by determining the OD<sub>600</sub>.

### 2.2. Media and growth conditions

Yeast were grown non-selectively in liquid or solid YEPD medium (1% yeast extract, 2% bactopectone, 2% glucose, 0.003% adenine). For derepression of invertase, YEPD contained 0.1% glucose. YEPD medium at pH 2.5-6.0 contained 10 g/L succinic acid and was adjusted to the appropriate pH with phosphoric acid. YEPD medium at pH 6.5-7.5 contained 50 mM MOPS and was adjusted to the

**Table 1. Yeast strains used in this study**

Strain	Relevant genotype	Parental Strain/ Source
W303/1a	<i>MATa ade2-1 ura3-1 leu2-3,112 his3-11,15 trp1-1</i>	(136)
AU5-4	<i>MATa/α NCR1/ncr1Δ::URA3</i>	W303
AU5-4/2c	<i>MATα ncr1Δ::URA3</i>	AU5-4
WUN6	<i>MATα NCR1</i>	AU5-4/2c
WUN7	<i>MATα NCR1</i>	AU5-4/2c
CTY182	<i>MATa ura3-52 Δhis3-200 lys2-801<sub>am</sub></i>	(32)
CTY1-1a	<i>MATa ura3-52 Δhis3-200 lys2-801<sub>am</sub> sec14-1<sup>ts</sup></i>	(32)
CTY10/5d	<i>MATa gal4 gal80 his3-200 trp1-901 ade2 ura3-52 leu2-3,112 URA3:: (lexA<sub>OP</sub>)<sub>8</sub>-lacZ</i>	(10)
HK580-10A	<i>MATα ade2-1 ura3-1 leu2-3 his3-11 trp1-1 ade3Δ::hisG-URA3-hisG</i>	(9)
HK580-10D	<i>MATa ade2-1 ura3-1 leu2-3 his3-11 trp1-1 ade3Δ::hisG-URA3-hisG</i>	(9)
AF-1A	<i>MATα ade2-1 ura3-1 leu2-3 his3-11 trp1-1 ade3Δ</i>	HK580-10A
AF-1D	<i>MATa ade2-1 ura3-1 leu2-3 his3-11 trp1-1 ade3Δ</i>	HK580-10D
AFD1	<i>MATa/α NCR1/ncr1Δ::TRP1</i>	31-7 and AF-1D
AF-2I	<i>MATα ade2-1 ura3-1 leu2-3 his3-11 trp1-1 ade3Δ ncr1Δ::LEU2</i>	AF-1A
AF-3	<i>MATa ade2-1 ura3-1 leu2-3 his3-11 trp1-1 ade3Δ ncr1Δ::LEU2</i>	AF-1D
AFD3	<i>MATa/α NCR1/ncr1Δ::TRP1 YGL250w/ygl250wΔ::LEU2</i>	AFD1
Y2454	<i>MATα mfa1Δ::MFA1pr-HIS3 can1Δ his3ΔI leu2Δ0 ura3Δ0 MET15 lys2Δ0</i>	(155)

**Table 1 (Cont'd). Yeast strains used in this study**

Y1239	<i>MATa his3Δ1 leu2Δ0 met15Δ0 ura3Δ0</i>	(176)
SYNK-1	<i>ncr1Δ::kanMX4</i>	Y2454
Y1239NK-1	<i>ncr1Δ::kanMX4</i>	Y1239
SYNN-1	<i>ncr1Δ::natR</i>	SYNK-1
Y1239NN-6	<i>ncr1Δ::natR</i>	Y1239NK-1
Y1239-nhx1Δ	<i>nhx1Δ::kanMX4</i>	Y1239
EDN4	<i>MATa/α NCR1/ncr1Δ::natR</i> <i>NHX1/nhx1Δ::kanMX4</i>	SYNN-1 and Y1239-nhx1Δ
Euroscarf Deletion Set	<i>MATa his3Δ1 leu2Δ0 met15Δ0 ura3Δ0</i> <i>orfΔ::kanMX4</i>	(176)
Y1239-vma6Δ	<i>vma6Δ::kanMX4</i>	Y1239
EDN66	<i>MATa/α NCR1/ncr1Δ::natR</i> <i>VMA6/vma6Δ::kanMX4</i>	SYNN-1 and Y1239-vma6Δ
EDN66/7a	<i>NCR1 VMA6</i>	EDN66
EDN66/7b	<i>ncr1Δ::natR VMA6</i>	EDN66
EDN66/7c	<i>NCR1 vma6Δ::kanMX4</i>	EDN66
EDN66/7d	<i>ncr1Δ::natR vma6Δ::kanMX4</i>	EDN66

appropriate pH with NaOH. YEPD medium at pH 8.0-9.0 contained 50 mM TAPS and was adjusted to the appropriate pH with NaOH. YNB minimal medium contained 0.67% yeast nitrogen base (YNB) without amino acids, 2% glucose, 0.002% uracil, 0.002% tryptophan, 0.003% adenine, 0.009% leucine and 0.002% histidine. Synthetic defined (SD) medium contained 0.67% YNB without amino acids, 2% glucose, 1.4 g/L NaOH, 0.0117% adenine, 0.0078% each of alanine, cysteine, aspartic acid, glutamic acid, phenylalanine, glycine, isoleucine, inositol, lysine, methionine, asparagine, proline, glutamine, serine, threonine, valine, tyrosine, and tryptophan, 0.004% leucine, 0.002% each of histidine and arginine, and 8 mg/L para-aminobenzoic acid. Synthetic complete (SC) medium was YNB minimal medium buffered with 10 g/L succinic acid, brought to pH 5.5 with 6 g/L NaOH and supplemented with 1% casamino acids, 0.002% uracil, 0.002% tryptophan and 0.003% adenine. APG medium was used in testing hygromycin B sensitivity and contained 1.7 g/L YNB without amino acids or ammonium sulphate, 8 mM phosphoric acid, 2.12 g/L arginine, 2% glucose, 0.009% leucine, 0.002% uracil, 0.00002% methionine, 0.003% lysine, 0.002% histidine and was adjusted to pH 4.0 with NaOH (132). For induction of the galactose-inducible *GALI-10* promoter, yeast were grown in medium containing 2% galactose rather than glucose.

Histidine, uracil or leucine was omitted from medium for growth of yeast harbouring *HIS3*, *URA3* or *LEU2* plasmids, respectively. To counterselect against the

*URA3* gene, yeast were grown on YNB medium containing 5-fluoro-orotic acid (5-FOA) (BioVectra) at a concentration of 1 g/L. Selection for *natR* and *kanMX4* gene replacements was obtained by inclusion of 100 mg/L clonNat (Werner BioAgents) or 200 mg/L G418 (Sigma), respectively, in the medium. G418 is not effective in medium containing ammonium sulphate (155), so SD or SC media containing G418 was prepared with 1 g/L monosodium glutamate and 1.7 g/L YNB without amino acids or ammonium sulphate.

*MATa* haploids derived from Y2454/Y1239 diploids were selected in synthetic defined medium lacking arginine and histidine but containing 50 mg/L canavanine (155). Omission of arginine prevents induction of the general amino acid permease, so uptake of canavanine is dependent on the *CAN1* gene (63). *CAN1* haploids and *CAN1/can1* diploids will not grow in the presence of canavanine, while only *MATa* cells express *MFA1pr-HIS3* to allow growth of *his3* yeast in the absence of histidine.

To assess growth on suboptimal levels of specific amino acids or nucleoside bases, SD medium was supplemented with normal levels of required amino acids or bases, but a suboptimal level of one amino acid or base (0.0004% uracil, 0.0004% tryptophan, 0.0015% leucine, or 0.004% histidine).

Other media were used to test conditional growth phenotypes (63, 83) and supplements and the concentrations employed for each are given in Table 2. YEP-

**Table 2. Chemical additions to media to assess growth phenotypes**

<b>Chemical</b>	<b>Concentration(s)</b>	<b>Medium</b>
caffeine	0.1%	YEPD
oligomycin	15 µg/mL	YEPD
formamide	3%	YEPD
sodium vanadate	2 mM	YEPD
LiCl <sub>2</sub>	100 mM	YEPD
KCl	1 M	YEPD
CaCl <sub>2</sub>	100 mM	SC
CaCl <sub>2</sub>	200 mM	YEPD
MgCl <sub>2</sub>	200 mM	SC
MgSO <sub>4</sub>	200 mM	SC
ethanol	6%	YEPD
nocodazole	2.5 µg/mL	YEPD
benomyl	10 mg/mL	YEPD
calcofluor white	20 µg/mL	YEPD
SDS	0.002%	YEPD
sorbitol	1 M	YEPD, SD
ZnCl <sub>2</sub>	10 mM	YEPD, SC
CdCl <sub>2</sub>	10 µg/mL	SC
CdCl <sub>2</sub>	20 µg/mL	YEPD
nystatin	5 µg/mL	YEPD
hydroxyurea	100 mM	YEPD
DTT	10 mM	YEPD
NaCl	0.9 M	YEPD
glycerol	2 M	YEPD
canavanine	60 µg/mL	YNB
hygromycin B	5-50 µg/mL	YEPD, APG
palmitic acid	500-800 µM	SD



acetate, YEP-glycerol and YEP-sucrose contained 1% yeast extract, 2% bacto-peptone and then respectively, either 2% potassium acetate, 3% (v/v) glycerol or 2% sucrose.

To induce meiosis, cells were cultured in Fogel's sporulation medium (1% potassium acetate, 0.25% yeast extract, 0.05% glucose and appropriate amino acids for plasmid selection) at 23°C for 5-7 d.

Cells were grown anaerobically in a chamber devoid of oxygen, prepared by inclusion of an Anaerocult A gas pack (Merck) saturated with 35 mL dH<sub>2</sub>O.

Anaerobic status was confirmed with an anaerobic indicator strip (EM Science).

*E. coli* were grown in LB or 2xYT as described by Sambrook *et al.* (137).

Media were supplemented with 50 µg/mL ampicillin to select for plasmids.

Expression of the *lacZ* gene, for blue-white screening of colonies, was monitored by inclusion of 33.3 µg/mL 5-bromo-4-chloro-3-indolyl-beta-D-galactopyranoside (X-gal) (American Biorganics, Inc.) and 33.3 µM isopropyl-beta-D-

thiogalactopyranoside (IPTG) (Biovectra) in the medium. To select for the presence of *URA3*-based plasmids, *E. coli* MC1066 cells were grown in M9 medium lacking uracil (137). M9 medium contained 6 g/L Na<sub>2</sub>HPO<sub>4</sub>, 3 g/L KH<sub>2</sub>PO<sub>4</sub>, 1 g/L NH<sub>4</sub>Cl, 0.5 g/L NaCl, 1 mM MgSO<sub>4</sub>, 500 µg/L thiamine, 0.002% of each of adenine, arginine,

histidine and threonine, 0.003% each of leucine, tyrosine, isoleucine and lysine, 0.002% methionine, 50 µg/mL ampicillin, and 2% glucose. Because uracil was omitted, only MC1066 *E. coli* cells that had a plasmid-borne *URA3* gene to complement the *pyrF* mutation were able to grow (5).

Media were solidified with 2% agar. All media reagents were obtained from DIFCO Laboratories or Sigma Chemical Co.

### **2.3. DNA isolation and analysis**

Plasmids were isolated from *E. coli* by the rapid boiling method or by alkaline lysis (137) and further purified using QiaPreps (Qiagen). The ten-minute plasmid preparation protocol (135) was used to rescue library plasmids from yeast and yeast genomic DNA for use as template in polymerase chain reaction (PCR) assays (135). For Southern blotting, yeast genomic DNA was isolated as described (46) and a 4-kbp *SmaI/XhoI* fragment encoding the *NCR1* gene was radiolabeled with <sup>32</sup>P-dCTP using a random-priming kit (Boehringer) for use as a probe for the *NCR1* locus. DNA was sequenced by the dideoxy chain-termination method using a Sequenase kit (USB) or by the John P. Robarts Research Institute in London, Ontario. Universal forward and reverse sequencing primers 213F and 213R were used to sequence library plasmid inserts. Plasmids were identified by restriction mapping.

## 2.4. PCR

Primers used in this study are listed in Table 3. High-fidelity PCR was performed using 1-10 ng template DNA in 1X PFX buffer (Invitrogen), 1X PCR Enhancer, 1 mM MgSO<sub>4</sub>, 0.003 µg of primers, 0.3 mM dNTPs and 0.04 U Platinum PFX Taq polymerase (Invitrogen). To amplify the *kanMX4* or *natR* genes with *NCR1* 5' and 3' flanking regions, (*ncr1Δ::kanMX4* and *ncr1Δ::natR*, respectively), high-fidelity PCR was performed using primers NCR16 and NCR17 and p4339 or pFA6-13MYC-KanR MX, respectively, as templates (Table 4). The reaction was initiated with a 2-min denaturation at 94°C, followed by 35 cycles of a 30-s denaturation at 94°C, a 45-s annealing at 58°C and a 2-min extension at 68°C. The reaction was terminated by a 5-min extension at 68°C.

For amplification of the *YGL250w* locus from genomic DNA, primers YGL250-F2 and YGL250-R2 were used. The reaction consisted of a 5-min denaturation at 94°C then 30 cycles of 1-min denaturation at 94°C, 2-min annealing at 48°C and 6-min extension at 72°C. A final 6-min extension period at 72°C concluded the amplification.

PCR to confirm deletion of yeast genes was performed using 1-10 ng template DNA in 1X PCR Buffer (Invitrogen), 1.5 mM MgCl<sub>2</sub>, 0.2 mM dNTPs (Amersham), 0.25 µl Platinum Taq Polymerase (Invitrogen), with 2 ng/µL of each primer. To

**Table 3. Primers used in the study**

Primer	Sequence
NCR1-F	5'-ccgaacgatagagtagtcaag
NCR1-R2	5'-caacgaagcctgtgttagtgt
NCR-F3	5'-agcttcgagctcatgaatgtgctatggattatagcactagtgg
NCR-R3	5'-ccaactagtgtataatccatagcacattcatgagctcga
NCR16	5'-aagataactaaattcatctccaaaaagaacaagagcagaacttca attagtaaaacatggaggcccagaataccc
NCR17	5'-acctatcttttactacgtaaaatagtagtataatctgctatggctaatt cttctgcagtatagcgaccagcattcac
YGL250-F2	5'-tcgtggtacatgatatg
YGL250-R2	5'-agaaactcaccgttgg
CYS1-F	5'-cgggaattcatggaaattcaattgggctag
CYS1-R	5'-cgcggatccctatctagacaacgtcaatgggtccc
NAT1	5'- ggactcccggacgttcgtcgc
YGL250-F1	5'-caggatccaagcttcaatggaatcaaagatg
YGL250-R1	5'-cactgcagttatctagagtcttcagaatcctca
213F	5'-tacttggagccactatcgactacg
213R	5'-cggcgatataggcgccagcaaccg
CHS5-A	5'-accggctgtaacgtacaataagtag
CHS5-D	5'-cggcctataaatagacagatttga
SAC1-A	5'-agtgtgaaaaattttgaaaaactcg
SAC1-D	5'-gaaacttacacggtacaatagggaa
DAL81-A	5'-tcaacagagatgatttgtgtcattt
DAL81-D	5'-gcaaagtataatagacgaggcaaaa
GOT1-A	5'-tattaattatgggggatcacaaga
GOT1-D	5'-agatctactgatagttccacatcg
BCK1-A	5'-gggaggtaacgaagagaagaatag
BCK1-D	5'-ttatagagactgtgcttgatgttgg
HFA1-A	5'-tcatagggttaaatactgtggaaag
HFA1-D	5'-gaatgtcagattttctcttttcgg
BEM1-A	5'-taaaccgaaatccaaaaactttaca
BEM1-D	5'-catgcattatgattgagtggaata
LIP2-A	5'-agaagggaatacatttgaccctatc

**Table 3. (Cont'd) Primers used in the study**

---

LIP2-D	5'-agaacaagaactctcaactgcatct
SPT3-A	5'-gcgtctcttagtttctttgcaatac
SPT3-D	5'-ttctatattttctttcaaaacatcg
IRA2-A	5'-tgcccaacgattatctattctacat
IRA2-D	5'-acagaaacactttcaactaagacgg
NHX1-A	5'-acacaaggagtagcagagcagtagt
NHX1-D	5'-tttcaatcaaaggcaaaaagtaaac
KAN-C	5'-tgattttgatgacgagcgtaat
VMA6-A	5'-gtacccttcttatcttacagacgca
VMA6-D	5'-acgcttgtaacaaactaaggatgtc

---

amplify the sequence at the *NCR1* locus, primers NCR1-F and NCR1-R2 were used. These primers anneal 294 bp upstream and 146 bp downstream of the *NCR1* ORF, respectively. The reaction was initiated with a 4-min denaturation at 94°C followed by 30 cycles of 1-min denaturation at 94°C, 2-min annealing at 52°C and 6-min extension at 72°C. The reaction was concluded with a 6-min extension at 72°C.

*ncr1Δ::natR* gene replacements were further confirmed using an internal *natR* primer (NAT1) paired with NCR1-R2. NAT1 anneals approximately 227 bp downstream of the *natR* initiation codon. The reaction was initiated with a 5-min denaturation at 94°C followed by 30 cycles of a 1-min denaturation at 94°C, 2-min annealing at 52°C and 2-min extension at 72°C. The reaction was completed with a final 5-min extension at 72°C.

To confirm deletion of yeast genes in strains from the Yeast Gene Deletion Set, primers annealing ~200 to 400 bp upstream and downstream of the open reading frame were used to amplify the locus (176). These reactions were initiated with a 3-min denaturation at 94°C followed by 35 cycles of a 15-s denaturation at 94°C, 15-s annealing at 57°C and 60-s extension at 72°C. The reactions concluded with a 3-min extension at 72°C. Deletions were further confirmed by the same program using the downstream primer paired with an oligonucleotide that anneals within the *kanMX4* cassette (KAN-C).

An ~700-bp portion of the *NCR1* ORF was generated by PCR using primers CYS1-F and CYS1-R to create an *EcoRI/BamHI* fragment encoding amino acids 769 to 1002 of Ncr1 with a methionine codon at the 5' end and a STOP codon at the 3' end. This fragment was subsequently identified as CYS when subcloned in other plasmids.

## 2.5. Plasmids

Plasmids used in this study are listed in Table 4. Yeast genomic DNA plasmid libraries used in this study were *Sau3A* partial restriction fragments cloned at the unique *BamHI* site in the single-copy *LEU2*-based p366 yeast vector (ATCC) and the high-copy *URA3*-based pRB114 yeast vector.

A high-copy *URA3*-based yeast plasmid in which the *NCR1* promoter drives expression of the *lacZ* gene (pNCR1p-lacZ) was created by replacing the *CYC1* promoter in pLG669-Z (61) with an 880-bp *EcoRV/BamHI* fragment from pRSNCR1 (161) containing the *NCR1* promoter and the first one-sixth of the *NCR1* open reading frame.

pSLNCR1, a single-copy *URA3*-based plasmid encoding *ADE3* and *NCR1*, has the *GALI-10* promoter situated adjacent to and upstream of the *CEN* sequence, rendering this plasmid unstable when transformants are grown on galactose. pSLNCR1 was generated by ligating an ~4-kbp *XhoI/BamHI* partial fragment from

**Table 4. Plasmids used in this study**

Plasmid	Relevant Features	Source
pLG669-Z	2 $\mu$ <i>URA3 CYC1p-lacZ</i>	(61)
pNCR1p-lacZ	2 $\mu$ <i>URA3 NCR1p-lacZ</i>	pLG669-Z
pRS313	<i>ARS CEN HIS3</i>	(143)
pRSHISNCR1	<i>ARS CEN HIS3 NCR1</i>	pRS313
pSLS1	<i>ARS GALpCEN URA3 ADE3</i>	(9)
pSLNCR1	<i>ARS GALpCEN URA3 ADE3 NCR1</i>	pSLS1
pTZ18R		Pharmacia
pNCR1-KO	<i>ncr1<math>\Delta</math></i>	pTZ18R
YE <sub>p</sub> 24	2 $\mu$ <i>URA3</i>	(16)
YE <sub>p</sub> 351	2 $\mu$ <i>LEU2</i>	(67)
pNCR1-KO::LEU2	<i>ncr1<math>\Delta</math>::LEU2</i>	pNCR1-KO
pHR81	2 $\mu$ <i>URA3 leu2-d</i>	(109)
pNCR1-KO::URA3	<i>ncr1<math>\Delta</math>::URA3</i>	pNCR1-KO
pLT11	<i>leu2::TRP1</i>	(38)
pLH7	<i>leu2::HIS3</i>	(38)
pUH7	<i>ura3::HIS3</i>	(38)
pRS315	<i>ARS CEN LEU2</i>	(143)
pRSNCR1-L	<i>ARS CEN LEU2 NCR1</i>	pRS315
pRS315-URA3	<i>ARS CEN LEU2 URA3</i>	pHR81
pRS314	<i>ARS CEN TRP1</i>	(143)
pRS314-URA3	<i>ARS CEN TRP1 URA3</i>	pHR81
pRS315-ADE3	<i>ARS CEN LEU2 ADE3</i>	pSLS1
pRS314-ADE3	<i>ARS CEN TRP1 ADE3</i>	pSLS1
pBluescript		Stratagene
pRSYGL250w	<i>ARS CEN HIS3 YGL250w</i>	pRS313
pBSYGL250w	<i>YGL250w</i>	pBluescript
pBSYGL250w $\Delta$ 1-300	<i>ygl250w<math>\Delta</math>1-300::LEU2</i>	pBSYGL250w
pBSYGL250w $\Delta$	<i>ygl250w<math>\Delta</math>::LEU2</i>	pBSYGL250w $\Delta$ 1-300
pRS316	<i>ARS CEN URA3</i>	(143)
pRSNCR1	<i>ARS CEN URA3 NCR1</i>	(161)
pGAD424	<i>GAL4<sub>AD</sub> TRP1</i>	Clontech



**Table 4. (Cont'd) Plasmids used in this study**

pGAD-CYS	<i>2μ LEU2 GAL4<sub>AD</sub>-CYS</i>	pGAD424
pET32	thioredoxin-His <sub>6</sub> - S-tag	Novagen
pET-CYS	thioredoxin-His <sub>6</sub> - S-tag-CYS	pET32
pRSNCR1-NoP	<i>ARS CEN URA3 NCR1-5'UTRΔ</i>	pRSNCR1
pEMBLyEX4	<i>2μ URA3 LEU2-d GALp</i>	(26)
pEMBL-NCR1	<i>2μ URA3 LEU2-d GALpNCR1</i>	pEMBLyEX4
pEMBL-HIS	<i>2μ HIS3 LEU2-d GALp</i>	pEMBLyEX4
pEMBL-NCR1-HIS	<i>2μ HIS3 LEU2-d GALpNCR1</i>	pEMBL-NCR1
pGAL-BCK1-20	<i>ARS CEN LEU2 GALp-BCK1-20</i>	pPAD91, (44)
pGBTNHX1-C	<i>2μ TRP1 GAL4<sub>BD</sub>-NHX1-C</i>	(1)
pGADNHX1-C	<i>2μ LEU2 GAL4<sub>AD</sub>-NHX1-C</i>	pGBTNHX1-C
pSHCYS	<i>2 μ HIS3 LEXA-CYS</i>	pGAD-CYS
pSH2-1	<i>2μ HIS3 LEXA</i>	(10)
pSH2-REP2	<i>2μ HIS3 LEXA-REP2</i>	(142)
pGADREP1	<i>2μ LEU2 GAL4<sub>AD</sub>-REP1</i>	(142)
pFA6-13MYC-KanR MX	<i>kanMX4</i>	(166)
p4339	<i>natR</i>	(155)

pRSNCR1 encoding *NCR1* with a 9.3-kbp *SalI/EcoRI* fragment from pSLS1 (9) (Joyce Chew, personal communication).

The 5' and 3' *NCR1* flanking noncoding genomic sequences were isolated from pRSNCR1 as 0.6-kbp *EcoRI/SphI* and 0.24-kbp *SphI/HindIII* fragments, respectively, and ligated together in *EcoRI/HindIII* digested pTZ18R (Pharmacia) to give pNCR1-KO (Joyce Chew, personal communication). A 2.3-kbp *HpaI/SphI* fragment encoding the *LEU2* gene was isolated from YEp351 and inserted between the 5' and 3' *NCR1* flanking sequences in *MscI/SphI* digested pNCR1-KO to yield pNCR1-KO::LEU2 (Joyce Chew, personal communication). A 2.25-kbp *HpaI/SphI* fragment from this plasmid was used for targeted replacement of the *NCR1* gene with *LEU2*. For targeted replacement of the *NCR1* gene with *URA3*, a 1.1-kbp *SmaI/SphI* fragment encoding the *URA3* gene was isolated from pHR81 and inserted between the 5' and 3' *NCR1* flanking sequences in *MscI/SphI* digested pNCR1-KO to yield pNCR1-KO::URA3 (Melanie Dobson, personal communication).

A 5.3-kbp *SmaI/SalI* fragment encoding the *ADE3* gene isolated from pSLS1 was subcloned in pRS314 and pRS315 to give pRS314-ADE3 and pRS315-ADE3, respectively.

A 1.1-kbp *SmaI/SalI* fragment encoding the *URA3* gene isolated from pHR81 was ligated in pRS314 and pRS315 to give pRS314-URA3 and pRS315-URA3, respectively.

A p366 library plasmid containing a 10.6-kbp genomic insert encoding *YGL250w* from *S. cerevisiae* chromosome VII was digested with *Sst*I and *Eco*RV to release a 2.3-kbp fragment. This fragment was subcloned into pRS313 and pBluescript to give pRSYGL250w and pBSYGL250w, respectively.

pBSYGL250w was digested with *Sna*BI and *Eco*RI to remove a 350-bp fragment encoding the 5' third of the *YGL250w* gene. This was replaced with a 2.7-kbp *Eco*RI/*Pvu*II fragment from pGAD424, encoding the *LEU2* gene, creating pBSYGL250w $\Delta$ 1-300. To completely delete *YGL250w*, pBSYGL250w $\Delta$ 1-300 was digested with *Bam*HI and *Sst*I to release a 6.1-kbp fragment. pBSYGL250w was digested with *Sst*I and *Sau*3A and a 386-bp fragment was purified. The 6.1-kbp and 386-bp fragments were ligated together to yield pBSYGL250w $\Delta$ , in which the entire *YGL250w* open reading frame is replaced with the *LEU2* gene.

A 700-bp *Eco*RI/*Bam*HI fragment (CYS) encoding the *NCR1* cysteine-rich loop was inserted in the yeast 2-hybrid vector pGAD424 (Clontech) to give pGAD-CYS, expressing the Ncr1 cysteine-rich loop fused to the carboxy terminus of the Gal4 activation domain.

An *Eco*RI/*Sal*I fragment was isolated from pGAD-CYS and subcloned into the *E. coli* expression vector pET32 (Novagen) and into the yeast 2-hybrid vector pSH2-1 (10) to give pETCYS and pSHCYS, respectively. The Ncr1 CRL is

expressed with an amino-terminal thioredoxin-polyhistidine tag from pET-CYS, and fused to the C terminus of LexA from pSH-CYS.

A 0.3-kbp *EcoRI/PstI* fragment encoding the C-terminal portion of Nhx1 was obtained from pGBT9NHX1-C (1) and ligated in pGAD424, to create pGADNHX1-C, in which the C-terminal tail of Nhx1 is fused to the carboxy-terminal end of the Gal4 activation domain.

The *NCR1* open reading frame lacking its promoter region was generated by first creating a 70-bp *HindIII/MscI* fragment encoding the start codon and the first 32 nucleotides of the *NCR1* open reading frame, by annealing primers NCR-F3 and NCR-R3. This fragment was used to replace the *NCR1* upstream non-coding region in pRSNCR1, to give pRSNCR1-NoP, in which *HindIII* and *SstI* sites immediately precede the *NCR1* initiation codon. A 3.7-kbp *SstI/XbaI* fragment encoding the complete *NCR1* gene without the upstream noncoding sequence was isolated from pRSNCR1-NoP and ligated in pEMBLyEX4 to give a high-copy yeast plasmid with *NCR1* under the control of a galactose-inducible promoter (pEMBL-NCR1).

## **2.6. Transformation of yeast and *E. coli***

Yeast were transformed using the LiAc/ss-DNA/PEG method (54). Strains or plasmids were marker-swapped from *LEU2* or *URA3* to *TRP1* or *HIS3* by transforming with linearized marker swap plasmids pLT11, pLH7, or pUH7 as

described (38). One-step gene replacements were carried out as described (136). The *YGL250w* ORF was replaced with the *LEU2* gene by transforming yeast with a 3.4-kbp *SpeI/SstI* fragment from pBSYGL250w $\Delta$  and selecting for leucine prototrophy. A 2.8-kbp *BamHI/EcoRI* fragment isolated from plasmid pNCR1-KO::*LEU2* encoding the *LEU2* gene flanked by the *NCR1* gene 5' and 3' noncoding regions was used to transform yeast to leucine prototrophy. Similarly, the *NCR1* gene was replaced with the *URA3* gene using a 1.6-kbp fragment isolated from plasmid pNCR1-KO::*URA3*. The *ncr1* $\Delta$ ::*kanMX4* and *ncr1* $\Delta$ ::*natR* amplicons were used to transform yeast to G418 or ClonNat resistance, replacing *NCR1* with either the G418- or ClonNat-resistance markers *kanMX4* or *natR*, respectively. To regenerate *NCR1* wild-type yeast from an *ncr1* $\Delta$ ::*URA3* strain, a *HindIII/SstI* fragment encoding wild-type *NCR1* was used to transform these yeast to 5-FOA resistance. When selecting for transformants on medium containing 5-FOA, G418 or clonNat, strains were incubated for 4 h in rich medium prior to plating to allow disappearance of the *URA3* gene product or accumulation of the *kanMX4* or *natR* gene products, respectively. All gene deletions were confirmed by PCR and/or Southern blotting.

*E. coli* were made competent and transformed by electroporation using a BioRad Gene Pulser at a voltage of 2.5 kV, 200  $\Omega$  resistance and 25  $\mu$ F capacitance as described by the manufacturer.

## **2.7. Plasmid Loss**

Yeast containing a plasmid to be lost were grown for several generations in medium containing the nutritional supplement specified by the marker gene on the plasmid. Under these conditions, cells that lost plasmid were not at a selective disadvantage and could be identified by replica plating onto medium containing or lacking the particular amino acid or base and screening for the desired auxotrophy.

## **2.8. Extraction of proteins from yeast**

Proteins were isolated from yeast by glass-bead disruption. After harvesting, cell mass was determined and cells were resuspended in an equal volume of RIPA buffer (50 mM Tris pH 8.0, 150 mM NaCl, 1% NP-40, 0.5% deoxycholate, 0.1% SDS, 1 mM PMSF, 1 mM DTT, 1X Complete protease inhibitors (Roche)). Acid-washed siliconized glass beads (40 mesh) were added to the meniscus and tubes were vortexed at maximum speed for 4 min, keeping the samples cold. After vortexing, an equal volume of RIPA buffer was added and tubes were vortexed an additional 3 min. The bottom of each tube was punctured with a 30-gauge needle, and the cell lysate was collected in a second tube by centrifugation.

## **2.9. Extraction of proteins from *E. coli***

*E. coli* BL21 DE3 transformants were grown in LB+ampicillin. After incubation at 37°C overnight, cultures were ten-fold diluted into fresh medium and incubated until cells were in log phase. Protein expression was induced by the addition of IPTG to a final concentration of 0.3 mM and incubation at 25°C for 6 h. Cells were harvested by centrifugation at 5,500 rpm at 4°C for 10 min, were resuspended in cold TBS (25 mM Tris-HCl pH 7.4, 137 mM NaCl, 2.7 mM KCl) and lysed by sonicating 6 x 30 sec on a Branson Sonifier 250 at power level 2 (~20% output). Triton X-100 was added to a final concentration of 1%, followed by 1 mM DTT, 1 mM PMSF and 1X Complete protease inhibitors (Roche). The solutions were incubated at 4°C with gentle rocking for 45 min, and then centrifuged at 20,000 x g for 20 min at 4°C. Both soluble and insoluble fractions were saved.

## **2.10. Purification of His<sub>6</sub>-tagged insoluble proteins**

The Ncr1 cysteine-rich loop was expressed as a thioredoxin-His<sub>6</sub> fusion protein (CRL-His<sub>6</sub>) in *E. coli* from plasmid pET-CYS. Insoluble proteins were resuspended in 12 mL lysis buffer (50 mM NaH<sub>2</sub>PO<sub>4</sub>, 10 mM Tris, 300 mM NaCl, pH 7) containing 8 M urea and solubilization was facilitated by sonicating 4 x 20 sec on power level 2 (~20% output). The sample was centrifuged as above and CRL-His<sub>6</sub>

was purified from the supernatant by affinity purification using Talon slurry (Clontech). Resin (4 mL of a 50% solution in lysis buffer with 8 M urea) was added to the CRL-His<sub>6</sub> urea-solubilized fraction. The solution was rocked gently for 30 min at room temperature to allow adsorption of CRL-His<sub>6</sub> to the resin. The resin was pelleted by centrifugation and the unbound proteins were removed. The resin was washed 2 x 10 min with 25 mL cold lysis buffer + 8 M urea. The resin was resuspended in 6 mL cold lysis buffer + 8M urea and transferred to a column. The protein was renatured by sequentially washing proteins adsorbed to the resin with 10 mL lysis buffer containing urea at decreasing concentrations, then finally with lysis buffer without urea. CRL-His<sub>6</sub> was eluted from the column with 10 mL elution buffer (45 mM NaH<sub>2</sub>PO<sub>4</sub>, 270 mM NaCl, 150 mM imidazole, pH 7) and the eluate was collected in 1-mL fractions. Fractions containing CRL-His<sub>6</sub> were pooled, transferred to dialysis tubing (Molecular Weight Cut Off of 8,000, BioDesign, Inc. of New York) and dialyzed against 2 litres of PBS (8 g/L NaCl, 0.2 g/L KCl, 1.44 g/L Na<sub>2</sub>HPO<sub>4</sub>, 0.24 g/L KH<sub>2</sub>PO<sub>4</sub>) for 2 d at 4°C. Protein samples were aliquotted dropwise from a P1000 into liquid nitrogen and were stored as beads at -70°C. Samples of the denatured and renatured CRL-His<sub>6</sub> were used for production of anti-Ncr1 polyclonal antibodies in rabbit (Chemicon).



### **2.11. SDS-PAGE analysis**

Protein concentrations were determined by Bradford assay and samples were prepared for electrophoresis by resuspending in an equal volume of 2X protein gel loading buffer (87). Prior to separation by electrophoresis, protein samples were incubated at 37°C for 5 min when Ncr1 protein was present or at 100°C for all other samples. Ncr1 cysteine-rich-loop-His<sub>6</sub> fusion proteins were resolved in 12% SDS-polyacrylamide gels. Samples containing native Ncr1 or immunoprecipitated Gas1 were resolved in 6% or 8% SDS-polyacrylamide gels, respectively and proteins were detected by staining with Coomassie Blue.

### **2.12. Western analysis**

Proteins resolved by SDS-PAGE were transferred to PVDF membranes (BioRad) using a Hoeffer Transphor apparatus in transfer buffer (25 mM Tris, 192 mM glycine, 20% (v/v) methanol, 0.0375% SDS (w/v)) for 1 h at 300 mA. After transfer, membranes were washed in PBST (8 g/L NaCl, 0.2 g/L KCl, 1.44 g/L Na<sub>2</sub>HPO<sub>4</sub> 0.24 g/L KH<sub>2</sub>PO<sub>4</sub>, 0.001% (v/v) Tween-20), blocked for 1 h in 5% skim milk powder in PBST, and then washed with PBST. Primary and secondary antibody incubations were carried out in PBST containing 5% skim milk powder. Affinity-purified anti-Ncr1 polyclonal antibodies (J. Chew) were used at a 1:2,000 dilution while the anti-CPY antibody (Molecular Probes) was used at a 3:5,000 dilution.

Proteins tagged with S-peptide were recognized with HRP-conjugated S protein (Novagen), employed at a dilution of 1:5,000. Bound antibodies were detected with HRP-conjugated goat secondary antibodies at a dilution of 1:5,000 and visualized by chemiluminescence using a Lumiglo kit (KPL), followed by exposure to x-ray film.

### **2.13. Yeast two-hybrid and $\beta$ -galactosidase assays**

Yeast two-hybrid assays were performed as described (10) using the reporter yeast strain CTY10/5d and a  $\beta$ -galactosidase filter assay to detect fusion-protein interaction (135). Expression of the *E. coli lacZ* gene under the control of the *NCR1* promoter in yeast was determined using a permeabilized-cell  $\beta$ -galactosidase assay (135).

### **2.14. Plating assays**

For all plating assays, untransformed yeast were grown in YEPD and transformed yeast were grown in selective medium overnight. Five- or ten-microlitre volumes of serial dilutions of cells were deposited on plates.

### **2.15. Recovery from deep stationary phase**

Yeast were grown in YEPD for 24 h and then incubated at room temperature for 3 months prior to plating on YEPD. Their ability to form colonies was compared to YEPD cultures incubated overnight prior to plating.

### **2.16. Heat-stress viability assay**

Cells were grown to log phase in YEPD at 30°C and then incubated at 44°C for the indicated amounts of time. Equal numbers of cells taken before and after this heat shock were plated on YEPD, incubated at 30°C for 2 days and the number of colonies on each plate were counted to determine survival. Percentage of survival was calculated using the survival of non-heat-shocked cells as 100%. The percentage of respiration deficient [ $\rho$ -], cells was also determined, counting white, glycerol-auxotrophic petite colonies as [ $\rho$ -].

### **2.17. Generation of petites**

To monitor production of [ $\rho$ -] yeast, respiration-competent [ $\rho$ + ] yeast strains were grown to saturation in YEPD and plated on YEPD. A well in the centre of each plate was filled with dH<sub>2</sub>O, or with 0.1 mg/mL, 1 mg/mL or 10 mg/mL ethidium bromide. The plates were incubated for one week. The following were determined

for each plate: region of inviability (distance from the well to the closest [ $\rho$ +] or [ $\rho$ -] colony), the region of [ $\rho$ -] growth (distance from the first [ $\rho$ -] colony closest to the well to the first [ $\rho$ +] colony), and the region of wild-type growth (distance from the first [ $\rho$ +] colony to the outside edge of the plate). Ethidium bromide plates were replica-plated to YEP-glycerol to ensure that small white colonies were unable to use glycerol as a carbon source, as expected if they were [ $\rho$ -].

### **2.18. Hygromycin assays**

Yeast transformants were incubated at 28°C in synthetic complete medium lacking uracil until the cells were in stationary phase, and then used to inoculate APG medium lacking uracil and containing different concentrations of hygromycin B (Sigma) to a starting OD<sub>600</sub> of 0.004. The cultures were incubated on a roller at 28°C for 24 h and cell densities of each culture were determined by measuring OD<sub>600</sub>.

### **2.19. Secretion of invertase**

The secretion of invertase was monitored as described (32, 56). Yeast cells were grown in YEPD to log phase, harvested by centrifugation at 2,500 rpm for 5 sec, washed twice, and incubated in 0.1% glucose YEPD at 30°C for 2 h. Cells were then harvested, washed and resuspended in 10 mM NaN<sub>3</sub>. Half of each cell sample was

treated with 0.2% Triton X-100, then stored at  $-70^{\circ}\text{C}$  for 10 min to permeabilize the cell membrane. Cells were transferred to test tubes and the volumes were brought to 200  $\mu\text{L}$  with 0.1 M NaOAc, pH 5.1. A blank containing no cells was included. Sucrose (50  $\mu\text{L}$ , 0.5M) was added, the tubes incubated at  $30^{\circ}\text{C}$  for 3 min, and reactions stopped by the addition of 300  $\mu\text{L}$  0.2 M  $\text{KPO}_4$ , pH 7, 10 mM NEM. Samples were incubated at  $100^{\circ}\text{C}$  for 3 min, then equilibrated to  $30^{\circ}\text{C}$ . Two mL glucostat reagent (0.1 M  $\text{KPO}_4$ , 2.75 units/mL glucose oxidase, 2.5  $\mu\text{g/mL}$  peroxidase, 100  $\mu\text{M}$  NEM, 150  $\mu\text{g/mL}$  o-dianisidine) was added and tubes incubated at  $30^{\circ}\text{C}$  for 1 h. Reactions were stopped by the addition of 2 mL 6 N HCl. The absorbance of each sample was determined at 540 nm. The ratio of the external (determined from intact cells) to total (from permeabilized cells) invertase was determined. The experiment was carried out in triplicate for each strain. A strain known to secrete invertase (CTY1-1a) was included as a positive control.

## **2.20. Radiolabeling and immunoprecipitation of Gas1**

Maturation of Gas1 was monitored as described (151). Log-phase cells were harvested, resuspended at  $1 \times 10^8$  cells/mL in medium lacking methionine and cysteine, and incubated with 435  $\mu\text{Ci}$  EXPRE<sup>35</sup>S<sup>35</sup>S <sup>35</sup>S-methionine and <sup>35</sup>S-cysteine (NEN, catalog number NEG-072 in 50 mM Tricine-HCl, pH 7.4, 10 mM  $\beta$ -

mercaptoethanol) for 10 min at 30°C or 37°C. The chase was initiated by adding a 1/100 volume of chase mixture (5 mg/mL methionine and 5 mg/mL cysteine). At the indicated chase times, 1-mL samples were removed and NaN<sub>3</sub> and NaF were added to a final concentration of 10 mM each. Cells were harvested and resuspended in 200 µL Laemmli buffer (62.5 mM Tris-HCl, pH 6.8, 2% SDS, 10% glycerol, 5% β-mercaptoethanol, 1 mM PMSF, 4 µM pepstatin) and lysed by vortexing for 10 min with acid-washed glass beads. The lysates were boiled for 5 min, then centrifuged at 14,000 rpm for 5 min. Two hundred µL of supernatants were added to 800 µL IP Dilution Buffer (60 mM Tris-HCl, pH 7.4, 1.25% (v/v) Triton X-100, 190 mM NaCl, 6 mM EDTA) and were pre-cleared by incubation with Protein A-Sepharose (Amersham Biosciences) at 4°C overnight. Proteins that interacted with Protein A were removed by centrifugation. Anti-Gas1 rabbit polyclonal antibody (4 µL, provided by Howard Reizman) was incubated with the pre-cleared supernatant at 4°C overnight and subsequently incubated with 50 µL 50% slurry of Protein A-Sepharose at 4°C overnight. The resin was pelleted and washed three times with IP buffer (50 mM Tris-HCl, pH 7.4, 1% Triton X-100, 0.2% SDS, 150 mM NaCl, 5 mM EDTA), once with high-salt wash buffer (IP Buffer with 500 mM NaCl) and finally with IP buffer. Resins were resuspended in Laemmli buffer containing 0.05% Bromphenol

Blue. Samples were boiled for 5 min before resolution by SDS-PAGE and visualized by Phosphorimaging (BioRad) and autoradiography.

### **2.21. Lipid labeling**

Log-phase cells were labeled with [ $^{14}\text{C}$ ]acetate (1.4  $\mu\text{M}$ , 4  $\mu\text{Ci}$ ) (New England Nuclear, NEC-084H) at 30 or 37°C for the indicated times. Duplicate samples were harvested and lipids were isolated as described (180). Cells were washed with water, resuspended in 1 mL  $\text{CHCl}_3/\text{MeOH}$  (1:1), and lysed for 1 min at 4°C using a BioSpec Multi-Bead Beater containing 0.5 mL acid-washed glass beads. Extracts were removed and beads were washed with 1 mL  $\text{CHCl}_3/\text{MeOH}$  (2:1), which was pooled with the extracts. Samples were removed for total uptake determinations. One half mL  $\text{CHCl}_3/\text{MeOH}$  (2:1), 0.5 mL  $\text{CHCl}_3$  and 1.5 mL  $\text{dH}_2\text{O}$  were added to the extracts. Tubes were vortexed and samples were centrifuged at 2,500 rpm for 10 min at 4°C. The aqueous phases and protein interfaces were aspirated and the organic phases were transferred to microfuge tubes. Samples were removed to determine the total incorporation of [ $^{14}\text{C}$ ]acetate into lipids.

Lipids were separated by thin layer chromatography (TLC). For each condition, equal amounts of radioactivity were loaded on two silica gel 60 Å LK6D 20 cm x 20 cm TLC plates (Whatman). Standards were also loaded on the TLC plates.

Phospholipids were separated using  $\text{CHCl}_3$ :MeOH:dH<sub>2</sub>O:CH<sub>3</sub>COOH (70:30:4:2) and neutral lipids were separated using petroleum ether:diethyl ether:CH<sub>3</sub>COOH (80:20:1) as solvent systems. After resolution, standards were stained with iodine vapor. Plates were sprayed with EnHance (NEN) and exposed to autoradiography film at -70°C. Appropriate areas on the TLC plates were scraped into scintillation vials. Scintillation fluid (2.5 mL) was added to the vials and radioactivity in each vial was determined using a Beckman scintillation counter.

The amount of phosphorus in the lipid samples was determined by the method of Ames and Dubin (2). Lipid samples were resuspended in 300  $\mu\text{L}$  dH<sub>2</sub>O and 150  $\mu\text{L}$  perchloric acid and incubated at 160°C overnight in test tubes covered with glass marbles to prevent evaporation. 750  $\mu\text{L}$  dH<sub>2</sub>O was added to each tube, followed by 500  $\mu\text{L}$  0.9% ammonium molybdate and 150  $\mu\text{L}$  10% ascorbic acid, and the samples incubated at 45°C for 30 min. OD<sub>820</sub> readings were used to determine the amount of phosphorus incorporated into lipids.

## **2.22. Secretion of carboxypeptidase Y**

$2.5 \times 10^5$  stationary-phase cells were spotted on synthetic complete solid medium lacking uracil and containing either glucose or galactose, overlaid with nitrocellulose membranes and incubated for 35 h. Membranes were washed with



dH<sub>2</sub>O and extracellular CPY was detected by immunostaining with anti-CPY antibody (Molecular Probes).

### **2.23. Thin-section electron microscopy**

Fresh overnight cultures of yeast transformed with pEMBLyEX4 or pEMBL-NCR1 were grown in synthetic complete medium lacking uracil until log phase. Cells were diluted in synthetic complete galactose medium lacking uracil and incubated at 30°C for 18.5 h. For permanganate fixation, cells were washed with PBS, incubated in 10 volumes of 1.5% KMnO<sub>4</sub> for 20 min at 23°C, washed with PBS, incubated with 10 volumes of 1% sodium periodate for 15 min at 23°C, washed again with PBS and incubated with 1% NH<sub>4</sub>Cl for 10 min at 23°C and processed for electron microscopy (48).

### **2.24. Screen for mutants that are synthetic lethal with *ncr1Δ***

A colony-colour assay (9) based on adenine auxotrophy was used to identify *ncr1Δ* yeast that carried mutations rendering cells dependent on an *NCR1*-encoding plasmid for survival. The plasmid, pSLNCR1, was designed with a centromere sequence adjacent to a galactose-inducible promoter, so that plasmid loss could be enhanced by growing yeast containing the plasmid on galactose. The plasmid is

maintained under these conditions only when it is essential. The presence of an *ADE3* gene on the plasmid results in the *ade2 ade3* host yeast giving rise to red colonies, typical of an *ade2* mutant yeast. Absence of the plasmid results in the *ade2 ade3* yeast forming white colonies.

Yeast were mutagenized with either ~5000 µJ UV irradiation to ~50% survival, or by treatment with ethylmethanesulphonate (EMS) as described by Rose *et al.* (135). Plates were incubated for 7 days, to allow colour to develop in the colonies. For UV-irradiated cells, plates were kept dark to prevent photorepair. Derivatives that produced red colonies after three consecutive growths on YEP-galactose were retained.

## **2.25. Synthetic genetic array (SGA) analysis**

SGA analysis was conducted as described by Tong *et al.* (155), with the following differences. The query yeast strain (Y2454) was transformed with either pEMBLyEX4 or pEMBL-NCR1, mated to the complete viable yeast gene deletion set and pinned onto synthetic complete medium lacking uracil and containing G418 to select for the *URA3*-based plasmids to ensure that only diploids could grow. Plates were incubated for 2 days at 30°C. Diploids were sporulated and *MATa* haploid cells were selected on medium lacking histidine and arginine but containing canavanine, as described by Tong *et al.* (155). Haploids having the gene deletion being tested and

retaining the plasmid were selected in a subsequent step by pinning to synthetic defined medium lacking histidine, arginine and uracil but containing canavanine and G418, and incubation for 2 days. To screen for deletion mutants that exacerbate toxicity of *NCR1* overexpression, the strains were then pinned to synthetic defined medium lacking uracil with either glucose or galactose as the carbon source. To screen for deletion mutants that suppress toxicity of *NCR1* overexpression, the strains were first pinned from synthetic defined medium lacking uracil to synthetic defined medium lacking leucine. This step allowed time for cells to attain a higher copy number of the pEMBLyEX4 or pEMBL-NCR1 plasmids as compared to growth on medium lacking uracil. Due to the poor expression of the *leu2-d* allele on these plasmids, cells with higher copy number are favoured on medium lacking leucine (49). Plates were scored for growth after 4 days incubation at 30°C. Deletion mutations identified by the SGA analysis were tested by sequential streaking for single colonies on media and under conditions mimicking those used in the SGA screen.

## **2.26. Digital analysis of SGA plates**

Images of SGA plates were obtained using an Epson scanner. All digital manipulations of plate images were performed using Adobe Photoshop version 5.5. Yeast colonies were pseudo-coloured red for deletion mutants overexpressing *NCR1*

on galactose, blue for deletion mutants harbouring pEMBL-NCR1 and grown on glucose, and green for deletion mutants harbouring pEMBLyEX4 and grown on galactose. Images from different plating conditions were overlaid and merged to compare growth at each spot on the array.

### 3. Results

#### 3.1. *NCR1* is not an essential gene

The similarity of the *Saccharomyces cerevisiae* Ncr1 protein to human NPC1 (25) suggests that the function of the protein may be conserved. To determine the function of the Ncr1 protein, the growth of wild-type yeast (*NCR1*) was compared to that of yeast with a deletion of the *NCR1* gene (*ncr1Δ*). Yeast lacking *NCR1* were found to be indistinguishable from an otherwise isogenic wild-type *NCR1* strain under standard plating conditions (Fig. 4). This demonstrates that *NCR1* is not required for cell proliferation under normal laboratory conditions for the strain backgrounds used in this study. This finding is consistent with two recent studies that examined the consequences of *NCR1* deletion (98, 183).

#### 3.2. Loss of *NCR1* does not affect lipid metabolism

While *NCR1* deficiency does not affect viability of yeast, its loss might influence lipid metabolism, based on the lipid accumulation defects observed in mammalian NPC cells (85, 122, 153). To determine if lipid levels were affected by loss of *NCR1*, wild type *NCR1* and *ncr1Δ* yeast were radiolabeled with [<sup>14</sup>C]acetate. Acetate is incorporated into endogenous fatty acids, which subsequently acylate lipids, allowing the levels of phospholipids and neutral lipids to be analyzed.

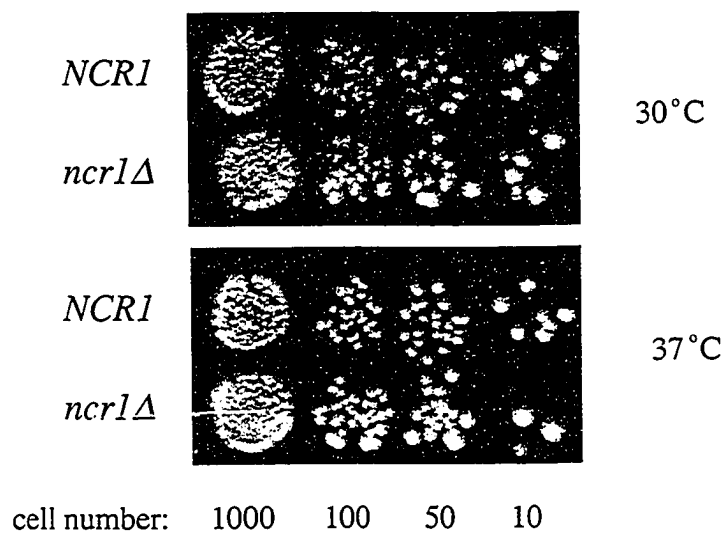


**Figure 4. Loss of *NCR1* has no effect on viability of yeast cells.** Yeast were grown in YEPD for 16 h, then spotted on YEPD solid medium and incubated at 30 °C or 37 °C, for 3 d. The number of cells in each spot is shown.

Metabolic and steady-state labeling of lipids are achieved following incubation with [ $^{14}\text{C}$ ]acetate for 1 h or 16 h, respectively. Since *ncr1* $\Delta$  yeast were previously demonstrated to have endocytic defects when grown at 37°C, possibly suggestive of a membrane perturbation at this elevated temperature (161), lipid metabolism was monitored at 37°C in addition to 30°C (Fig. 5).

Steady-state lipid profiles for *NCR1* and *ncr1* $\Delta$  yeast were the same, whether they were grown at 30°C or 37°C. The similarity of the steady-state lipid profiles extends recent results demonstrating that loss of *NCR1* does not alter sphingolipid metabolism (data not shown) (98) or sterol metabolism (98). Metabolic lipid profiles for *NCR1* and *ncr1* $\Delta$  yeast were also identical at 37°C. The lack of effect on lipid levels at 37°C suggests that altered lipid metabolism is not responsible for the delay in endocytic trafficking observed at 37°C (161). Yeast lacking *NCR1* incorporated significantly more [ $^{14}\text{C}$ ]acetate into diacylglycerol (DAG) after 1 h at 30°C but not at 37°C, but the significance of this observation was not investigated.

### **3.3. *NCR1* is not required for secretion of invertase**

In mammalian NPC cells both the efflux of a marker of fluid-phase endocytosis as well as sorting of the mannose-6-phosphate receptor are perturbed (81,

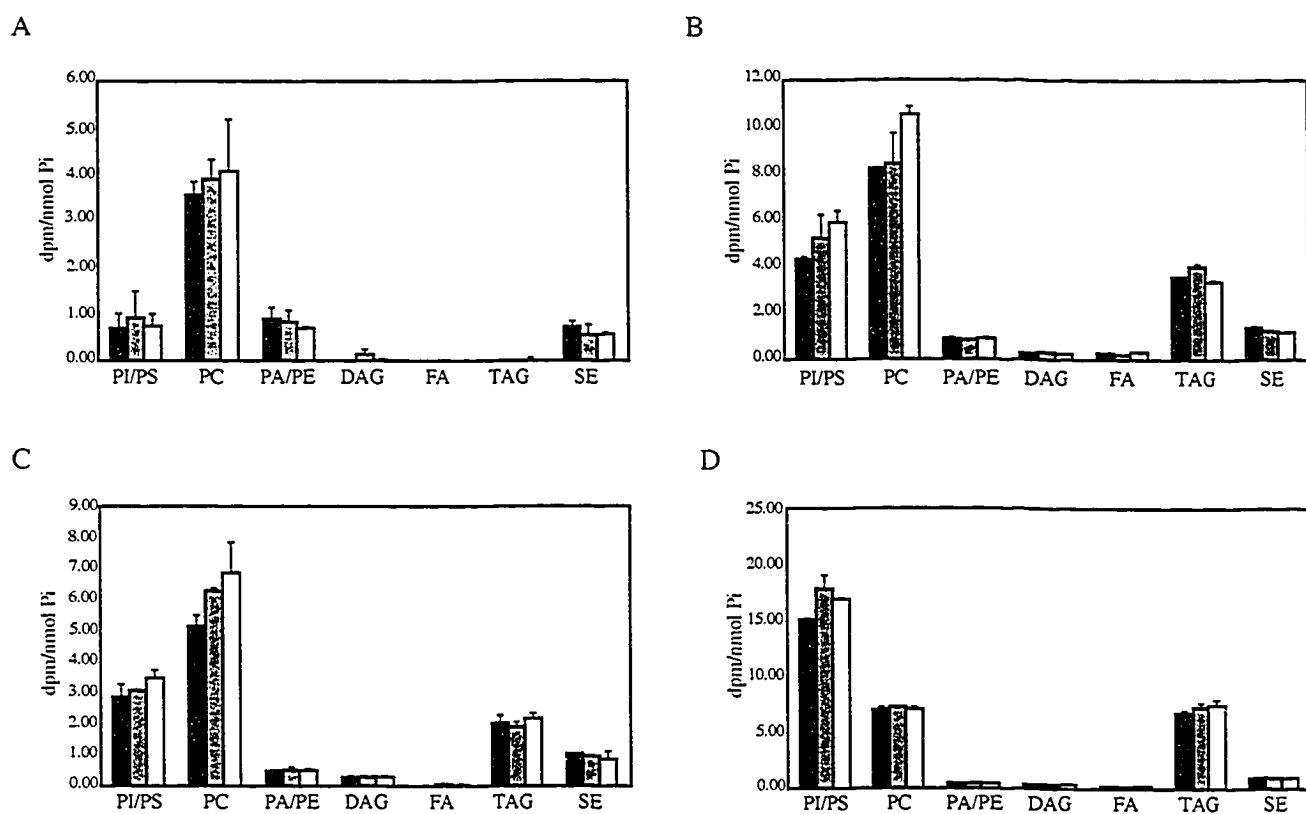


**Figure 5. Loss of *NCR1* does not affect metabolic or steady-state lipid metabolism at 30°C or 37°C.** *NCR1* yeast transformed with pRS313 (black) and *ncr1*Δ yeast transformed with pRS313 (grey) or pRSHISNCR1 (white) were labeled with [ $^{14}$ C]acetate at 30°C (A and B) or 37°C (C and D) for 1 h (A and C) or 16 h (B and D). Neutral and phospholipids were extracted, then separated by thin-layer chromatography. Lipids identified based on migration of standards were phosphatidylinositol/phosphatidylserine (PI/PS), phosphatidylcholine (PC), phosphatidic acid/phosphatidylethanolamine (PA/PE), diacylglycerol (DAG), fatty acids (FA), triacylglycerols (TAG), and sterol esters (SE). Results are the average  $\pm$  SD of 2 replicates.



110). To test whether intracellular trafficking is affected in *ncr1* $\Delta$  yeast, an invertase secretion assay was performed.

Invertase is a sucrose-cleaving enzyme that is secreted from yeast and maximally expressed when glucose levels are low (63, 154). Mutants blocked in the secretion pathway accumulate intracellular invertase (113). The ability of yeast cells to secrete invertase can be measured by a colorimetric assay that estimates the amount of glucose released from the hydrolysis of sucrose by invertase (56). After the derepression of invertase by incubation in 0.1% glucose, the ratio of external to total invertase activity was 90.5% for *NCR1* yeast and 99.4% for *ncr1* $\Delta$  yeast. In the same experiment, a ratio of 34.4% was obtained for a strain known to be defective for secretion (CTY1-1a) due to a temperature-sensitive mutation in the *SEC14* gene (8). Normal extracellular invertase activity in *ncr1* $\Delta$  yeast suggests that trafficking through intracellular compartments is not perturbed.

### **3.4. Ncr1 is not required for sorting of GPI-anchored proteins.**

While *NCR1* deficiency did not affect secretion of invertase, loss of *NCR1* could affect other intracellular trafficking events. In human NPC cells, cholesterol and sphingolipids accumulate (85, 122, 153). In eukaryotic cell membranes, sphingolipids and sterols are enriched in lipid domains termed rafts (144), and in

yeast, sterols and sphingolipids are required for the correct intracellular trafficking of raft-associated proteins (6, 167). One well-studied yeast protein localized in rafts is Gas1. Gas1 receives a glycosylphosphatidylinositol (GPI) moiety and is extensively glycosylated in the ER, forming an immature 105-kDa protein that partitions into sphingolipid-rich membrane domains (128). The immature protein is then packaged in COPII vesicles and transported to the Golgi, where it is further glycosylated, resulting in the mature 125-kDa form that is directed to the plasma membrane without subsequent modification (128). Yeast lacking *NCRI* are wild type with respect to sterol and sphingolipid metabolism (data not shown) (98). However, a dominant mutant form of *NCRI* has been found to cause complex sphingolipids to accumulate in the yeast vacuole, implicating Ncr1 in sphingolipid trafficking (98). To determine if trafficking of Gas1 is impeded in *ncr1Δ* cells, indicative of a perturbation in ER/Golgi sphingolipid or sterol levels, maturation of Gas1 was monitored at both 30°C and 37°C, since *ncr1Δ* endocytic defects are observed only at 37°C. Maturation of Gas1 was found to be indistinguishable in wild-type *NCRI* and *ncr1Δ* yeast at both 30°C (Fig. 6) and at 37°C (data not shown), suggesting that in *ncr1Δ* yeast the formation of nascent raft domains is normal, implying that sphingolipid and sterol levels are unaffected and balanced in ER and Golgi membranes.

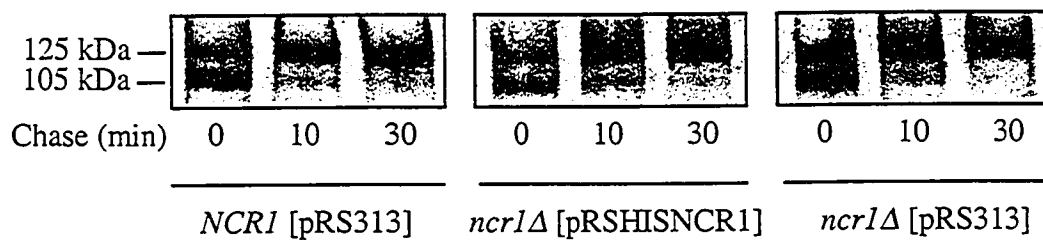


**Figure 6. Maturation of Gas1 is indistinguishable in *NCR1* and *ncr1Δ* yeast.** *NCR1* and *ncr1Δ* yeast transformed with either pRS313 or pRSHISNCR1 were labeled with [ $^{35}$ S]methionine and [ $^{35}$ S]cysteine for 10 min and chased for the indicated amount of time at 30°C. Gas1 was immunoprecipitated from total cell lysates, separated by SDS-PAGE and detected by autoradiography.

### 3.5. Effects of drugs or inhibitors

Sterol-ester formation was indistinguishable in *NCR1* and *ncr1Δ* yeast (Fig. 5), but if deletion of *NCR1* impacts sterol metabolism only slightly, this experiment may not have been sensitive enough to detect subtle differences between the two strains. Therefore, *NCR1* and *ncr1Δ* yeast were subjected to growth conditions known to influence sterol metabolism, to assess whether more subtle changes are produced by deletion of *NCR1*. Nystatin is a polyene antibiotic that interacts with ergosterol, the yeast equivalent of cholesterol, in the plasma membrane (14). Resistance or sensitivity to nystatin often reflects a decrease or increase in the plasma-membrane ergosterol content, respectively. *NCR1* and *ncr1Δ* yeast grown on nystatin-containing medium were indistinguishable, suggesting that loss of *NCR1* does not affect sterol levels in the plasma membrane (data not shown). Molecular oxygen is required for sterol synthesis (78), so under anaerobic conditions yeast are dependent on the uptake of exogenous sterol from the medium (57). Yeast lacking *NCR1* grew as well as their wild-type counterparts under anaerobic conditions (data not shown), suggesting that Ncr1 does not participate in sterol uptake.

To determine if the Ncr1 protein is involved in trafficking fatty acids, as has been hypothesized based on the ability of human NPC1, when expressed in *E. coli* cells, to transport oleic acid across the cell membrane (41), *NCR1* and *ncr1Δ* yeast

were grown on medium containing palmitic acid. The mutant grew as well as *NCR1* yeast (data not shown), indicating that an excess of this fatty acid did not perturb growth.

Although loss of *NCR1* did not seem to affect lipid metabolism, the secretory pathway, assembly of sterol-sphingolipid-rich membrane domains or viability under normal laboratory conditions, it was possible that a deleterious effect of *NCR1* deletion might only be observed under specific conditions. Therefore, *ncr1Δ* yeast were exposed to a range of agents that have previously been shown to impair various processes (63, 83). These included addition of caffeine, canavanine, oligomycin, ethanol, formamide, vanadate, DTT, divalent cations, nocodazole, benomyl, hydroxyurea, SDS, calcofluor white, sorbitol, glycerol and high concentrations of NaCl and KCl (Table 5). No differences in growth were observed under any of these conditions, suggesting that loss of *NCR1* does not impair signaling pathways, oxidative phosphorylation, protein folding or glycosylation, microtubule cytoskeleton formation, DNA synthesis, or cell membrane or wall assembly (Table 5). In addition to these conditions, *ncr1Δ* yeast were tested for the ability to recover from deep stationary phase and to use galactose, sucrose, acetate or glycerol instead of glucose as a carbon source. Under each of these conditions, *NCR1* and *ncr1Δ* yeast were indistinguishable (data not shown).

**Table 5. Cellular processes affected by chemical additions**

Chemical	Target	Reference
caffeine	phosphodiesterase	(63)
canavanine	arginine analog	(30)
oligomycin	oxidative phosphorylation	(159)
formamide	protein stability / hydrogen bonding	(63)
ethanol	protein stability / hydrogen bonding	(63)
DTT	protein disulfide bonds	(73)
sodium vanadate	protein glycosylation	(7)
nocodazole	microtubule polymerization	(127)
benomyl	microtubule depolymerization	(147)
SDS	cell membrane	(69)
hydroxyurea	DNA synthesis	(185)
calcofluor white	cell wall chitin	(133)
acetate	tricarboxylic acid cycle	(88)
divalent cations (LiCl <sub>2</sub> , ZnCl <sub>2</sub> , CdCl <sub>2</sub> )	ATPases or oxidoreductases	(63)
CaCl <sub>2</sub>	protein kinase C pathway	(111, 117)
	cell cycle	
high osmolarity (1 M sorbitol, 2 M glycerol, 0.9 M NaCl, 1 M KCl)	cell wall	(112)
	high osmolarity glycerol pathway	(21)

Finally, the effect of growth on suboptimal levels of amino acids or nucleoside bases was compared for *NCRI* and *ncr1Δ* yeast. When yeast are grown in rich medium, amino acids can be stored in the vacuole, to be subsequently released during nitrogen starvation (79). If Ncr1 alters vacuolar membrane composition, thus altering the conformation of an amino-acid or base permease, or otherwise regulates a permease, *ncr1Δ* yeast may be less able to mobilize amino acids from the vacuole. *NCRI* and *ncr1Δ* yeast were grown to stationary phase in rich medium, and were then grown on SD medium containing suboptimal levels of either uracil, histidine, tryptophan or leucine. Growth of both strains was indistinguishable under these conditions (data not shown) indicating that the amino-acid and base permeases are not impaired by loss of *NCRI*.

These experiments reveal that loss of *NCRI* is inconsequential to many cellular processes, and suggest that either *NCRI* is required under circumstances that have not yet been tested or there is complete functional overlap between the Ncr1 protein and other proteins.

### 3.6. *NCR1* expression is not induced by elevated temperature

Examination of the upstream untranslated region of *NCR1* revealed a single copy of the thermal stress-responsive element (*STRE*), CCCCT (80), 131 bp upstream of the translation initiation codon. While two copies of the C<sub>4</sub>T pentanucleotide in the promoter induce high levels of gene expression when yeast are exposed to elevated temperature, a single copy of the element can increase expression 2-3 fold (80). To test whether the *NCR1* promoter might only be activated when cells are subjected to high temperature, as might be expected by the presence of this element, yeast transformed with a plasmid containing the *lacZ* gene under the control of the *NCR1* promoter, pNCR1p-*lacZ*, were grown at 30°C and then shifted to 44°C.  $\beta$ -galactosidase expression from the *NCR1* promoter at 30°C was very low ( $\sim 1 \times 10^5$   $\beta$ -galactosidase units) and the expression level was unchanged at 44°C. This is in contrast to a reference promoter, the *CYC1* promoter, which when fused to the *lacZ* gene on plasmid pLG669-Z (61) expressed  $\beta$ -galactosidase to a much higher level ( $\sim 9 \times 10^5$   $\beta$ -galactosidase units). This indicates that at 30°C, the *NCR1* gene was expressed at only a low level and was not activated by growth at the elevated temperature of 44°C.



### **3.7. *NCR1* and *ncr1Δ* yeast have similar survival at high temperature, but *ncr1Δ* yeast produce fewer petites**

Although the *NCR1* promoter was not activated by exposure to heat stress, the presence of a *STRE* prompted us to determine if *NCR1* protects cells when they are exposed to thermal stress. To determine this, the viability of isogenic *NCR1* and *ncr1Δ* yeast was determined after exposure to 44°C (Fig. 7A). Wild-type *NCR1* yeast were more resistant than isogenic *ncr1Δ* yeast to challenge by high temperature. Upon inspection of the colonies arising from cells subjected to 44°C, it was noted that a larger proportion of the *NCR1* colonies were small and white, as opposed to large and red, than was observed for *ncr1Δ* yeast. Both strains contained the same mutant allele of *ADE2*, a gene in the adenine biosynthetic pathway that encodes phosphoribosylaminoimidazole carboxylase, responsible for catalyzing the conversion of the red intermediate P-ribosylaminoimidazole (AIR) to the colourless P-ribosylaminoimidazolecarboxylate (CAIR) (75). In *ade2* mutants, AIR accumulates and yeast give rise to pink or red colonies (158). The small colony size and colour suggested these were mitochondrial mutants, termed petites, and designated [ $\rho$ -], which do not accumulate the red pigment (27). Cells derived from the small white colonies were tested for the ability to grow on glycerol-containing medium and their inviability confirmed their identity as respiration-deficient petites

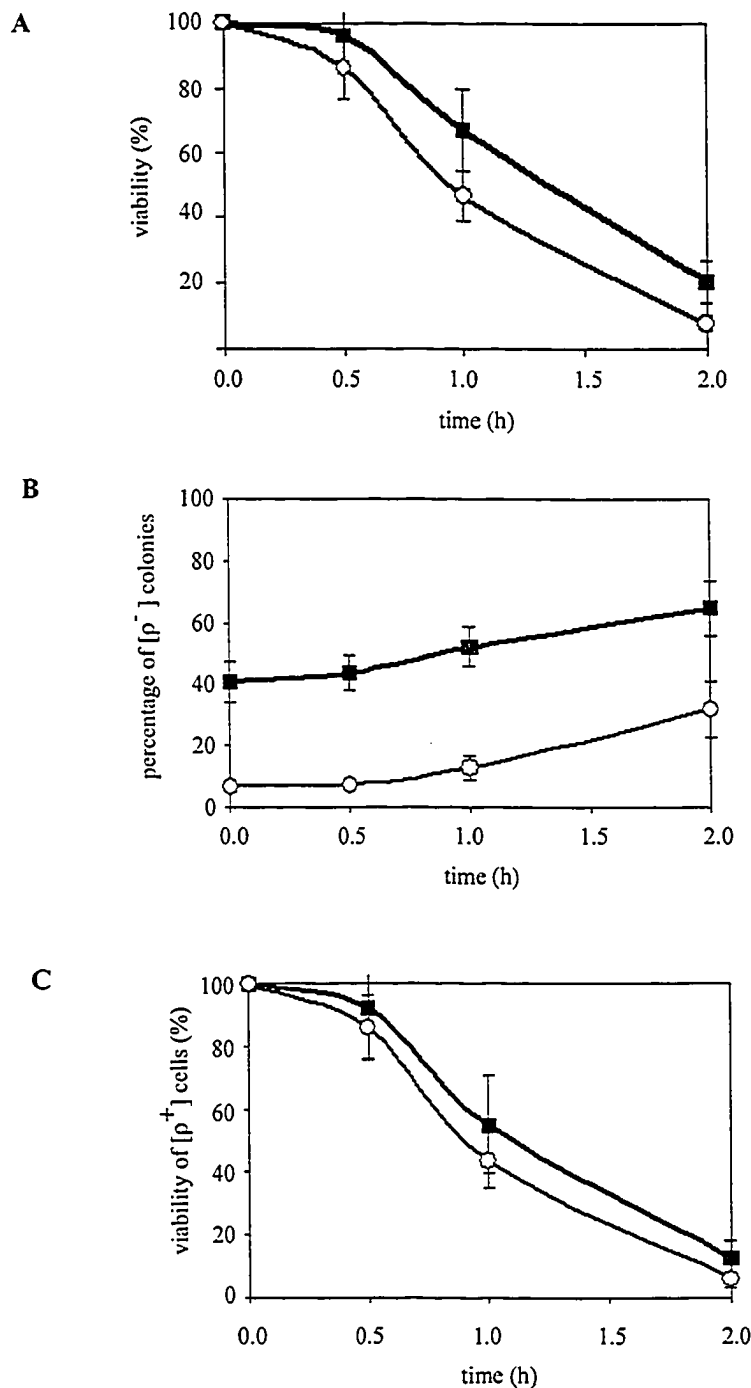


**Figure 7. Yeast lacking *NCR1* are more sensitive to thermal stress due to lower petite production.** Yeast grown at 30°C until log phase were incubated at 44°C for the indicated times and then plated on YEPD. (A) Survival of *NCR1* (closed squares) or *ncr1Δ* (open circles) yeast was determined as the percentage of colonies produced by heat-stressed relative to non-stressed cells. (B) The percentage of [%] colonies was determined by comparing the number of small white colonies to the total number of red and white colonies. (C) The relative survival of [%] cells was calculated by comparing the number of red colonies obtained with or without heat treatment. Results are from duplicate cultures of two independent isolates for *ncr1Δ* and four independent isolates for *NCR1* in 2 separate experiments. Small white colonies were assumed to be petite and were verified as such by replica-plating to YEP-glycerol to ensure they could not grow.

(data not shown). Since *NCR1* yeast produced a larger proportion of petite [ $\rho$ -] mutants than *ncr1* $\Delta$  yeast (Fig. 7B), it was possible that the higher percentage of petite cells in the *NCR1* population contributed to their thermal resistance. Ceramide and the complex sphingolipid M(IP)<sub>2</sub>C are slightly elevated in [ $\rho$ -] yeast (62) and would be expected to increase thermotolerance (45, 74, 172). The higher thermosensitivity of the *ncr1* $\Delta$  yeast relative to the *NCR1* yeast could be explained by the lower percentage of [ $\rho$ -] cells generated by the *ncr1* $\Delta$  yeast under these conditions. When exposed to thermal stress, the survival of only the non-petite *NCR1* and *ncr1* $\Delta$  cells was identical (Fig. 7C), indicating that yeast bearing functional mitochondria respond to high temperature identically, whether *NCR1* is present or absent.

### **3.8. Loss of *NCR1* does not inhibit petite production in response to exposure to ethidium bromide**

The lower rate of petite production by *ncr1* $\Delta$  yeast exposed to heat stress prompted us to compare the ability of cells lacking *NCR1* to generate petites when exposed to ethidium bromide, which promotes deletions within the mitochondrial genome (55, 63). *NCR1* and *ncr1* $\Delta$  yeast were grown on solid medium in which a well was filled with an ethidium bromide solution. The radii of growth of wild-type

and petite cells were determined (Fig. 8) and found to be identical for *NCR1* and *ncr1* $\Delta$  yeast, demonstrating that [ $\rho$ -] cells can be produced by *ncr1* $\Delta$  yeast.

### 3.9 Screen for mutants that are synthetic lethal with *ncr1* $\Delta$

The deletion of *NCR1* may not confer a discernable phenotype if another gene (or genes) can compensate for its loss. Identification of the putative compensating gene/genes provides another approach to determine the cellular function of *NCR1*. The identity of genes sharing functional overlap with a gene of interest can be revealed by screening for genes that, when mutated, are lethal only in a strain lacking the gene of interest. In this study, a synthetic-lethal genetic screen was undertaken to reveal genes that, when mutated, make the wild-type *NCR1* gene essential for viability.

The synthetic-lethal genetic screen employed in this study exploits a strain carrying two mutations in the adenine biosynthetic pathway, *ade2* and *ade3* (9). Yeast lacking *ADE2* accumulate a red pigment and give rise to red or pink colonies, as described above. The *ADE3* gene product catalyzes an earlier step in the adenine biosynthetic pathway than *ADE2*. Yeast containing mutations in *ADE3* are blocked at this earlier step in the pathway, do not accumulate the red AIR pigment and remain white (84). Transformation of the *ade2 ade3* yeast with a plasmid containing *ADE3* results in red colonies that become white if the plasmid is lost (84). In the present

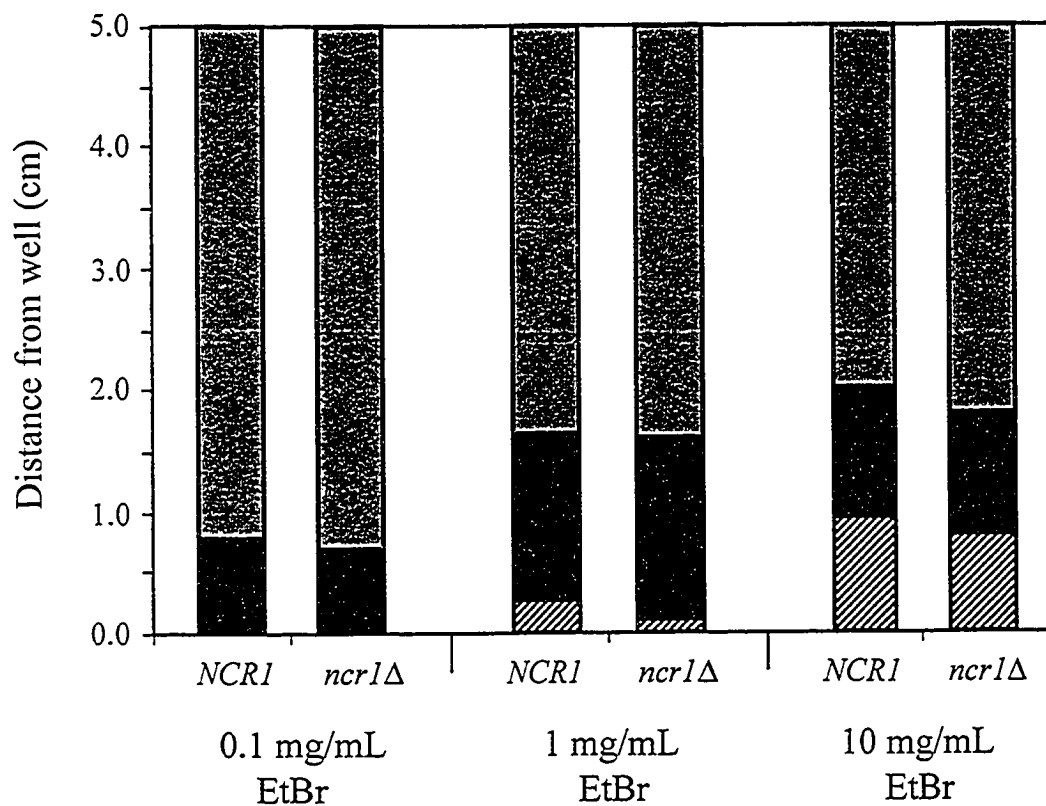


**Figure 8. Deletion of *NCR1* does not prevent production of petites in response to ethidium bromide.** Wells formed in YEPD solid medium on which *NCR1* and *ncr1Δ* yeast were spread were filled with ethidium bromide (EtBr) solutions. The plates were incubated at 30 °C for 7 d and the regions of inviability (hatched), [p<sup>-</sup>] colonies (black) and [p<sup>+</sup>] colonies (grey) were determined.

screen, yeast mutants retain the plasmid pSLNCR1 (a single-copy *ARS CEN* plasmid encoding wild type *NCR1* and the selectable marker *URA3*, in addition to containing the *ADE3* gene for colour) gave rise to red colonies and were thus identified. A unique feature of pSLNCR1 is the placement of the *GALI-10* promoter adjacent to the centromere sequence, *CEN*. Growth of transformed yeast on galactose activates transcription from the *GALI-10* promoter through the plasmid's centromere sequence, abolishing plasmid stability and thereby facilitating loss of the plasmid (9).

For the genetic screen, *ncr1Δ ura3 ade2 ade3* yeast were transformed with the single-copy pSLNCR1 plasmid and transformants were selected on the basis of uracil prototrophy. The transformants gave rise to red colonies due to the presence of the *ADE3* gene on pSLNCR1. These yeast were then mutagenized by UV irradiation or EMS treatment to introduce mutations throughout the genome and were plated on galactose to destabilize pSLNCR1. Mutants dependent on the plasmid-borne copy of *NCR1* for survival were identified based on their formation of red colonies, even after growth on galactose-containing medium which would reduce the mitotic stability of the *NCR1*-containing plasmid.

Mutants that were dependent on the plasmid for survival and that had a low frequency of reversion were identified by their inability to grow on medium containing 5-FOA. 5-FOA is converted to the cytotoxic 5-fluorouracil by the *URA3* gene product. In this screen, inclusion of 5-FOA is toxic to yeast that retain the

*URA3*-containing plasmid but allowed growth of *ura3* cells that had lost pSLNCR1.

All mutants were then backcrossed to *ncr1Δ* yeast to produce diploids heterozygous for the unknown mutated gene. The heterozygous diploids were tested for growth on medium supplemented with 5-FOA to determine whether new mutations were recessive or dominant. Twenty-seven robust recessive mutations were identified.

The mutants, which had been generated in yeast of both *a* and *α* mating types, were classified into complementation groups by mating all possible pairwise combinations to each other and by scoring the ability of mutant diploids to lose pSLNCR1 using medium containing 5-FOA. Haploid parents of the diploid were assumed to have a mutation in the same gene (the same complementation group) if the diploid they formed could not grow on 5-FOA. Six different complementation groups were identified, with three mutants unclassified because the phenotype proved unstable after long-term storage at  $-70^{\circ}\text{C}$ . In these latter cases, the instability may have arisen either because the original mutation began to revert at a high frequency or second-site suppressing mutations occurred.

Mutants that could not lose the *NCR1*-containing plasmid pSLNCR1 might reflect a requirement for any one of the three genes on the plasmid (*NCR1*, *URA3*, or *ADE3*), or a need for a combination of these genes. To identify those mutants that required pSLNCR1 for a gene other than *NCR1*, mutants were transformed with *LEU2*-based

plasmids that contained, respectively, the *URA3*, *ADE3* or *NCR1* genes, pRS315-*URA3*, pRS315-*ADE3*, or pRSNCR1-L. Transformants were selected on medium lacking leucine and tested for loss of pSLNCR1 as evidenced by growth on 5-FOA or by formation of red colonies on YEP-galactose. The majority (14 out of 27) of the mutants were able to lose pSLNCR1 if they were transformed with pRS315-*URA3*, indicating that they had maintained pSLNCR1 only because they required the *URA3* gene. Consistent with this hypothesis, one mutant that was able to lose pSLNCR1 when transformed with pRS315-*URA3* was also complemented by a *LEU2 CEN* library plasmid carrying the *FUR1* gene, encoding uracil phosphoribosyltransferase, an enzyme involved in pyrimidine salvage. Eight out of 27 mutants were complemented by plasmids encoding *ADE3*, suggesting that they were only dependent on *ADE3*, also present on pSLNCR1. None of the mutants were complemented by *NCR1* alone, indicating that none of the mutants were solely dependent on the presence of the *NCR1* gene on pSLNCR1. Despite this apparent lack of dependence on the *NCR1* gene, four mutants (33-13, 45-6b, 41-6 and 36-7) were not able to lose pSLNCR1 when they were transformed with either pRS315-*ADE3*, pRS315-*URA3* or pRSNCR1-L, suggesting they might require more than one of the genes present on pSLNCR1.

To identify the mutated gene in strains that could not lose the pSLNCR1 plasmid, the mutant yeast were transformed with a single-copy plasmid yeast genomic DNA



library and tested for loss of pSLNCR1 on YEP-galactose or 5-FOA. Mutants transformed with the library plasmid were subsequently tested for the ability to lose the library plasmid, to confirm that it was essential. Complementing library plasmids were rescued, inserts were fingerprinted by *Sau3A* digests and plasmids were retransformed into the mutant to ensure the rescued library plasmid allowed loss of pSLNCR1 on YEP-galactose or 5-FOA. Inserts were sequenced and complementing inserts, which contained 5-7 genes, were strategically deleted to identify the gene responsible for complementation. Finally, the single gene was subcloned and tested for its ability to render pSLNCR1 nonessential.

### **3.9.1. Characterization of synthetic-lethal mutant 33-13**

One of the mutants (33-13) not complemented by pRS315-ADE3, pRS315-URA3 or pRSNCR1-L, was transformed with the yeast genomic DNA library to identify the wild-type version of the mutated gene. After screening approximately 15,000 library plasmid transformants, two different plasmids were found to render pSLNCR1 nonessential in mutant 33-13. Sequencing revealed that the two inserts consisted of an overlapping region of *S. cerevisiae* chromosome VII, each encoding in entirety *YGL250w*, *ZIP2*, *PDE1* and *YGL247w*. Plasmids containing various deletions of this region were constructed and only those plasmids containing *YGL250w* were found to complement the 33-13 mutation. A plasmid encoding

*YGL250w*, pRSYGL250w, was created and tested for its ability to complement the other mutants identified in this screen. The 45-6b, 36-7 and 41-6 mutants were not complemented by pRSYGL250w, suggesting, as expected from their placement in different complementation groups from 33-13 and each other, that these represent mutations in different genes.

Complementation of the 33-13 mutation with the *YGL250w* gene would be expected if the mutation were within the *YGL250w* gene, but it could also result from suppression of a mutation in a different gene by the plasmid-borne copy of *YGL250w*. To determine if the 33-13 mutant yeast was indeed mutated at the *YGL250w* locus, a diploid heterozygous for deletions of the *YGL250w* and *NCR1* genes was created and tetrad analysis was performed. Out of 38 informative tetrads, 40 *ncr1Δ ygl250wΔ* double mutants were identified and all of them were viable (Fig. 9). The viability of the double mutants demonstrates that *ncr1Δ* and *ygl250wΔ* are not synthetically lethal when present in the same strain.

It was possible that only the particular point mutation in the *YGL250w* allele in 33-13 (*ygl250w-13*), but not complete deletion of *YGL250w* (*ygl250wΔ*), is synthetically lethal with *ncr1Δ*. To test this hypothesis, a linear DNA fragment encoding the 5' and 3' flanking sequences of *YGL250w* interrupted by the *LEU2* gene (*ygl250wΔ::LEU2*) was transformed into the 33-13 mutant. The *YGL250w* locus in

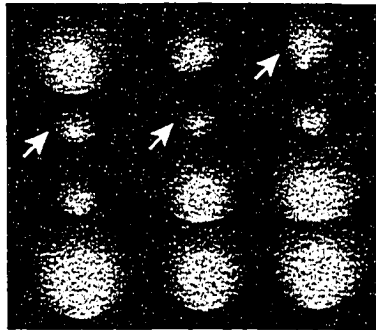


**Figure 9. The *ncr1Δ* and *ygl250wΔ* mutations are not synthetically lethal.**  
White arrows indicate viable *ncr1Δ ygl250wΔ* double mutants.

33-13 was therefore gene converted to *ygl250wΔ::LEU2*. This strain could not lose pSLNCR1 when plated on galactose, proving that *ygl250w-13* and *ncr1Δ* do not participate in a synthetic lethal interaction. Therefore, the plasmid-borne *YGL250w* may have been identified by its ability to suppress the synthetic lethal mutation in the 33-13 mutant, and may have precluded identification of plasmids that complemented this mutation.

### **3.9.2. Characterization of synthetic-lethal mutant 45-6b**

Synthetic lethal mutant 45-6b was not complemented by pRS315-URA3, pRS315-ADE3 or pRSNCR1-L, suggesting that the pSLNCR1 plasmid was not maintained in this strain for *URA3*, *ADE3* or *NCR1* alone. Because this mutant had a tendency to develop reversion or second-site suppressing mutations, the wild-type version of the mutated gene was cloned by complementation of a formamide-sensitive phenotype found to segregate with the 45-6b mutation. After screening ~92,000 yeast genomic DNA library transformants, one plasmid was found to permit growth on 3% formamide. This library plasmid, containing five complete genes, also allowed 45-6b mutants to lose pSLNCR1 on galactose. Transformation of different deletion plasmids created from this library plasmid revealed that *GFAI* complemented the formamide-sensitivity of 45-6b mutants and permitted loss of pSLNCR1.

*GFAI* encodes glutamine-fructose-6-phosphate amidotransferase, required for the first step in the biosynthesis of the cell-wall component chitin (171). Because *GFAI* is an essential gene, yeast deleted at both the *NCR1* and *GFAI* loci could not be created. To determine if these mutants were dependent on *NCR1* for growth, diploids heterozygous for deletion of *NCR1* were produced, by mating 45-6b with a strain wild-type for *NCR1* and *GFAI*. Diploids that could grow on 5-FOA because they had lost pSLNCR1 were sporulated, producing two live spores to two dead or ungerminated spores, suggesting that the putative *gfa1-45* mutation does not promote germination after sporulation (Fig. 10A). To establish the dependence of this mutant on *NCR1* for survival, the heterozygous diploids were transformed with the low-copy *URA3*-marked plasmid pRS316 and with pRSNCR1, which encodes *NCR1*. When diploids transformed with pRS316 were sporulated, most tetrads (33 out of 35) resulted in only two live (or germination-competent) progeny, but a minority (one out of 35) gave rise to two large colonies, one small colony and one dead or ungerminated spore, or two large colonies and two small colonies (two out of 35 tetrads) (Fig. 10B). Two percent of total spores resulted in small colonies and suggests that the *URA3* gene on pRS316 contributed slightly to the viability of these spores. Diploids transformed with pRSNCR1 also gave rise to some tetrads (17 out of 36) consisting of two live and two dead or ungerminated progeny. However, a higher proportion, compared to the pRS316 transformants, gave rise to a small

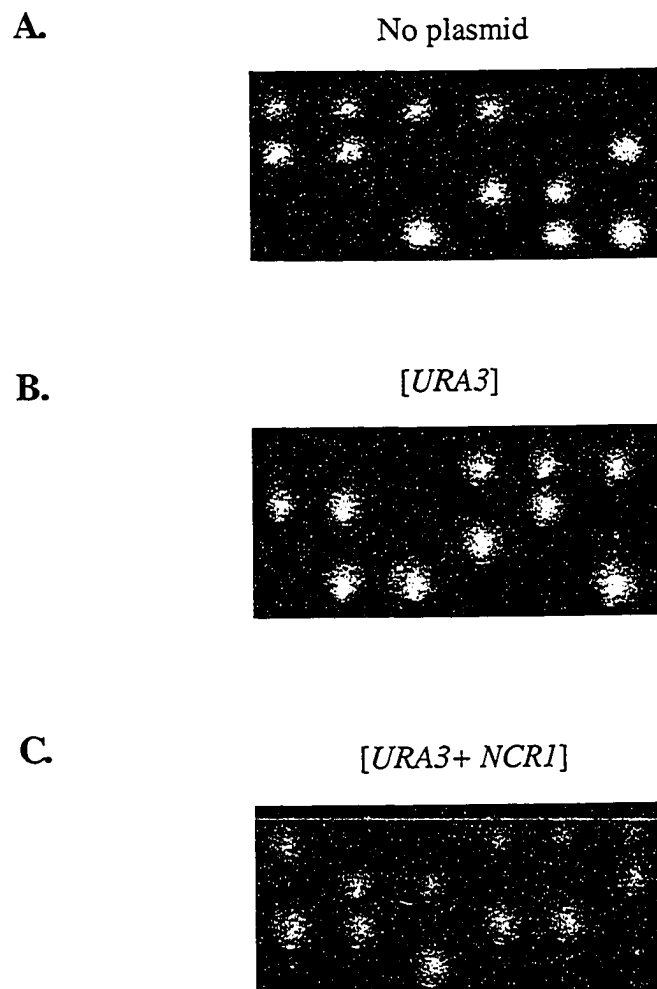


**Figure 10. Viability of presumptive *gfa1-45* spores is improved with plasmid encoding *NCR1* and *URA3*.** Diploids heterozygous for *NCR1* (*NCR1/ncr1Δ*) and *GFA1* (*GFA1/gfa1-45*) were sporulated before (A) and after transformation with (B) the single-copy *URA3* plasmid pRS316, or (C) the single-copy plasmid pRSNCR1 encoding *URA3* and *NCR1*. Tetrads were dissected on YEPD medium and incubated at 30°C for 5 d.

colony, and when a small colony was formed, it was generally bigger than those produced by pRS316-transformed diploids (Fig. 10C). In total, 16% of spores gave rise to small colonies. This suggests that the presence of the *NCR1* gene on the *URA3*-based plasmid improved the germination and enhanced the survival of the presumptive *gfa1-45* mutant spores. However, viability of these spores was not linked to the genomic *NCR1* gene: half of these spores were *NCR1* and half were *ncr1Δ*. Because *URA3* alone improved viability and *NCR1* combined with uracil prototrophy contributed even more to the viability of these spores, it suggests that *NCR1* and *URA3* deliver additive effects promoting colony formation. This was our first indication that phenotypes of *ncr1Δ* yeast may be influenced by nutritional status. Subsequently, the endocytic delay of *ncr1Δ* yeast was found to be improved if yeast were uracil or histidine prototrophs (161). This synthetic lethal screen is based on the assumption that the nutritional markers present on pSLNCR1 do not impact the identification of synthetic lethal genetic interactions. However, we had established that the nutritional status of *ncr1Δ* yeast was not neutral. This may explain why a mutation dependent solely on *NCR1* was not identified by this screen. Interestingly, we have performed a synthetic genetic array high-throughput screen to reveal gene deletions synthetic-lethal with *ncr1Δ* and none were identified (M. Dobson, personal communication). This suggests that a single gene might not exist that, when mutated,

renders *NCR1* essential, under normal laboratory growth conditions. It may be necessary to create multiple mutants to observe synthetic lethal interactions with *NCR1*.

### **3.10. Overexpression of wild type *NCR1* is toxic**

The lack of *ncr1Δ*-specific phenotypes, despite thorough investigation, and the inability to identify genes with functional overlap with *NCR1* via synthetic-lethal genetic screens, led us to probe the function of the *NCR1* gene by studying the effects of its overexpression. Overexpression of human NPC1 in Chinese hamster ovary cells disrupts cholesterol trafficking, leading to increased delivery of LDL-derived cholesterol to the ER and endosomal cholesterol to the plasma membrane (104). To assess whether *NCR1* overexpression confers any effect on yeast, the *NCR1* ORF was cloned adjacent to a *GAL1-10* promoter on a high-copy vector, pEMBLyEX4, producing pEMBL-NCR1, where *NCR1* is expressed only when cells harbouring the plasmid are grown on galactose. pEMBLyEX4 and pEMBL-NCR1 encode two selectable markers, *URA3* and an allele of *LEU2*, *leu2-d*. The *leu2-d* allele lacks most of the promoter, so this gene produces only ~5% of the wild-type *LEU2* gene product (49). Plasmids based on pEMBLyEX4 can be maintained at high copy number in *ura3* mutant yeast grown on medium lacking uracil and a 4-5 fold higher



copy number can be achieved in *leu2* mutant yeast grown on medium lacking leucine (49).

To examine the expression of *NCR1*, polyclonal antibodies recognizing the cysteine-rich loop of Ncr1 were raised in rabbits. These antibodies detect an ~115-kDa protein in total protein extracts from wild-type *NCR1*, but not from *ncr1Δ* yeast (Fig. 11). To determine the extent of overexpression of *NCR1* from pEMBL-NCR1, total proteins were extracted from *NCR1* yeast transformed with the empty vector, pEMBLyEX4, the high-copy *NCR1* plasmid, pEMBL-NCR1, and the single-copy *NCR1* plasmid pRSNCR1, and Ncr1 protein was detected by Western blotting (Fig. 11). A single band of ~115 kDa was observed in proteins extracted from yeast transformed with pEMBLyEX4 and was considered to be the steady-state level of Ncr1 protein expressed from the genomic *NCR1* gene. This signal doubled in intensity when yeast were transformed with the single-copy pRSNCR1 plasmid, consistent with the expected 2-fold increase in copy number of the gene. The intensity of this band increased dramatically when yeast transformed with pEMBL-NCR1 were grown on galactose, indicating that the protein is indeed overexpressed from this plasmid. Ncr1 levels for this transformant grown on glucose were indistinguishable from the level observed for yeast transformed with pEMBLyEX4 empty vector grown on galactose or glucose (data not shown), indicating that

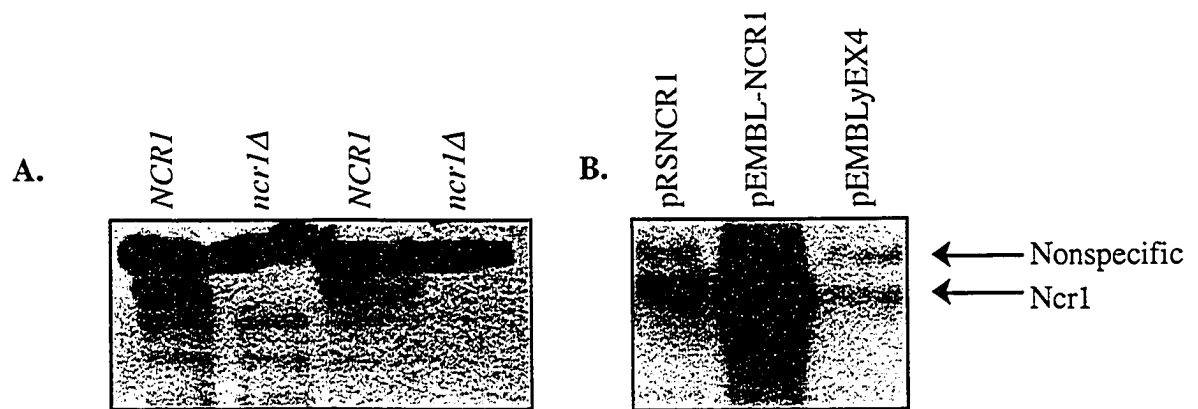


**Figure 11. Ncr1 is overexpressed from plasmid pEMBL-NCR1 on galactose.** Total protein was isolated from (A) isogenic *ncr1Δ* and wild type *NCR1* yeast grown in YEPD and (B) *NCR1* yeast transformed with pRSNCR1, pEMBLyEX4 or pEMBL-NCR1 and grown in synthetic complete galactose medium lacking uracil for 24 h. Proteins were separated by SDS-PAGE and analyzed by Western blotting using a polyclonal antibody raised against the cysteine-rich loop domain of Ncr1.

expression of *NCR1* from the *GAL1-10* promoter on pEMBL-NCR1 when cells are grown on glucose is negligible, as expected.

The consequence of *NCR1* overexpression was tested by growing yeast transformed with pEMBLyEX4 or pEMBL-NCR1 on synthetic complete medium lacking uracil or on synthetic defined medium lacking uracil or lacking leucine, to selectively grow yeast harbouring an increased copy number of the plasmid. The media contained either glucose, to repress, or galactose, to induce expression of *NCR1* from the *GAL1-10* promoter on pEMBL-NCR1 (Fig. 12). Yeast containing pEMBL-NCR1 grew slightly less well than empty-vector control cells on synthetic complete medium lacking uracil and containing galactose (Fig. 12D). The extent of toxicity of *NCR1* overexpression could be increased if yeast were grown in synthetic defined medium lacking leucine, to select for increased copy number of pEMBL-NCR1, prior to growth on synthetic complete galactose medium lacking uracil (Fig. 12C). Yeast containing pEMBL-NCR1 grew very poorly when *NCR1* was overexpressed on synthetic defined medium lacking uracil and containing galactose (Fig. 12B). The same yeast did not grow at all on synthetic defined medium lacking leucine to select for cells with an increased copy number of pEMBL-NCR1, and containing galactose to induce expression of *NCR1* (Fig. 12A). These findings indicate that overexpression of *NCR1* is deleterious to yeast, and the degree of toxicity is dependent upon the medium on which these yeast are grown.

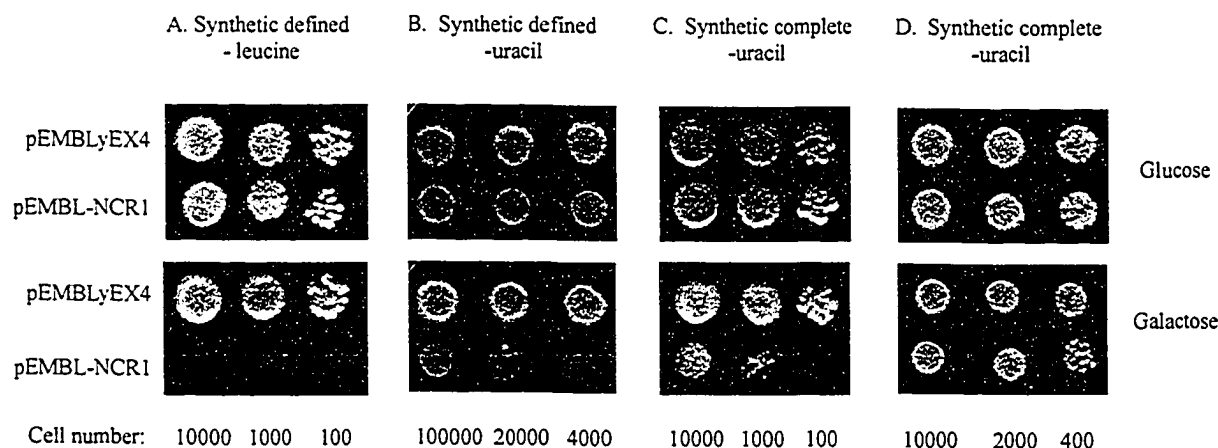


**Figure 12. Overexpression of *NCR1* is deleterious, but degree of toxicity is dependent on growth medium.** Wild-type *NCR1* yeast transformed with pEMBLyEX4 or pEMBL-NCR1 were grown to saturation (A) in synthetic defined medium lacking leucine (SD-Leu), spotted on SD-Leu or SD(galactose)-Leu and incubated at 30 °C for 7 d , or (B) in synthetic defined medium lacking uracil (SD-Ura) and spotted on SD-Ura or SD(galactose)-Ura and incubated at 30 °C for 7 d, or (C) in SD-Leu, spotted on synthetic complete medium lacking uracil (SC-Ura) or SC(galactose-Ura) and incubated at 30 °C for 5 d, or (D) in SC-Ura, spotted on SC-Ura or SC(galactose)-Ura and incubated at 30 °C for 3 d. The number of cells plated are indicated.

Synthetic defined and complete media differ in the concentrations and numbers of the amino acid and vitamin supplements they contain. In synthetic defined medium, specific concentrations of amino acids are present, while hydrolyzed casein satisfies these requirements in synthetic complete medium. Nucleoside bases such as uracil and adenine are added separately to both and therefore do not differ between the two. Viability of yeast overexpressing *NCR1* from pEMBL-NCR1 in synthetic defined galactose medium lacking uracil was found to be dramatically improved by the addition of leucine to the medium (M. Dobson, personal communication). A suboptimal level of leucine in synthetic defined medium lacking uracil may have selected for cells with a higher copy number of the pEMBL-NCR1 plasmid, which contains the poorly expressed *leu2-d* gene, inadvertently leading to a higher copy number of the plasmid than on synthetic complete medium lacking uracil. The greater loss of viability could reflect the higher expression of Ncr1 from increased plasmid levels in these cells, or because these yeast were contending with insufficient leucine in addition to excessive Ncr1, with each factor contributing to loss of viability.

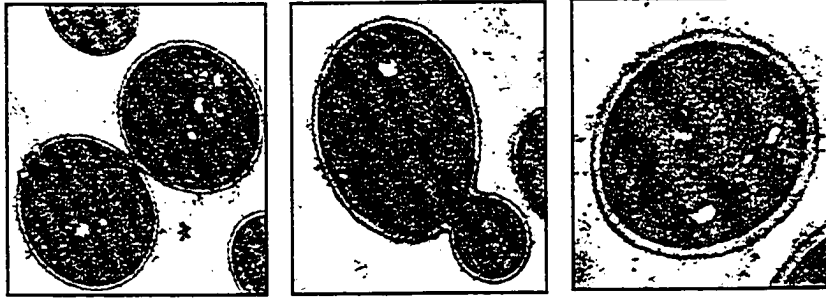
To examine whether overexpression of *NCR1* caused gross ultrastructural aberrations to the cell, electron microscopy was performed. Cells transformed with pEMBLyEX4 or pEMBL-NCR1 were grown to log phase in synthetic complete medium lacking uracil, then shifted to the same medium containing galactose to

induce expression of *NCR1*. Cells overexpressing *NCR1* looked identical to the cells harbouring empty vector with respect to bud morphology, thickness of the cell wall and basic cellular ultrastructure (Fig. 13). This is consistent with the robust growth of cells containing pEMBL-NCR1 on synthetic complete galactose medium lacking uracil (Fig. 12D).

### **3.11. $\text{CaCl}_2$ and sorbitol partially alleviate toxicity of *NCR1* overexpression**

To determine why excess *NCR1* is deleterious, various conditions were tested for the ability to alleviate this toxicity. Wild-type yeast transformed with pEMBLyEX4 or pEMBL-NCR1 were grown on medium containing galactose, to induce overexpression, and in the presence of different salts or sorbitol, to determine if these additives would influence the toxicity of *NCR1* overexpression. The presence of  $\text{MgCl}_2$ ,  $\text{MgSO}_4$  or  $\text{ZnCl}_2$  had no effect on viability. Cells grown on glucose were slightly inhibited by 10  $\mu\text{g/mL}$   $\text{CdCl}_2$ , so the inability of *NCR1*-overexpressing cells to grow under these conditions could be due to an additive effect with  $\text{Cd}^{2+}$  toxicity. However, this slight inhibition seems insufficient to explain the lack of growth for the most concentrated spot on galactose (Fig. 14). To be certain, the experiment would have to be repeated, exposing cells to a lower concentration of  $\text{CdCl}_2$  that does not compromise wild-type yeast. The toxicity of *NCR1* overexpression was partially suppressed by the addition of 100 mM  $\text{CaCl}_2$ , 1 M sorbitol or by incubation at 37°C.

A.



B.



**Figure 13. Overexpression of *NCR1* does not affect cell ultrastructure.** Electron micrographs of yeast transformed with pEMBLyEX4 (A) or pEMBL-NCR1 (B) are indistinguishable after growth for 18.5 h in synthetic complete medium lacking uracil and containing galactose to induce overexpression of *NCR1*.

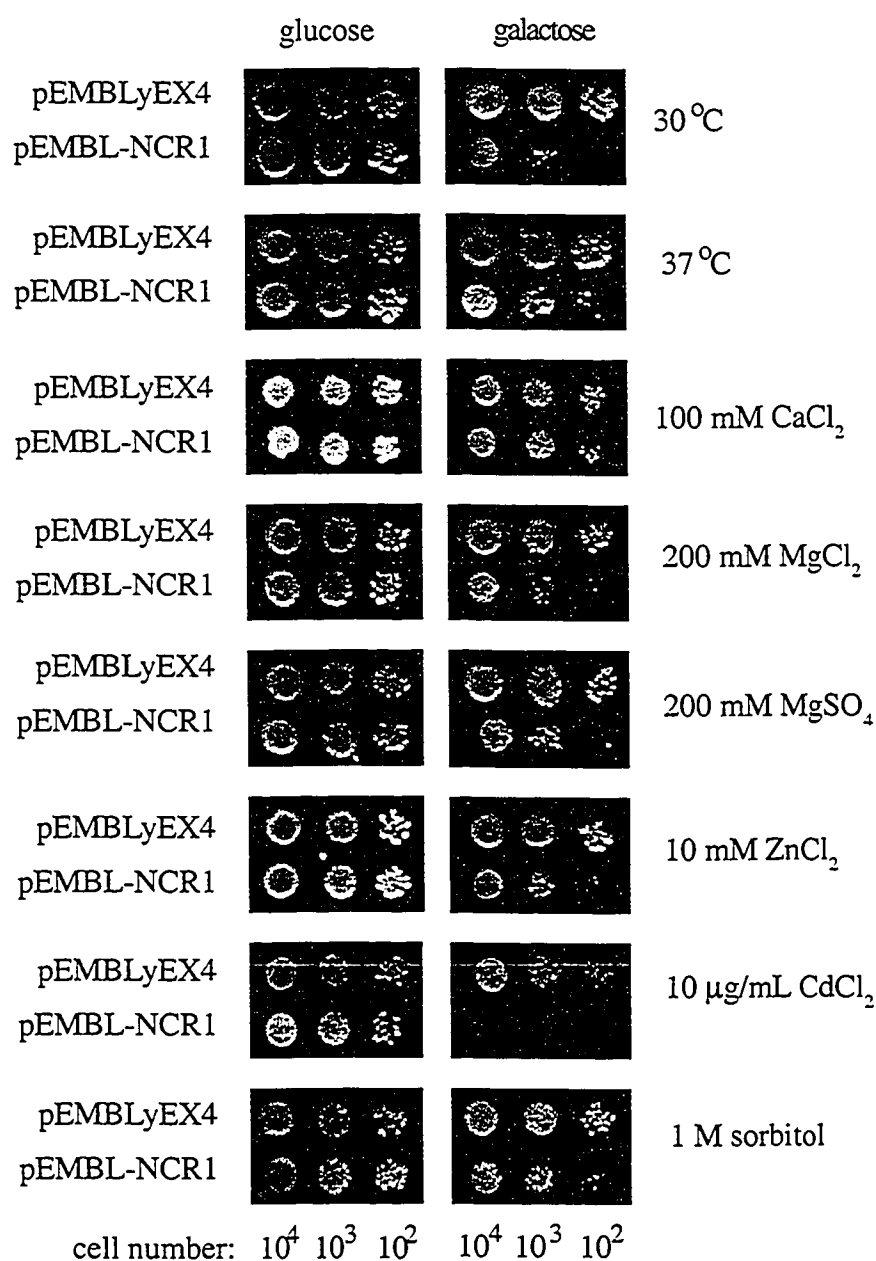


**Figure 14. CaCl<sub>2</sub> and sorbitol partially suppress, while CdCl<sub>2</sub> enhances, toxicity of *NCR1* overexpression.** Wild-type *NCR1* yeast transformed with pEMBLyEX4 or pEMBL-NCR1 were grown in synthetic defined medium lacking leucine (SD-Leu) to saturation, spotted on SC-Ura or SC(galactose)-Ura with the indicated additives and incubated at 30°C or 37°C for 5 days. The number of cells spotted is indicated.



Since 1 M sorbitol did not entirely rescue yeast from the toxicity of *NCR1* overexpression, this toxicity cannot be completely explained by increased fragility of the cells.

### **3.12. Screen for high-copy suppressors of *NCR1*-overexpression toxicity**

The toxicity observed when *NCR1* is overexpressed was exploited as the basis of a dosage-suppressor genetic screen. This screen would reveal the identity of genes whose products oppose the function of the Ncr1 protein, based on their ability to relieve the toxicity of excess Ncr1.

To produce the maximal level of *NCR1* expression, the suppression screen was performed on medium lacking leucine to maintain the pEMBL-NCR1 plasmid at a high copy number. The *URA3* gene on pEMBL-NCR1 was marker-swapped to *HIS3* (38) to enable selection for *URA3*-based high-copy yeast genomic DNA library plasmids in cells maintaining the *NCR1*-overexpression plasmid. Prior to the dosage-suppressor screen, overexpression of *NCR1* from the *HIS3*-marked pEMBL-NCR1 (pEMBL-NCR1-HIS), was tested and found to be equally toxic as from the pEMBL-NCR1 when transformed yeast were grown on synthetic defined medium containing galactose and lacking leucine (data not shown).

Yeast containing pEMBL-NCR1-HIS were transformed with a high-copy yeast genomic DNA library, grown on glucose and replica-plated to galactose to induce

expression of *NCR1*. Library plasmids that allowed cells to survive *NCR1* overexpression on synthetic defined medium lacking leucine were identified. Transformants that could grow under these conditions were then plated on medium that allowed them to lose the library plasmid while retaining pEMBL-NCR1-HIS. These strains, having lost the library plasmid, were retested for inviability on galactose medium lacking leucine to verify that the library plasmid was responsible for viability when *NCR1* was overexpressed.

Ninety out of 160 transformants identified in the primary screen were found to have become histidine auxotrophs once they lost the library plasmid, either because the library plasmid taken up encoded *LEU2*, or the genomic *leu2* allele had converted to wild-type *LEU2*, presumably by gene conversion with the *leu2-d* allele on pEMBL-NCR1-HIS. In either case, once the strain had become leucine prototrophic, it was able to lose the pEMBL-NCR1-HIS plasmid so the strain could no longer grow on medium lacking histidine. These were expected false positives from the screen.

Of the remaining 70 transformants, 25 were unable to grow on medium allowing overexpression of *NCR1* from pEMBL-NCR1-HIS once they had lost the library plasmid. This indicated that the library plasmid was responsible for suppression of *NCR1*-overexpression toxicity. The 25 library plasmids were rescued from yeast, amplified in *E. coli*, and after rechecking their ability to relieve the effects of *NCR1* overexpression, four were sequenced.

The first two inserts were found to encode chimeric Dengue virus vector sequences encoding the *ter<sup>R</sup>* gene, unfortunately not the first incidence of contaminating DNA arising from this library (T. Wong, personal communication). The third insert consisted of sequences from *S. cerevisiae* chromosome VII, encompassing the *MIG1* gene. The fourth insert consisted of sequences from *S. cerevisiae* chromosome XIII containing the *GAL80* gene.

Both *MIG1* and *GAL80* are genes that would be predicted to decrease *NCR1* overexpression from the *GALI-10* promoter on pEMBL-NCR1-HIS if they were present in high copy, due to their known roles in repressing expression from the *GALI-10* promoter (103, 134). These two genes represent a class of nonspecific suppressors that we expected to obtain in this screen, and validate this approach. Unfortunately, genes that specifically suppressed the toxicity of *NCR1* overexpression were not identified. The yeast genomic library may not have been representative of the entire yeast genome so that despite screening an adequate number of transformants, an authentic suppressor was missed. Alternatively, no single gene may exist that can specifically suppress the toxicity of *NCR1* overexpression.

### 3.13. Synthetic Genetic Array analysis to identify *NCR1* genetic interactions

Another approach taken to define genes that participate in similar or opposing pathways to *NCR1* was to identify genes that, when deleted, make yeast resistant or hypersensitive to *NCR1* overexpression, respectively. Synthetic genetic array (SGA) analyses were performed to identify these genetic interactions. The yeast genome consists of ~6000 genes, only about one-sixth of which are essential (176). The screens utilized a collection of the approximately 4,700 nonessential gene-deletion yeast strains, where each strain is precisely deleted at a particular locus. The genes are replaced with a *kanMX4* gene, facilitating selection of gene replacements by growth on medium containing G418. This collection was arrayed on solid medium such that the location of each strain in the array was known.

In this study, both screens were initiated identically. The query strain, Y2454, was transformed with either empty vector, pEMBLyEX4, or pEMBL-NCR1 and was robotically mated to each deletion strain in the Yeast Gene Deletion Set. Diploids were selected on synthetic complete medium lacking uracil and containing G418. Diploids were sporulated and *MATa* haploid meiotic progeny, deleted at each locus, were selected as previously described (155). Finally, these cells were pinned to medium that selected for the pEMBLyEX4 or pEMBL-NCR1 plasmid, while maintaining selection for *MATa* haploids carrying a gene deletion.

### 3.13.1. SGA screen for suppressors of *NCR1* overexpression toxicity

Overexpression of *NCR1* from pEMBL-NCR1 is severely toxic when yeast are grown on synthetic defined medium lacking leucine, to ensure maintenance of the plasmid at a maximal copy number (Fig. 12A). This phenotype was exploited in the screen for gene deletions that rescue cells from the effects of overexpression of *NCR1*. The *MATa* gene-deletion haploids containing pEMBLyEX4 or pEMBL-NCR1 were pinned to medium lacking leucine, to ensure each strain harboured plasmids at a high copy number. Strains were then grown on medium lacking leucine but containing galactose, to induce expression of *NCR1* from pEMBL-NCR1. Yeast mutants that were able to grow on the galactose medium lacking leucine represented presumptive suppressors and were repinned to the same medium, allowing the strains to grow for several generations on galactose before scoring. Colonies derived from each presumptive suppressor strain containing pEMBL-NCR1 were compared with the same deletion mutant, grown on the same medium, but harbouring empty vector. This eliminated deletion mutants that grew more robustly than the majority of the strains on galactose even when *NCR1* was not overexpressed.

Strains with enhanced viability compared to the background colonies were selected as strains possibly resistant to the toxicity of *NCR1* overexpression. After three SGA iterations, each initiated with an independent isolate of Y2454 transformed with pEMBL-NCR1, a list of two hundred and six putative suppressors was compiled.

Presumptive suppressors were isolated from medium selecting for *MATa* haploids containing both a gene deletion and either plasmid. Their viability was retested on synthetic defined medium containing galactose and lacking leucine, by streaking or by serial dilutions (Fig. 15). Strains that were viable after streaking on the galactose plates, i.e. *loc1Δ*, were identified as strong suppressors of *NCRI* overexpression (Fig. 15A, Table 6). Suppression status of strains that grew, albeit poorly, on the galactose plates was confirmed by a more sensitive method, serial dilutions (Fig. 15B). Deletion of *CIT1* and *PAT1*, among others, permitted growth when *NCRI* was overexpressed. These analyses resulted in fifteen strong suppressors and forty-eight putative weaker suppressors.

The majority of the suppressors have unknown cellular functions, but other categories that were well-represented included metabolism, cell growth, transport, and transcription/translation. A link between these seemingly discrete cellular functions was obscure, and the significance of these interactions is not obvious. Therefore, we concentrated on gene-deletion mutants identified in the second SGA screen, the gene deletions that exaggerated the toxicity of *NCRI* overexpression.

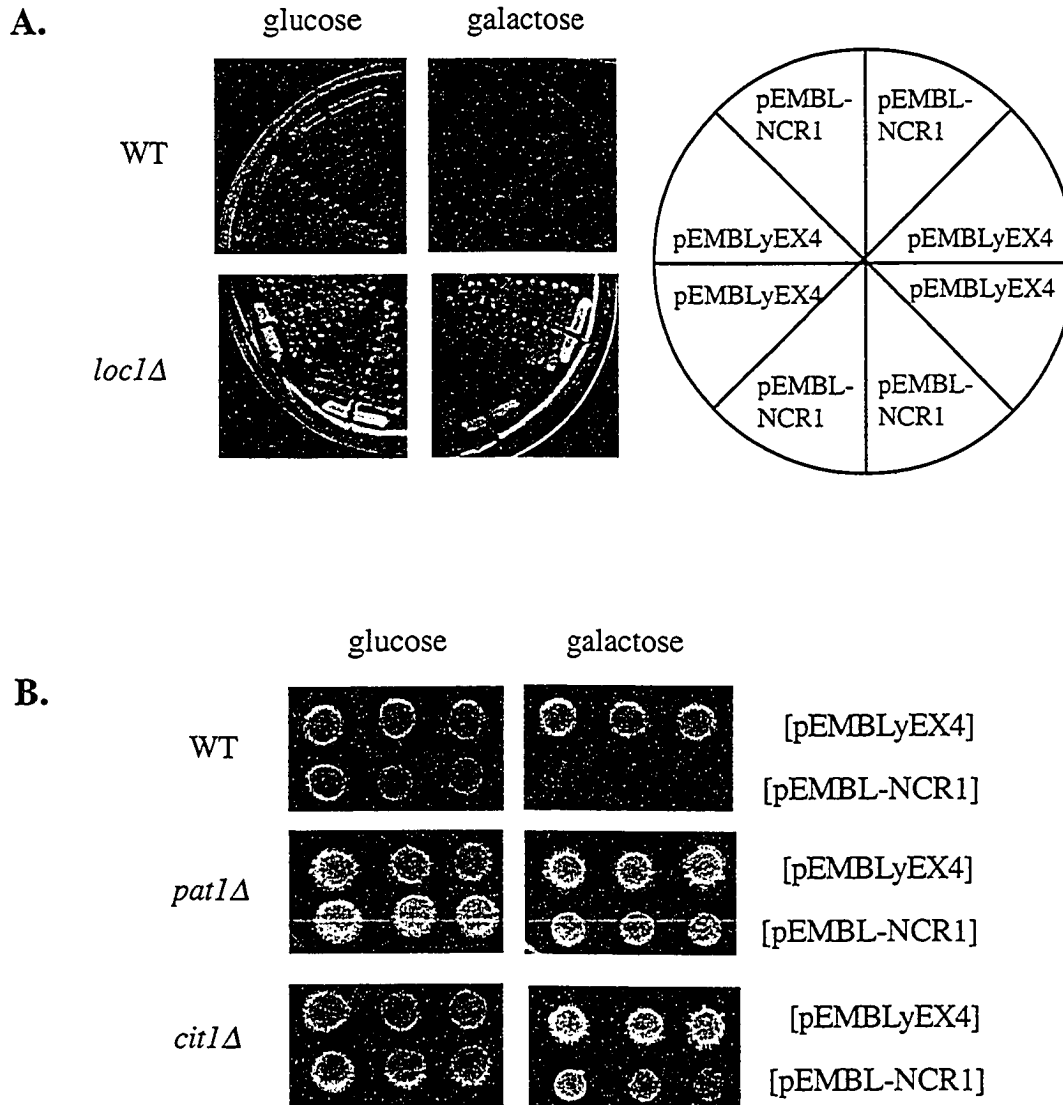


**Figure 15. Yeast gene deletions suppress the toxicity of *NCR1* overexpression.** (A) Transformed *MATa* haploid yeast strains with the indicated gene deletions were grown on solid synthetic defined glucose medium lacking leucine to select for increased dosage of pEMBLyEX4 and pEMBL-NCR1 and then streaked to isolate single colonies on synthetic defined medium lacking leucine and containing either glucose or galactose. The plates were incubated at 30°C for 7 d. Strong suppressors were identified as those deletion strains that permitted growth when *NCR1* was overexpressed on galactose. (B) *MATa* haploid deletion mutants harbouring either pEMBLyEX4 or pEMBL-NCR1 were grown for 2 d at 30°C in medium selecting for *MATa* haploid yeast strains carrying a gene deletion and either plasmid. The cultures were 4-fold serially diluted with dH<sub>2</sub>O and spotted on synthetic defined medium lacking leucine and containing glucose or galactose, beginning with 1x10<sup>6</sup> cells. Plates were incubated at 30°C for 7 d. Weak suppressors were identified as those deletion strains that permitted more growth than wild-type strains when *NCR1* was overexpressed on galactose.

**Table 6. Deletion suppressors of *NCR1*- overexpression toxicity**

<b>Gene</b>	<b>Function or gene product<sup>a</sup></b>
<b>Strong suppressors</b>	
<i>DAL7</i>	Malate synthase, degrades allantoin
<i>GAL3</i>	Involved in galactose induction of <i>GAL</i> genes
<i>GAL4</i>	Positive regulator of <i>GAL</i> genes
<i>LOC1</i>	Localization of mRNA
<i>NHP10</i>	Non-histone protein involved in nucleosome mobilization
<i>QDR1</i>	Multidrug resistance transporter, drug:H <sup>+</sup> antiporter
<i>RPL20b</i>	Protein component of the large (60S) ribosomal subunit
<i>RPS6b</i>	Protein component of small (40S) ribosomal subunit
<i>RTN2</i>	Member of reticulon family
<i>SXM1</i>	Nuclear import of mRNA-binding proteins
<i>XRS2</i>	DNA-repair protein
<i>YDR094w</i>	Unknown
<i>YOR315w</i>	Unknown
<i>YPL144w</i>	Unknown
<i>YPR059c</i>	Unknown
<b>Weak Suppressors</b>	
<i>BEM4</i>	Bud-emergence protein
<i>BUD9</i>	Required for bipolar budding
<i>CBP1</i>	Protein required for cytochrome b mRNA stability
<i>CCS1</i>	Copper chaperone for superoxide dismutase
<i>CIT1</i>	Citrate synthase
<i>DAL5</i>	Allantoin permease
<i>ESC2</i>	Protein involved in mating-type locus silencing
<i>GPH1</i>	Glycogen phosphorylase
<i>GPX2</i>	Glutathione peroxidase
<i>HLR1</i>	Protein involved in cell-wall composition and integrity
<i>HTA1</i>	Histone H2A
<i>IES5</i>	Associates with <i>INO80</i> chromatin remodeling complex
<i>MOG1</i>	Required for nuclear-protein import
<i>MPA43</i>	Unknown
<i>PAT1</i>	Protein associated with topoisomerase II



**Table 6. (Cont'd) Deletion suppressors of *NCR1* overexpression toxicity**

<i>PDR15</i>	Putative multidrug-resistance transporter
<i>PRM4</i>	Pheromone-regulated protein
<i>RCE1</i>	Protease involved in ras and a-factor terminal proteolysis
<i>RPL11Bb</i>	Protein component of the large ribosomal subunit
<i>SAC3</i>	Nuclear export of mRNA
<i>SMF1</i>	Manganese ion transporter
<i>SMF3</i>	Metal-ion transporter activity
<i>SWC1</i>	May establish boundaries of heterochromatin
<i>SWC2</i>	May establish boundaries of heterochromatin
<i>TMT1</i>	Trans-aconitate methyltransferase 1
<i>TNA1</i>	Transporter of nicotinic acid
<i>TOS6</i>	Unknown
<i>UAF30</i>	Component of Upstream Activation Factor complex
<i>UBC4</i>	Ubiquitin conjugating enzyme
<i>VID28</i>	Involved in degradation of fructose-1,6-bisphosphatase
<i>YAR1</i>	Involved in 40S ribosome biogenesis
<i>YBR225w</i>	Unknown
<i>YCR087w</i>	Unknown
<i>YDJ1</i>	ER and mitochondrial protein import
<i>YDR061w</i>	Mitochondrial ABC transporter activity
<i>YDR109c</i>	Unknown, kinase activity
<i>YDR198c</i>	Unknown
<i>YDR249c</i>	Unknown
<i>YDR391c</i>	Unknown
<i>YGL081w</i>	Member of Forkhead Associated Domain family
<i>YHL012w</i>	UTP-glucose-1-phosphate uridylyltransferase
<i>YML087c</i>	Contains oxidoreductase FAD-binding domain
<i>YML122c</i>	Unknown
<i>YMR258c</i>	Unknown
<i>YOR318c</i>	Unknown
<i>YPL030w</i>	Unknown
<i>YPL247c</i>	Unknown

<sup>a</sup> Function was assigned by the Yeast Proteome Database

### 3.13.2. SGA analysis to reveal genes that contribute to survival when *NCR1* is overexpressed

As an alternative approach to understand *NCR1* function, a second SGA analysis was undertaken to identify deletion mutants that are hypersensitive to overexpression of *NCR1*. The functions of the genes identified in this screen would be expected to oppose Ncr1 function and therefore contribute to survival when *NCR1* is overexpressed. Conversely, deletion of these genes would render cells intolerant to excess Ncr1 protein.

As with the SGA analysis described above, *MATa* haploid deletion strains containing pEMBLyEX4 or pEMBL-NCR1 were created by mating and sporulation, but instead of testing viability on medium lacking leucine, they were pinned to synthetic defined medium lacking uracil and containing galactose. Under these conditions, expression of the *NCR1* gene from pEMBL-NCR1 inhibits growth of wild-type yeast, but to a lesser extent than on medium lacking leucine (Fig. 12B). Gene deletions that specifically prevent the strain from growing when *NCR1* was overexpressed were expected to be a subset of those that impaired growth on the galactose medium lacking uracil. The other genes identified by this approach would include some that were unrelated to *NCR1* function, for example genes required for the use of galactose as a carbon source. To identify these, growth of each gene-deletion mutant harbouring pEMBL-NCR1 was compared to growth on the same

medium of the corresponding mutant but harbouring empty vector, pEMBLyEX4. If the strain containing empty vector could not grow on galactose, it demonstrated that the inviability was not due to a genetic interaction with *NCR1* and was due instead to galactose auxotrophy. In addition, the growth on galactose of each deletion mutant harbouring pEMBL-NCR1 was compared to the growth that had been observed on glucose prior to transfer to galactose. This comparison allowed identification of false positives, where inviability on the galactose medium was due to lower sporulation or germination efficiency, at earlier steps in the analysis (155). Gene-deletion mutants were scored as synthetic-lethal or sick with *NCR1* overexpression only if they grew under all conditions when transformed with empty vector and either failed to grow or grew poorly when transformed with the *NCR1*-overexpressing plasmid on synthetic defined galactose medium lacking uracil. Rapid identification of yeast deletion strains that were compromised only when *NCR1* was overexpressed was facilitated by digitally modifying scanned images of the plated arrays and overlaying the images (Fig. 16).

Upon completion of three SGA screens, each initiated with an independent isolate of Y2454 transformed with pEMBL-NCR1, thirty-one deletion mutants were identified on the basis of hypersensitivity to *NCR1* overexpression. These mutants were obtained from the Euroscarf collection and directly transformed with either pEMBLyEX4 or pEMBL-NCR1. Cell viability assays were performed to verify that,

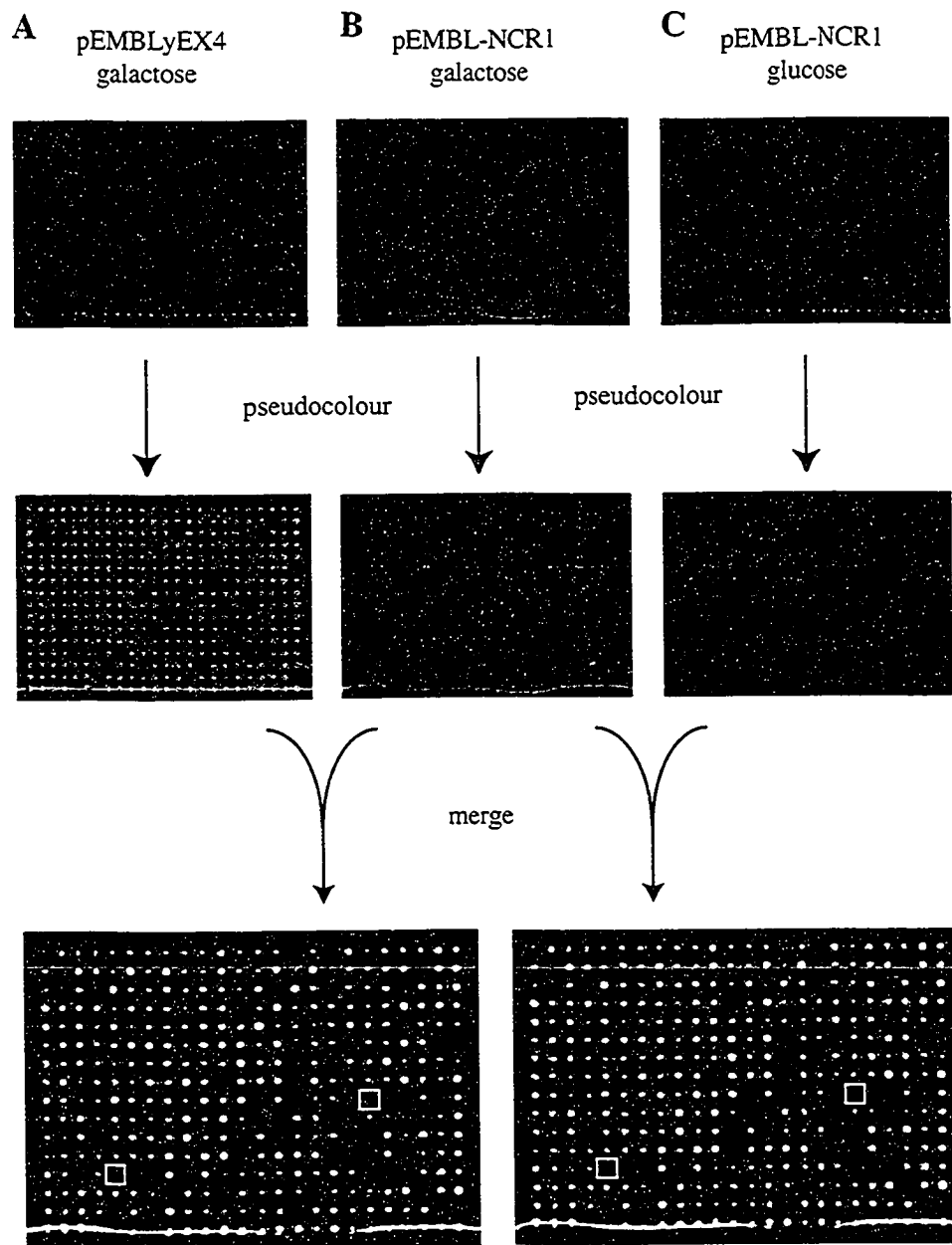


**Figure 16. Digital modification of SGA robot plates facilitates screening.** Haploid yeast carrying a gene deletion and either pEMBLyEX4 (A) or pEMBL-NCR1 (B and C) were pinned to synthetic defined medium lacking uracil and containing either glucose (C) or galactose (A and B). Colonies were pseudocoloured green (A) red (B) or blue (C) and merged with each other to facilitate identification of yeast gene-deletion strains that cannot grow in (B) because they are galactose auxotrophic (yellow box), due to decreased efficiency of sporulation or germination (white box), or because they cannot cope with the toxicity of *NCR1* overexpression (red box).

as observed in the SGA analysis where plasmids had been introduced into mutant cells by mating and sporulation, these deletions rendered cells more sensitive to overexpression of *NCRI* (Fig. 17). Fourteen genes were confirmed by this direct testing as contributing to survival when *NCRI* is overexpressed (Table 7). These genes may participate in pathways or cellular processes that oppose *NCRI* function (Table 7).

A quarter of the genes identified (*BEM1*, *BCK1* and *CHS5*) are directly involved in delivery of materials to polarized-growth sites. Polar growth is the asymmetric delivery of substrates to a distinct cellular location. *S. cerevisiae* displays polarized growth during budding, mating and pseudohyphal growth. During cell division, secretion is directed to the emerging bud. High concentrations of secretory vesicles can be visualized in small buds (97). During this process, the actin cytoskeleton becomes highly polarized and materials required for new wall assembly at the bud site are deposited at actin patches (97). Chitin, a polymer of N-acetylglucosamine and a constituent of the cell wall, is specifically localized at the incipient bud site in unbudded cells and later in the neck that separates mother from daughter cells (97). Another period of polarized growth occurs when yeast cells mate. During mating, yeast produce a mating pheromone. Upon detection of pheromone produced by a cell of the opposite mating type, the cell becomes deformed as growth is initiated in the direction of the mating partner, and a mating

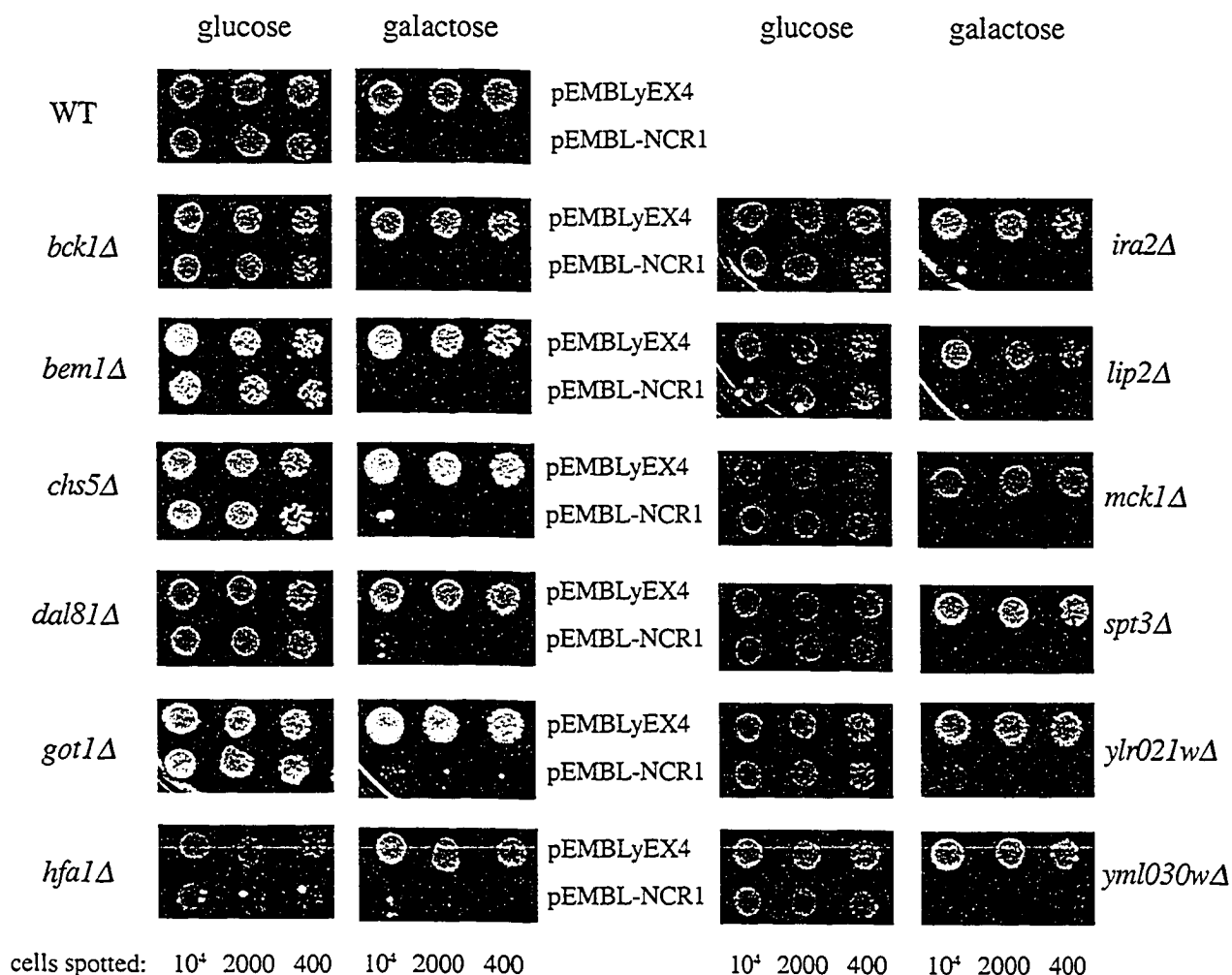


**Figure 17. Deletion mutations render cells hypersensitive to overexpression of *NCR1*.**

Yeast containing pEMBLyEX4 or pEMBL-NCR1 were grown in SD medium lacking uracil to saturation. Five-fold serial dilutions of cells were spotted on SD medium lacking uracil and containing glucose or galactose and were grown for 7 d. Two independent transformants were tested for each deletion mutant. The identity of each deleted gene was confirmed by PCR.

**Table 7. Genes that contribute to survival when *NCR1* is overexpressed**

<b>Gene</b>	<b>Function or gene product<sup>a</sup></b>
<b>Cell growth and intracellular trafficking</b>	
<i>BCK1</i>	MAP kinase kinase kinase in cell-wall integrity pathway
<i>BEM1</i>	Required for cell polarization and bud formation
<i>CHS5</i>	Required for polarized localization of chitin synthase III
<i>GOT1</i>	Required for ER to Golgi transport
<i>MCK1</i>	Member of the GSK3 subfamily of protein kinases
<b>Metabolism</b>	
<i>DAL81</i>	Transcription factor
<i>HFA1</i>	Mitochondrial acetyl-CoA carboxylase
<i>LIP2</i>	Protein with similarity to <i>E. coli</i> lipoic acid ligase
<b>Other</b>	
<i>IRA2</i>	GTPase-activating protein for Ras1 and Ras2
<i>SPT3</i>	Member of the nucleosomal histone acetyltransferase complex SAGA
<i>YLR021<sub>w</sub></i>	Possibly required for full induction of <i>IME1</i>
<i>YML030<sub>w</sub></i>	Possibly involved in mitochondrial function

<sup>a</sup> Function was assigned by the Yeast Proteome Database

projection emerges (97). Many proteins required for budding are also essential for mating (97). Since loss of genes required for polarized growth exacerbates toxicity of *NCR1* overexpression, excess Ncr1 may result in enhanced flow of materials away from sites of polarized growth.

The product of one of the genes identified in this screen, *BCK1*, is a component of a signal-transduction pathway in yeast, the protein kinase C (PKC)/cell-wall integrity pathway. Signal-transduction pathways are triggered by proteins at the cell surface that respond to the environment by initiating a cascade of protein phosphorylations that ultimately activate the expression of genes required to protect the cell from damage. In response to high temperature or low osmolarity, Pkc1 phosphorylates, and thereby activates, Bck1 (64). Bck1 then phosphorylates Mkk1 and Mkk2, which in turn phosphorylate the mitogen-activated protein (MAP) kinase Slt2 (64). Phosphorylated Slt2 activates transcription factors that induce expression of cell-wall biosynthetic genes, including *FKS1*, *FKS2*, *MNN1* and *CHS3*, which encodes chitin synthase (64). It was striking that *BCK1* was identified in this screen in isolation from other members of the PKC pathway. Tong *et al.* (156) have estimated the frequency of false negatives in an SGA screen to be 17-41%. To determine if other members of the PKC pathway were false negatives in this screen, yeast deleted for different components of the PKC pathway were transformed with pEMBLyEX4 and pEMBL-NCR1 and viability was tested on synthetic defined



galactose medium lacking uracil. Cells lacking *SLT2* were found to be intolerant to excess *NCR1*, indicating that *BCK1* is not the only member of this pathway that participates in a genetic interaction with *NCR1* (Fig. 18).

It is unsurprising that *mkk1Δ* and *mkk2Δ* cells survived *NCR1* overexpression, as they comprise an essential gene pair, with one wild-type gene compensating for loss of the other (64). The other gene deletions that were inconsequential in combination with *NCR1* overexpression included *sac7Δ* and *rlm1Δ*. Sac7 is a GTPase-activating factor for Rho1 (a G protein that activates Pkc1), while Rlm1 is a transcription factor that is activated in response to phosphorylation of Slr2 (64).

The inviability of *bck1Δ* cells overexpressing *NCR1* may reflect excessive flux through a pathway that opposes the PKC pathway. To determine if the reciprocal genetic interaction existed, *NCR1* and *ncr1Δ* yeast were transformed with the single-copy *LEU2*-marked plasmid pRS315 or with pGAL-BCK1-20, that encodes a constitutively activated allele of *BCK1*, *BCK1-20*, under the control of a galactose-inducible promoter (44). Cell viability was tested on synthetic defined medium lacking leucine or the same medium containing galactose (Fig. 19). Overexpression of activated *BCK1* impairs growth of *NCR1* cells, but deletion of *NCR1* did not exacerbate this toxicity. This may suggest that *NCR1* does not oppose

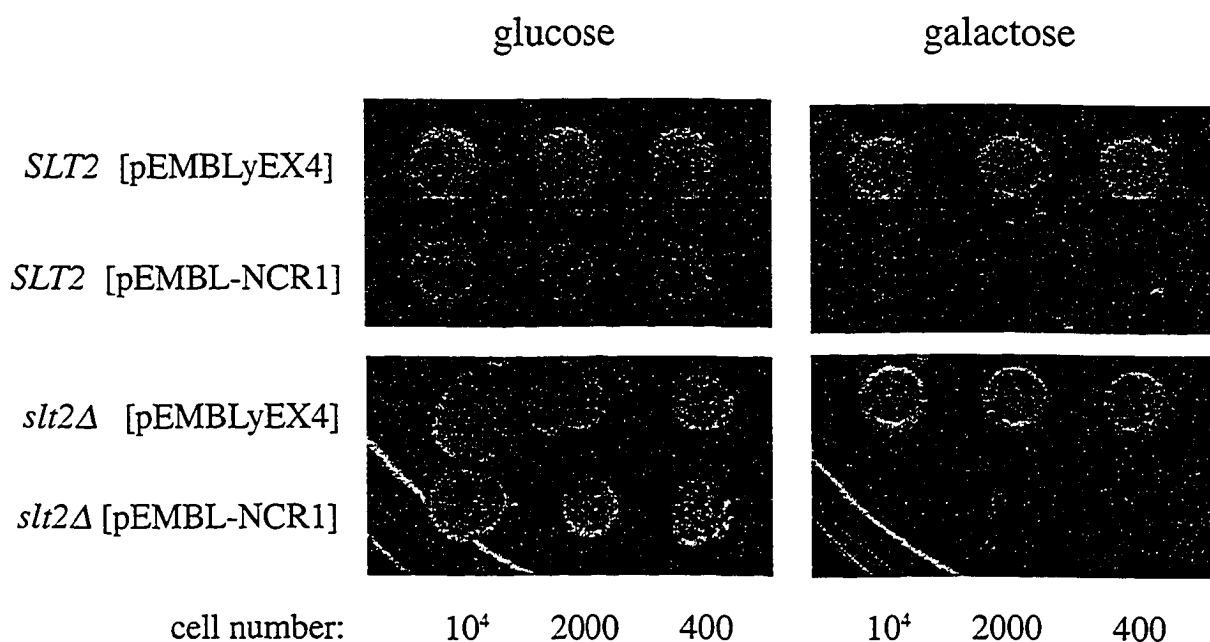


**Figure 18. *slt2Δ* cells are hypersensitive to excess *NCR1*.** Isogenic *SLT2* or *slt2Δ* cells transformed with pEMBLyEX4 or pEMBL-NCR1 were grown to stationary phase in synthetic defined medium lacking uracil. Cells were 5-fold serially diluted and equal numbers of cells, beginning with 10<sup>4</sup> cells, were deposited on synthetic defined medium lacking uracil and containing glucose or galactose and incubated at 30° C for 7 days.

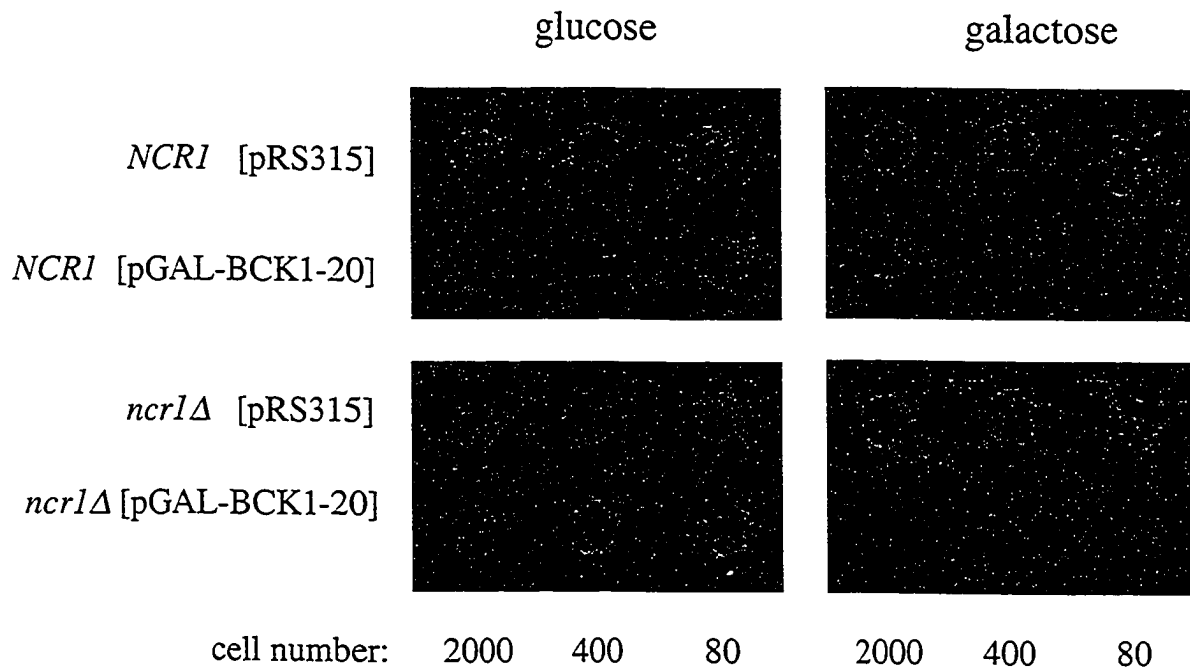


**Figure 19. *ncr1Δ* cells are not hypersensitive to excess *BCK1-20*.**

Isogenic *NCRI* or *ncr1Δ* cells transformed with pRS315 or pGAL-BCK1-20 were grown to stationary phase in synthetic defined medium lacking leucine. Cells were 5-fold serially diluted and equal numbers of cells, beginning with 2000 cells, were deposited on synthetic defined medium lacking leucine and containing glucose or galactose and incubated at 28°C for 3 days.

flux through the *BCK1* pathway. Alternatively, *NCR1* may contribute only slightly to an opposing pathway, such that the effects of its loss in this context are undetectable.

### **3.14. Loss of *NHX1* impairs cells overexpressing *NCR1***

The *NHX1* gene was found to contribute to survival when *NCR1* is overexpressed. Deletion of *NHX1* exacerbated toxicity of *NCR1* overexpression in only one of three SGA screens, but this phenotype was found to be reproducible when directly tested. The *nhx1* $\Delta$  mutations differed from the other enhancers in that it was deleterious only when cells were induced to overexpress *NCR1* on synthetic complete, but not on synthetic defined medium (Fig. 20). This conditional phenotype may have prevented the *nhx1* $\Delta$  mutant from being consistently identified in all three screens, which were performed on synthetic defined medium.

The genetic interaction between *NCR1* and *NHX1* was confirmed by tetrad analysis. Wild-type cells harbouring pEMBL-NCR1 were mated to *nhx1* $\Delta$  cells and the diploids were sporulated. Haploid segregants were tested for growth on synthetic complete medium lacking uracil and containing galactose to induce expression of *NCR1* from the plasmid. All *nhx1* $\Delta$  meiotic progeny overexpressing *NCR1* on galactose grew more poorly than either *nhx1* $\Delta$  cells transformed with empty vector or *NHX1* segregants transformed with either plasmid (data not shown). The genetic

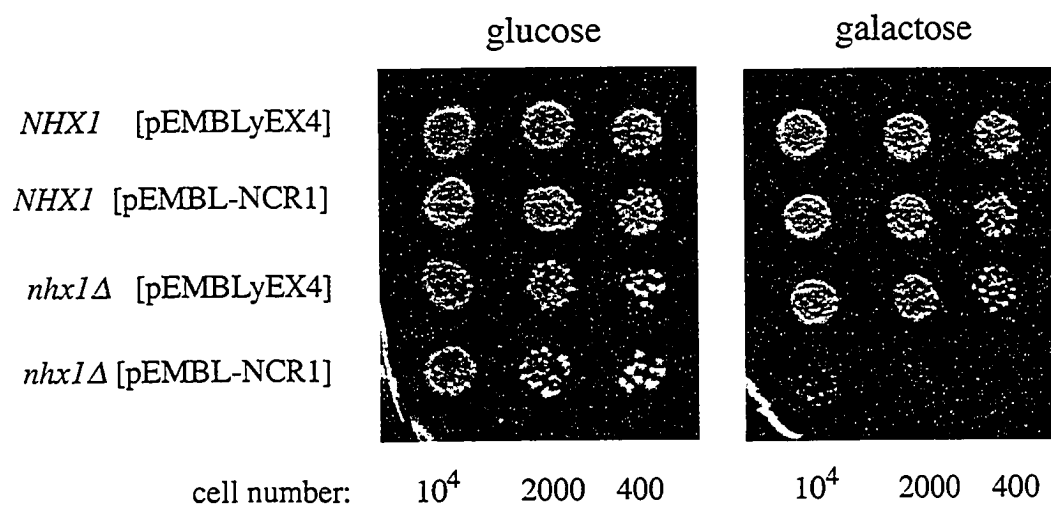


**Figure 20. Yeast lacking *NHX1* are hypersensitive to overexpression of *NCR1*.** Isogenic *NHX1* and *nhx1Δ* yeast were transformed with pEMBLyEX4 and pEMBL-NCR1 and grown in synthetic complete liquid lacking uracil to stationary phase. Cells were 5-fold serially diluted and deposited on synthetic complete medium lacking uracil and containing either glucose or galactose, starting with 10<sup>4</sup> cells. The plates were incubated at 30 °C for 3 d.

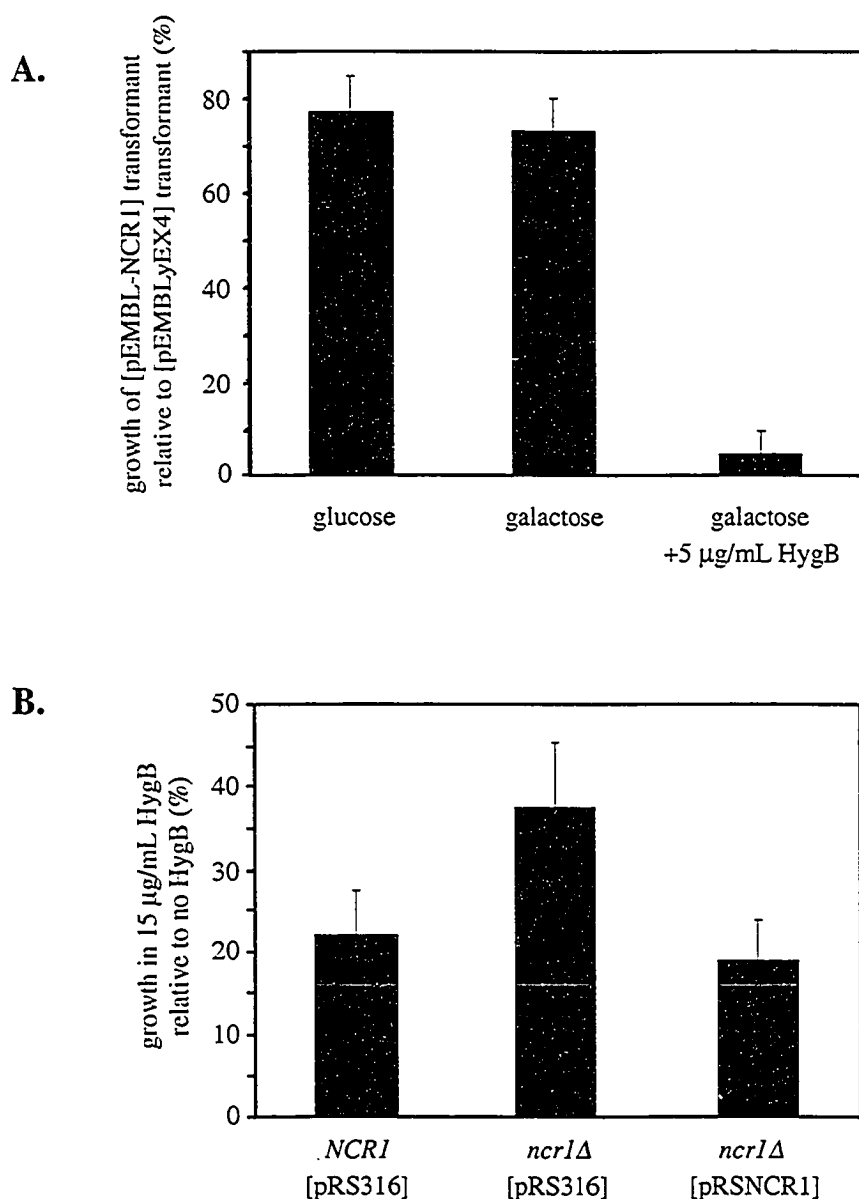
linkage of *nhx1Δ* with the inviability proves that loss of this protein renders cells intolerant to overexpression of *NCR1*.

Based on sequence homology with mammalian NHE proteins, *NHX1* encodes a sodium-proton antiporter (106), localized to the prevacuolar compartment (107). The Nhx1 protein is believed to participate in sodium homeostasis by sequestering Na<sup>+</sup> ions in the PVC (106, 107). The inviability observed when cells lacking this sodium-proton transporter overexpress *NCR1* suggests that Ncr1 may also participate in sodium or pH homeostasis.

Since *NHX1* allows cells to cope with excess *NCR1*, I assessed the consequence of loss of the *NCR1* gene when *NHX1* is absent. Diploids heterozygous for *ncr1Δ* and *nhx1Δ* were created and sporulated. Analysis of the meiotic products from these crosses did not reveal any difference between *ncr1Δ nhx1Δ* and *NCR1 nhx1Δ* haploid segregants when these were grown on YEPD medium at 30°C (data not shown). The lack of a synthetic phenotype suggests that *NCR1* may not directly participate in maintaining intracellular sodium or pH balance. On the other hand, if Ncr1 negatively regulates Nhx1, loss of Ncr1 in a strain already lacking Nhx1 may have no further effect.

### 3.15. As with *NHX1* deletion, *NCR1* overexpression results in hygromycin B sensitivity

*NHX1*-deficient yeast are sensitive to NaCl under acidic conditions (106), and also to other cations such as K<sup>+</sup>, tetramethylammonium and the aminoglycoside antibiotics hygromycin B and G418 (20, 53). The uptake of hygromycin B, a divalent cation that inhibits translation, is driven by the electrical membrane potential and may occur through nonspecific channels in the plasma membrane (160). The loss of Nhx1 has been hypothesized to decrease the concentration of protons in the cytosol, resulting in a hyperpolarized plasma membrane, allowing greater uptake of positively charged molecules such as hygromycin B, and decreased sequestration of the drug (1). Since overexpression of *NCR1* is particularly detrimental to cells lacking *NHX1*, we hypothesized that cells overexpressing or lacking *NCR1* might have altered sensitivity to hygromycin B, reflecting an influence on an Nhx1-dependent process. Yeast overexpressing *NCR1* were found to be hypersensitive to even low levels of hygromycin B (5 µg/mL), while yeast lacking *NCR1* were significantly more resistant ( $P < 0.05$ ) than *NCR1* wild-type yeast to growth in 15 µg/mL hygromycin B (Fig. 21). This suggests that *NCR1* prevents intracellular sequestration or promotes polarization of the cell membrane, so when in excess, there is increased uptake of hygromycin B or decreased storage.

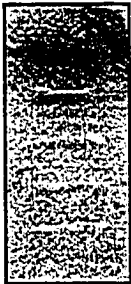


**Figure 21. Hygromycin B is toxic to cells overexpressing *NCR1*, while deletion of *NCR1* confers hygromycin B resistance.** Transformed yeast were grown at 28 °C to saturation in synthetic complete liquid medium lacking uracil. Yeast were inoculated into APG pH 4 medium lacking uracil, containing glucose or galactose, with or without hygromycin B (HygB) and incubated at 28 °C. (A) *NCR1* yeast transformed with pEMBLyEX4 or pEMBL-NCR1 were inoculated at OD<sub>600</sub>=0.005 and grown for 48 h. Growth was measured as OD<sub>600</sub> and pEMBL-NCR1 transformant growth as a percent of the pEMBLyEX4 transformant growth in the same medium. (B) *NCR1* and *ncr1Δ* yeast, transformed with either pRS316 or pRSNCR1, were inoculated at OD<sub>600</sub>=0.004 and grown for 24 h. Growth was measured as OD<sub>600</sub> and expressed as percent of the control cultures containing no hygromycin. Results are the average  $\pm$  SD of 3 replicates with a minimum of two independent transformants for each.



### 3.16. The Nhx1 C-terminal tail and Ncr1 cysteine-rich loop do not interact by yeast two-hybrid analysis

The Nhx1 protein is an integral membrane protein localized to the PVC (1). The amino-terminal domain is predicted to contain 12 transmembrane spans and to mediate ion exchange (173). The carboxy-terminal domain is hydrophilic and luminal (173), and has previously been shown to interact with Gyp6, a GTPase Activating Protein (GAP) for Ypt6. Ypt6 is a small GTP-binding protein implicated in retrograde vesicular trafficking from the PVC to the Golgi (1). The colocalization of both Nhx1-GFP and Ncr1-GFP to the same compartment and the discovery that Nhx1 is required to survive excess *NCR1* suggested that the two proteins might physically interact *in vivo*. Both the Nhx1 carboxy-terminal tail and the cysteine-rich loop of Ncr1 are predicted to be luminal (42, 173); therefore, interaction of these hydrophilic domains was tested using a two-hybrid genetic assay (Fig. 22). The Nhx1 and Ncr1 domains were not found to interact in this assay. This lack of interaction may indicate these proteins do not normally interact *in vivo*, but improper folding of these two domains or interference from the protein sequences to which they are fused may have prevented interaction in this assay. The other two predicted luminal domains of Ncr1 (42) could not be tested for interaction in this assay, as they activate the reporter gene when fused to a DNA-binding domain even in the absence of an authentic interacting partner protein (data not shown). Interestingly, I found

<u>LexA<sub>DB</sub></u>	<u>Gal4<sub>AD</sub></u>	
Rep2	Rep1	
-	Nhx1-C	
Rep2	Nhx1-C	
Ncr1-CRL	Nhx1-C	
Ncr1-CRL	Rep1	

**Figure 22. The Nhx1 C-terminal tail and Ncr1 cysteine-rich loop do not interact in a two-hybrid assay.** Yeast expressing the Nhx1 C-terminal tail (Nhx1-C) and Ncr1 cysteine-rich loop (Ncr1-CRL) fused to either the LexA DNA-binding domain or the Gal4 transcription-activation domain were assayed by a  $\beta$ -galactosidase filter assay for expression of a *lacZ* reporter gene controlled by the LexA-binding site. Two proteins known to interact, Rep1 and Rep2, were used as controls (142) for fusion-protein interactions, detected as a dark colour on the filter.

that fusion of the carboxy terminal portion of Nhx1 with the LexA DNA-binding domain was also capable of activating reporter-gene expression in the absence of an interacting partner. Coimmunoprecipitation of native Ncr1 and Nhx1 will need to be performed to determine if these proteins do interact.

### **3.17. Excess *NCRI* does not cause cells to missort carboxypeptidase Y**

In addition to its role in Na<sup>+</sup> homeostasis, Nhx1 also participates in intracellular trafficking. Yeast deficient in *NHX1* were isolated in a screen for mutants that inappropriately secrete a fraction of their carboxypeptidase Y (CPY) into the growth medium (17). CPY is normally a vacuolar protease. The CPY precursor protein is synthesized in the endoplasmic reticulum and transported to the vacuole *via* the Golgi and prevacuolar compartment (148). Its proper delivery to the vacuole is dependent on the receptor Vps10 (34, 99). Vps10 recognizes CPY in the late Golgi and delivers it to the PVC. A retrieval signal in its cytosolic domain facilitates the recovery of Vps10 to the Golgi (34). If insufficient Vps10 is delivered to the Golgi, either due to impaired synthesis or inefficient retrieval from the PVC, CPY accumulates at the Golgi and is diverted to the plasma membrane, where it is secreted (99). Secretion of CPY is detectable and this approach can be used to identify perturbations in trafficking between the Golgi and PVC compartments (34, 148).

In yeast lacking *NHX1* the PVC becomes enlarged and proteins such as Vph1, (normally a vacuolar protein), and the CPY receptor Vps10 are both improperly localized to this compartment (17). Because of increased acidity in the PVC, the Vps10 receptor is prematurely degraded when *NHX1* is absent (17). These features all suggest that movement of proteins from the PVC to the vacuole or Golgi is restricted in *nhx1Δ* mutants. Supporting this, two markers of endocytosis, the lipophilic dye FM4-64 and GFP-tagged  $\alpha$  mating factor receptor, Ste3-GFP, accumulate in the PVC when *NHX1* is absent (17). In wild-type cells, FM4-64 and Ste3 are internalized at the PM and enter the PVC before delivery to the vacuole (28, 165). Therefore, Nhx1 participates in trafficking between the prevacuolar compartment and the vacuole or Golgi (17).

The exacerbated toxicity of *NCR1* overexpression in *nhx1Δ* yeast suggests that the function of Ncr1 may oppose that of Nhx1. Ncr1 might directly participate in ion transport or could negatively regulate Nhx1. Ncr1 function could also oppose Nhx1 function more indirectly. For example, Nhx1-mediated transport between the PVC and the vacuole or Golgi may be balanced by Ncr1 facilitating delivery of materials to the PVC, either from the Golgi, the vacuole or from an early endocytic compartment. This function of Ncr1 is consistent with loss of *NCR1* delaying endocytic traffic (161). In this case, overexpression of *NCR1* might be predicted to induce excessive

delivery of cargo to the PVC. This enhanced anterograde transport might impair recycling of Vps10 to the Golgi, causing CPY at the Golgi to be diverted to the cell surface. Additionally, overexpression of *NCR1* in *NHX1*-deficient cells might be expected to exaggerate the secretion of CPY in *nhx1Δ* cells.

To test these hypotheses, *NHX1* and *nhx1Δ* yeast transformed with pEMBLyEX4 or pEMBL-NCR1 were grown on nitrocellulose membranes overlaid on synthetic complete medium lacking uracil and containing galactose to induce expression of *NCR1*. Secretion of CPY by the yeast was assayed by probing the membrane with anti-CPY antibodies (Fig. 23). Neither *NHX1* yeast transformant secreted detectable CPY, suggesting that overexpression of *NCR1* does not impair retrograde trafficking from the PVC. This implies that Ncr1 is not a negative regulator of Nhx1. In addition, CPY secretion by *nhx1Δ* cells, with or without *NCR1* overexpression, was comparable (Fig. 23). Therefore, the overexpression of *NCR1* in cells lacking *NHX1* did not enhance the *nhx1Δ* CPY secretion defect, suggesting the toxicity associated with *NCR1* overexpression in these cells does not reflect an exaggerated obstruction of traffic from the PVC to the Golgi.

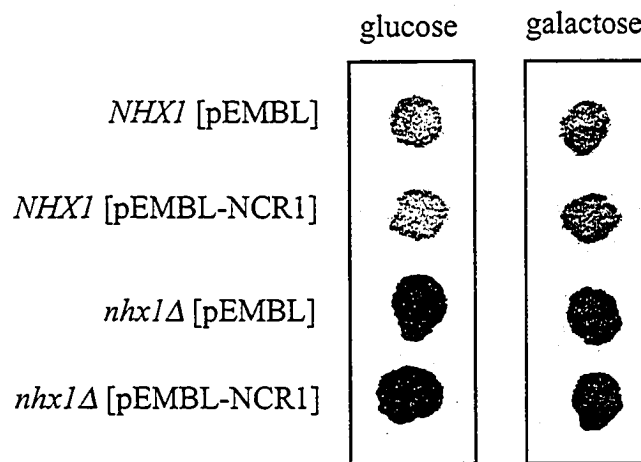


**Figure 23. Effect of *NCR1* overexpression on CPY secretion.** Equal numbers of cells from stationary-phase yeast cultures were spotted on nitrocellulose membranes overlaid on synthetic complete medium lacking uracil and containing glucose or galactose. Following 35 h at 30 °C, the membranes were washed to remove cells. Extracellular CPY secreted from isogenic *NHX1* or *nhx1*Δ yeast, harbouring pEMBLyEX4 or pEMBL-NCR1, was detected by immunostaining with anti-CPY antibody.

### 3.18. *NCR1* contributes to pH homeostasis in the absence of V-ATPase

Since overexpression of *NCR1* does not promote secretion of CPY, either in the presence or the absence of *NHX1*, sufficient Vps10 must be recycled to the Golgi for CPY binding and anterograde transport. If Ncr1 does not function in delivery of cargo from the Golgi to the PVC, its ability to oppose Nhx1 may be due to another aspect of Nhx1 function. Bowers *et al.* (17) have proposed that retrograde trafficking is impaired in *nhx1*Δ cells because they cannot alkalinize the PVC. The resulting increase in luminal pH contributes to protein-trafficking defects of *nhx1*Δ cells. This hypothesis has been supported by the observation that the addition of weak base to the culture medium can correct the mislocalization of endocytosed Ste3-GFP or delayed efflux of FM4-64 in *nhx1*Δ cells (20). Conversely, accumulation of Ste3-GFP in the PVC could be induced in wild-type cells by supplementation of the culture medium with weak acid (20). In wild-type cells, the sodium import/proton export activity of Nhx1 is dependent on a proton gradient across the PVC membrane, established by the import of protons into the PVC by the vacuolar H<sup>+</sup>-ATPase (V-ATPase) (17). Nhx1 activity has been proposed to neutralize the V-ATPase-mediated acidification of the PVC (17), suggesting that defective retrograde trafficking in *nhx1*Δ cells could be alleviated by impairing import of protons into the PVC (17). However, deletion of *VMA2*, encoding a subunit of the V-ATPase, fails to correct the

trafficking phenotypes of *nhx1Δ* cells (17). Bowers *et al.* concluded that either the protein-trafficking defects of *nhx1Δ* cells are independent of its ion exchange function, or another protein could acidify the PVC. Since Ncr1 function may oppose Nhx1 function, Ncr1 could be the other protein that promotes import of protons when cells lack V-ATPase activity. To test this hypothesis, *ncr1Δ*, *vma6Δ* and *ncr1Δ vma6Δ* double mutants were grown on media of varying pH and viability was assessed relative to a *NCR1 VMA6* wild-type strain. *VMA6* encodes a subunit of the V-ATPase and is required for its assembly. Wild-type *NCR1 VMA6* yeast and those lacking only *NCR1* grew well at every pH used, except at the extreme alkaline pH of 9 (data not shown). Yeast lacking *VMA6* grew slightly less well than wild-type yeast at pH 2.5, 3, 7.5 and 8 (Fig. 24). However, sensitivity to high and low pH was exacerbated dramatically by loss of *NCR1* in this background (Fig. 24). This suggests that *NCR1* allows cells to maintain pH homeostasis at low and high pH, in the absence of *VMA6*. We subsequently confirmed that inviability of the *ncr1Δ vma6Δ* strain at low and high pH was due to loss of *NCR1* because a single copy of *NCR1* on a plasmid rescued *vma6Δ ncr1Δ* cells at alkaline and acidic pH, while the corresponding empty vector did not suppress the inviability (M. Dobson, unpublished results).



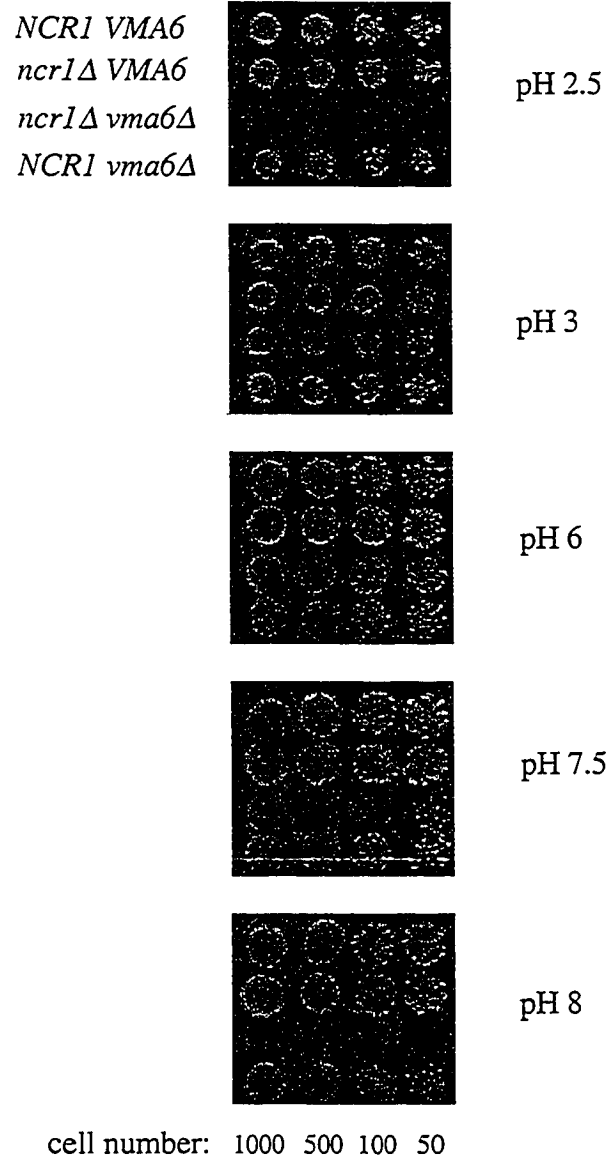


**Figure 24. Yeast cells lacking both *VMA6* and *NCR1* are sensitive to acidic and alkaline pH.** Haploid yeast of the genotypes indicated were grown to saturation in YEPD and deposited on YEPD plates buffered at the indicated pH. The numbers of cells deposited are indicated. The orientation of the strains spotted on the plates is the same for each pH condition. The plates were incubated at 28°C for 5 d.

## 4. Discussion

The primary biochemical defect in NPC1 mutant cells is unidentified. While the underlying cause of the pathology of NPC disease was initially believed to be defective cholesterol transport, more recent studies have suggested that intracellular transport in general may be affected by dysfunctional NPC1, leading to accumulation of sterols and sphingolipids as a secondary effect (110). I have used, as a model, the yeast *Saccharomyces cerevisiae* to examine the effects of deletion or overexpression of its single NPC1 homologue, *NCR1*.

This investigation commenced with an extensive examination of the consequences of *Ncr1* deficiency in yeast. Given that mutation of the human NPC1 homologue results in a fatal cholesterol storage disorder, we expected that loss of *Ncr1* would evoke an observable phenotype in yeast cells. *ncr1* $\Delta$  cells grew as well as their *NCR1* counterparts under a range of normal and stressful growth conditions. This is compatible with recent reports demonstrating that loss of *Ncr1* is inconsequential (98, 183).

While *ncr1* $\Delta$  yeast responded similarly to *NCR1* yeast under all plating conditions to which they were subjected, it was possible that subtle biochemical differences between *NCR1* and *ncr1* $\Delta$  yeast could be detected by specific biochemical assays. Incorporation of [<sup>14</sup>C]acetate into lipids was indistinguishable in *NCR1* and

*ncr1Δ* yeast at 37°C, a temperature at which endocytosis is impaired but not blocked in the mutant (161). This was in accordance with a recent extensive comparative analysis of sterol metabolism in *NCR1* and *ncr1Δ* yeast, where no differences were observed (98). Subcellular localization of endogenously synthesized lipids could be examined, as it is still possible that their distribution may be altered in *ncr1Δ* yeast, particularly at 37°C, even if total lipid levels are unaffected. A significant increase in diacylglyceride (DAG) levels in *ncr1Δ* yeast was observed following [<sup>14</sup>C]acetate labeling for one hour at 30°C. Increased DAG has been shown to activate protein kinase C (Pkc1) (115), which in turn activates Bck1 and Slr2, two downstream effectors in the maintenance of cellular integrity pathway. If deletion of *NCR1* causes an increase in DAG, overexpression of *NCR1* may result in decreased DAG, and correspondingly reduce the activity of Bck1 and Slr2, leading to impaired growth. Consistent with this hypothesis, deletion of either *BCK1* or *SLR2* were found to enhance the toxicity resulting from overexpression of *NCR1*. What is the source of the elevated DAG when *NCR1* is deleted? DAG is produced in many reactions within the cell: it is released during the formation of inositol phosphoceramide (65) or can be produced by the dephosphorylation of phosphatidic acid by phosphatidic acid phosphatase (24). Since elevated DAG levels were only observed in *ncr1Δ* mutants following a one hour pulse with [<sup>14</sup>C]acetate, and had normalized by 16 h, the most

likely source of DAG is that produced by the glycerol acyltransferase synthetic pathway, rather than by a catabolic process. In the synthetic pathway, Gat1 or Gat2 catalyze the acylation of glycerol-3-phosphate, forming lysophosphatidic acid, which can be subsequently acylated by Slc1 to form phosphatidic acid (180). At 37°C, DAG levels in yeast lacking *NCR1* were normal but an endocytic delay was observed (161), suggesting that the increase in DAG at 30°C might be associated with the unimpaired trafficking. If excess DAG suppresses the effects of *NCR1* deletion at 30°C, then simultaneous loss of *NCR1* and one of the DAG biosynthetic enzymes might confer a phenotype.

Subtle changes in the lipid composition of membranes, including alterations in DAG levels, can perturb intracellular trafficking events. To assess this in *ncr1Δ* yeast, the maturation of Gas1, a GPI-linked protein found in the plasma membrane, and extracellular levels of invertase, a protein that is normally secreted, were monitored. Gas1 maturation was normal in *ncr1Δ* yeast at both 30°C and 37°C, indicating normal raft trafficking from the ER to the Golgi in these mutants. Invertase secretion was unaffected by deletion of *NCR1*, but this experiment was performed only at 30°C, not at 37°C. Since endocytic defects in *ncr1Δ* yeast are only observed at 37°C (161), it is possible that secretory defects could arise at the elevated temperature as well. Additionally, in this experiment, yeast were induced to express

invertase for 2 h prior to assaying enzyme activity. Subtle defects in secretion, which could be identified following shorter incubation times, might not have been detected. Regardless, these results contribute to previous findings that sphingolipid and sterol metabolism are unaffected by loss of *NCR1* (98) and that *NCR1* does not seem to influence intracellular trafficking under standard growth conditions (183).

Despite *ncr1Δ* yeast having no discernable plating phenotypes or differences in intracellular trafficking, they were found to be more sensitive to thermal stress than *NCR1* yeast. This sensitivity was found to be due to decreased production of mitochondrial mutants. Yeast lacking functional mitochondria have altered sphingolipid composition that can affect their viability at high temperature (45, 62, 74, 172). The wild-type *NCR1* strain, in which the *ncr1Δ* mutation was created for this experiment, produced petite colonies at an unusually high frequency of ~40%, while yeast normally produce petite colonies at a frequency of 1% (55). Since freeze-thawing damages *E. coli* DNA (23), the increased propensity of this yeast strain to generate mitochondrial mutants may have arisen during long-term storage at -70°C. The tendency to produce petites at an increased frequency was lost when this strain was mated to other yeast, suggesting mitochondrial DNA damage was responsible for this phenotype. In any case, deletion of *NCR1* in this strain diminished the extent to which petite colonies were formed. Reintroduction of the wild-type *NCR1* gene

restored the high rate of petite production, demonstrating a dependence of this phenotype on *NCR1* status. Exposure to ethidium bromide, an agent that is known to induce mitochondrial DNA damage (55), affected *NCR1* and *ncr1Δ* yeast equally, so the significance of decreased petite production upon loss of *NCR1* is unclear.

Interestingly, a recent report has shown that mouse NPC1<sup>-/-</sup> neurons have severe mitochondrial abnormalities leading to a decrease in cellular ATP, resulting in neurodegeneration (179). This finding may be connected to my observation that loss of Ncr1 diminishes production of mitochondrial DNA mutants; however, this relationship was not pursued due to the difficulties associated with studying a potentially mitochondrion-linked trait.

The failure of *ncr1Δ* cells to exhibit a phenotype under normal laboratory conditions and when treated with various agents implies that the role performed by Ncr1 either has no significant influence on cell biology under the conditions examined or that other wild-type genes protect *ncr1Δ* yeast from exhibiting an observable phenotype.

Genetic approaches were undertaken to attempt to identify these protecting genes. The first was a classical synthetic-lethal screen to identify genes required when *NCR1* is absent. All but four of 27 synthetic-lethal mutants were found to be dependent on one of the nutritional marker genes, either *URA3* or *ADE3*, that were

present on the pSLNCR1 plasmid employed in this approach, but did not require the *NCR1* gene for survival. One of the 4 mutants that did require the plasmid pSLNCR1 for survival was able to lose the plasmid in the presence of one extra copy of *YGL250w*. Unfortunately, the mutant locus remains unidentified and the biological role of *YGL250w* has not been elucidated. According to a study in which virtually every yeast protein was tagged with green fluorescent protein, the Ygl250w protein resides in the cytoplasm and nucleus (70). High-throughput genome-wide yeast two-hybrid analyses revealed that Ygl250w interacts with Atp14, Avo2, Bdp1, Sas10 and Soh1 (72). One must discriminate when considering these findings, since Atp14 localizes to mitochondria where it would be unlikely to interact physically with cytoplasmic or nuclear Ygl250w. Bdp1 (a component of the RNA Polymerase III transcription factor), Sas10 (a component of the small ribosomal subunit processosome) and Soh1 (a protein with sequence similarity to RNA polymerase) are all nuclear proteins, so their interactions with Ygl250w may be valid. Since some of these proteins participate in transcription or may be required for efficient translation, it is reasonable to predict that Ygl250w may be involved in gene expression as well. Changes in gene expression are difficult to interpret, since many genes may be influenced; therefore it is not obvious how one extra copy of a gene involved in gene expression could rescue yeast from loss of *NCR1* and mutation of the unidentified gene. Interestingly, one of the Ygl250w -interacting proteins, Avo2 (72), is a

component of a complex required for cell growth (96), and loss of *YGL250w* was found to impair cells lacking *ARP2* (155). *Arp2* encodes an actin-related protein that is required for actin patch assembly and motility during endocytosis and establishment of cell polarity (50, 105). These findings may imply a role for *YGL250w* in cell growth and polarity, which is intriguing considering that some genes required to establish cell polarity are also required for yeast to survive high expression of *NCRI*.

The second gene identified in the colony colour-based synthetic-lethal screen was *GFAI*. *GFAI* encodes glutamine:fructose-6-phosphate aminotransferase, which catalyzes the first step in chitin biosynthesis, the transfer of an amino group from glutamine to fructose-6-phosphate, forming glucosamine-6-phosphate and glutamate (171). Since *GFAI* is an essential gene, the synthetic-lethal mutant 45-6b must carry a point mutation that retains the essential function of *GFAI* but renders *NCRI* essential. Alternatively, since linkage analysis was not conducted for this mutant it is also possible that, as was observed for another mutant, a gene other than *GFAI* carries the mutation and the plasmid-borne copy of wild type *GFAI* rescues cells deficient in the second gene and *NCRI*. The method of suppression by *GFAI* was not investigated; however, sporulation of diploids heterozygous for both *NCRI* and the mutant gene (either *gfaI* or an unknown locus) resulted in only two live progeny per tetrad. Sporulation is dependent on functional *GFAI* (174) and the inability of the



mutant spores to recover from meiosis (possibly due to spore wall defects associated with loss of *GFAI*) may support their identification as *gfaI* mutants, but this evidence is indirect.

When tetrads were isolated from the diploids heterozygous for loss of *NCR1* and the *gfaI* mutation, the presence of *NCR1* on a plasmid, in combination with *URA3*, was found to promote viability of spores. This first illustration that nutritional status affects *ncr1Δ* phenotypes highlights the importance of studying the effects of loss of *NCR1* only in nutritionally matched, isogenic strains. This contribution of nutritional markers to *ncr1Δ*-dependent phenotypes may explain why the colony colour-based synthetic-lethal screen, performed on the assumption that nutritional status is inconsequential to loss of the gene of interest, was not successful in identifying mutations solely dependent on *NCR1*. Nonetheless, if wild-type *NCR1* partially rescues *gfaI* meiotic progeny, which are compromised because they lack a cell-wall biosynthetic enzyme, this may imply a role for *NCR1* in wall biosynthesis, or mobilization of cell-wall material. Expression of the *GFAI* gene is positively regulated by the mating pheromone response and by the PKC pathway (184). This is interesting in light of the SGA findings that components of the PKC pathway and genes participating in mating-projection formation contribute to viability when yeast overexpress *NCR1*. In both cases, either loss of *NCR1* or its overexpression might alter critical flux in the polarized secretion and recycling pathways.

Synthetic lethal interactions with *ncr1* $\Delta$  were sought by SGA, which is less reliant on nutritional markers, and instead utilizes drug-resistance gene replacements to select for gene deletions. This method probes for synthetic lethal interactions between the gene of interest and every nonessential gene in the Yeast Gene Deletion Set. No synthetic lethal interactions were identified by this approach (data not shown). Therefore, under normal plating conditions, *ncr1* $\Delta$  yeast do not require a nonessential gene for survival. It is possible that two or more genes must be simultaneously deleted for *NCR1* to become essential. Indeed, it has been found that only the simultaneous deletion of all seven oxysterol-binding protein homologues is lethal in yeast (13). Alternatively, a synthetic-lethal SGA screen could be performed under conditions of stress, such as high or low pH, or in the presence of specific inhibitors, to reveal novel *NCR1* genetic interactions.

My second approach to investigate the function of Ncr1 examined the effects of *NCR1* overexpression in yeast. The *NCR1* gene was placed under the control of a galactose-inducible promoter on a high-copy plasmid. The copy number of the pEMBL-NCR1 plasmid could also be controlled by altering the medium on which yeast were grown to select for either uracil or leucine prototrophy. As anticipated, the presence of galactose rather than glucose did result in a dramatic increase in the level of Ncr1 protein expressed by yeast transformed with pEMBL-NCR1 over wild-type levels, as detected by Western blotting (Fig. 11). Viability of these transformed yeast

varied greatly, depending on whether the medium was synthetic complete or synthetic defined and whether selection was for uracil or leucine prototrophy (Fig. 12). These media differences may provide a means to further dissect the nature of the toxicity of *NCRI* overexpression. Initial steps towards this elucidation were taken in this study.

$\text{CaCl}_2$  was found to partially suppress the toxicity of *NCRI* overexpression on both synthetic complete medium lacking uracil (Fig. 14) and on synthetic defined medium lacking leucine (data not shown). The inability of  $\text{MgCl}_2$ ,  $\text{MgSO}_4$  and  $\text{ZnCl}_2$  to rescue cells from the effects of *NCRI* overexpression suggests that this effect was specific to  $\text{Ca}^{2+}$ . The addition of 1 M sorbitol slightly alleviated the inviability due to overexpression of *NCRI* on synthetic complete medium lacking uracil (Fig. 14) but not on synthetic defined medium lacking leucine (data not shown). Since sorbitol, which would be expected to osmotically stabilize cells, could not completely rescue cells from *NCRI* overexpression, the toxicity of *NCRI* overexpression was likely not due to generalized fragility of the cells and rescue by  $\text{Ca}^{2+}$  was not merely due to osmotic stabilization.  $\text{Ca}^{2+}$  has been found to activate protein kinase C (115). Activation of the protein kinase C pathway may explain the  $\text{Ca}^{2+}$ -specific rescue of yeast from *NCRI* overexpression toxicity, just as blocking this pathway by deletion of either *BCK1* or *SLT2* exacerbates the toxicity. Increased intracellular  $\text{Ca}^{2+}$  concentration has also been found to activate the mammalian Nhx1 homologue, NHE1, with the NHE1 C-terminal domain physically interacting with  $\text{Ca}^{2+}$ -

calmodulin (36). Supplementation of medium with  $\text{Ca}^{2+}$  may thus activate Nhx1, promoting alkalization of the PVC. If toxicity of overexpressed Ncr1 is due to acidification of the PVC, activation of Nhx1 by  $\text{Ca}^{2+}$  would be predicted to raise the pH of this compartment and hence alleviate the toxicity, while deletion of *NHX1* would exacerbate the toxicity and block the suppressive effect of  $\text{Ca}^{2+}$ .

The first of two SGA analyses performed in this study was designed to identify deletion mutations that allow yeast to cope with overexpression of *NCR1* (Fig 25). The majority (46%) of the genes identified in this screen have not yet been assigned cellular roles, so their identification as suppressors of the effects of *NCR1* overexpression will become more informative once experiments to test their functions are undertaken and as literature concerning their functions is published. Importantly, two genes expected to be false positives were identified in this screen. Deletion of either *GAL3* or *GAL4*, genes encoding transcription factors known to be required for induction of high-level expression from the *GAL1-10* promoter, rescued cells from the effects of the *NCR1* overexpression plasmid. As with the false-positive genes *MIG1* and *GAL80* identified in the dosage-suppressor screen, loss of *GAL3* or *GAL4* would be expected to diminish or prevent expression of *NCR1* from the *GAL1-10* promoter. Identification of these two genes indicates that authentic suppressors of *NCR1* overexpression were isolated in this screen. Likewise, other genes identified in this screen that participate in transcription or translation (11%) may suppress toxicity of

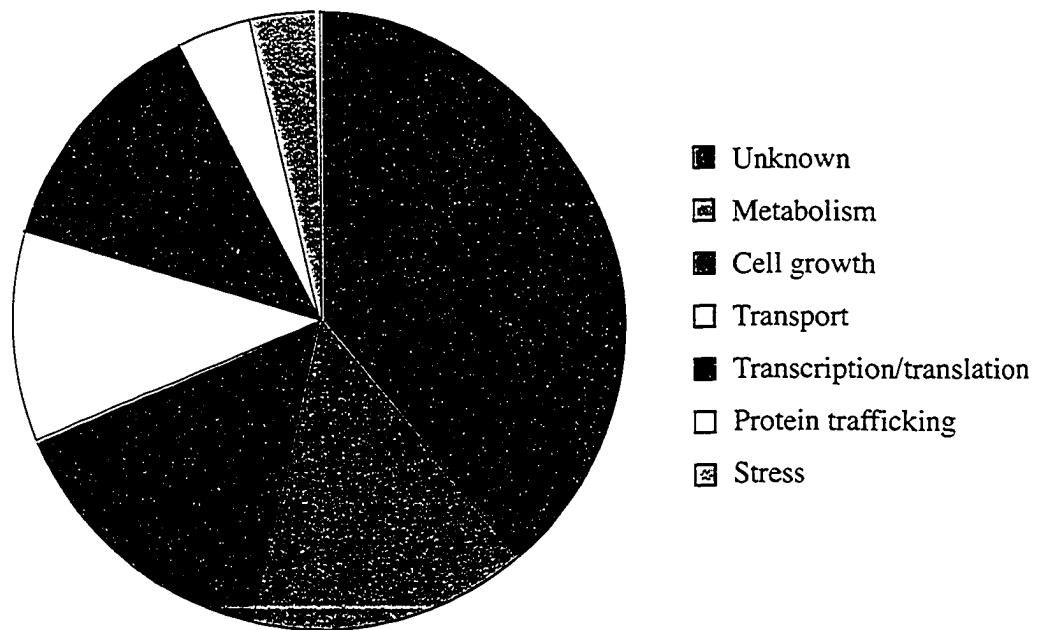


**Figure 25. Deletion suppressors of *NCR1* overexpression.** Genes that, when deleted, rescue cells from the toxicity of *NCR1* overexpression were classified on the basis of their Gene Ontology assigned by the Gene Ontology Consortium (4).

*NCR1* overexpression by attenuating expression of the gene from the pEMBL-*NCR1* plasmid. This could be tested by Western blot analysis of protein extracts from these mutants using anti-Ncr1 antibodies. Of the other genes identified whose effects could not be attributed to transcription or translation downregulation, ~15% participate in metabolism, 11% mediate transport, 6% are involved in protein trafficking, 5% are involved in stress response and 4% are involved in cell growth. The thread that binds the genes obtained in this screen to each other and to *NCR1* is not obvious. I expected to identify genes sharing functional overlap with Ncr1; however, the identity of these genes is most likely obscured by the simultaneous identification of many gene deletions that alleviate a deleterious secondary consequence of Ncr1 overexpression. This latter group of genes would provide less insight into Ncr1 function. Therefore, I focused on the results of the second SGA screen, that identified gene deletions that exacerbate the toxicity of *NCR1* overexpression.

In the second SGA screen conducted in this study, thirteen gene deletions were found to render cells hypersensitive to the toxicity of *NCR1* overexpression. In contrast to the gene deletions identified as rescuing cells from toxicity of *NCR1* overexpression, the “hits” identified in this second screen participate in related biological processes. This concept is illustrated in Fig. 26, showing all synthetic lethal interactions occurring among the identified genes. If two genes participate in a synthetic lethal interaction, they may be assumed to share functional overlap. The

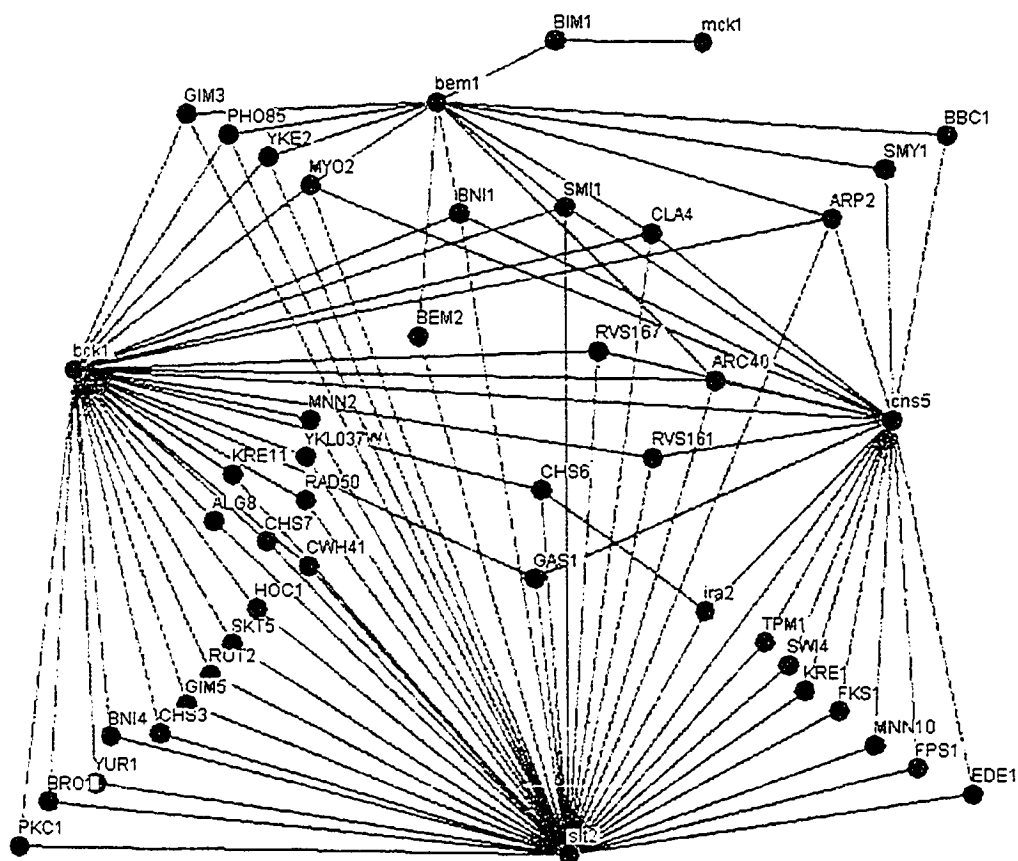


**Figure 26. Genetic interaction network representing the synthetic lethal/sick interactions.** Genes are represented as nodes and interactions are represented as edges that connect the nodes. Red nodes are gene deletions that were found to exacerbate the toxicity of *NCR1* overexpression, while blue nodes are other genes that interact. Any nodes with less than two edges are not shown. Synthetic lethal interactions were abstracted from the list in GRID (18), current as of July 2005, and visualized by Osprey (19).

high degree of connectivity among these hits suggests the majority are involved in related processes. Four of the identified genes, *BCK1*, *SLT2*, *BEM1* and *CHS5*, and many genes that participate in synthetic lethal interactions with these genes, are implicated in establishment of cell polarity.

One of the genes identified in this screen, *BEM1*, encodes a protein that is localized to the bud or shmoo tip and interacts with actin. Cells defective for *BEM1* are large and multinucleate and cannot form mating projections (125). Because Bem1 interacts with many proteins involved in polarized growth, it has been implicated as an organizing scaffold to help promote interactions between its binding partners (175). A second gene identified in this screen was *CHS5*. Chs5 resides in the late Golgi and secretory vesicles (140) and is part of the machinery that delivers a subset of vesicles to polar growth sites (138). In vegetatively growing cells, Chs5 delivers Chs3 (a chitin synthase) to the bud site (131, 140). In mating cells, Chs5 delivers Chs3 and Fus1 (a protein required for fusion during mating) to the shmoo tip (139, 140). In the absence of Chs5, these proteins are redistributed to cytoplasmic patches. While Chs5 clearly is important for the localization of some proteins, it does not transport all proteins that display polarized distribution (139). Cells lacking Bem1 or Chs5 may be less able to maintain materials at the bud site or mating projection due to loss of a stabilizing scaffold or to decreased vesicular trafficking to these destinations, respectively. If Ncr1 antagonizes these processes by participating



in removal of materials from the bud site or mating projection, overexpression of *NCR1* would further compromise the ability of *bem1Δ* or *chs5Δ* cells to replenish these sites with substrates required for budding, thus slowing proliferation.

Budding also involves components of the protein kinase C/cell-wall integrity pathway. Deficiency of two genes implicated in this pathway, *BCK1* or *SLT2*, results in phenotypes characteristic of cell-polarity mutants. Cells lacking *BCK1* exhibit a spectrum of morphological abnormalities (35). At high temperatures, *slt2* mutants accumulate secretory vesicles throughout the cytoplasm rather than at the bud tip and exhibit a depolarized distribution of chitin (102). Slt2 is phosphorylated, and therefore activated, during periods of highly polarized growth (64, 76). During bud emergence and formation of a mating projection, the cell wall and plasma membrane must be remodeled. This is believed to activate the PKC pathway to trigger new cell-wall synthesis (97).

Because cells lacking *BCK1* could not survive overexpression of *NCR1*, I tested the viability of cells lacking *NCR1* when an activated allele of *BCK1*, *BCK1-20*, was overexpressed. I found that overexpression of *BCK1-20* is not lethal when cells are deficient in *NCR1*. This lack of reciprocity might suggest that *NCR1* and *BCK1* do not have opposing functions, but the fact that *NCR1* shares a genetic interaction with *SLT2*, which acts downstream of *BCK1*, corroborates the hypothesis that Ncr1 is active in a process opposite to that in which *SLT2* and *BCK1* participate.

Given that *ncr1Δ* cells do not have a discernable phenotype, it may be unsurprising that Ncr1 loss does not further exaggerate the impairment produced by increased flux through the PKC pathway.

The Bck1, Slt2, Chs5 and Bem1 proteins are clearly implicated in polarized delivery of materials, even if their precise roles have not been elucidated. Since loss of these genes exacerbates the toxicity of *NCR1* overexpression, excess Ncr1 may result in enhanced flow of materials away from the bud or mating projection, resulting in an insufficiency of substrates required for polarized growth (Fig. 27). This substrate insufficiency in yeast overexpressing *NCR1* may precipitate phenotypes characteristic of cell-polarity mutants, in which delivery of substrates to these sites occurs less efficiently. Cells overexpressing Ncr1 may fail to polarize chitin or the actin cytoskeleton. Furthermore, these cells might have defective budding or inefficient mating. Experiments to address these questions are in progress. While *NCR1* overexpression may affect polarized growth in yeast due to accelerated removal of substances from these sites, yeast lacking *NCR1* may also exhibit phenotypes associated with cell-polarity mutants because recycling occurs less efficiently. It was previously determined that yeast lacking *NCR1* displayed budding defects at 37°C (161), supporting the hypothesis that Ncr1 participates in recycling from the bud. Interestingly, while homologues of the NPC1 protein can be found in many diverse organisms, the genome of the fission yeast,

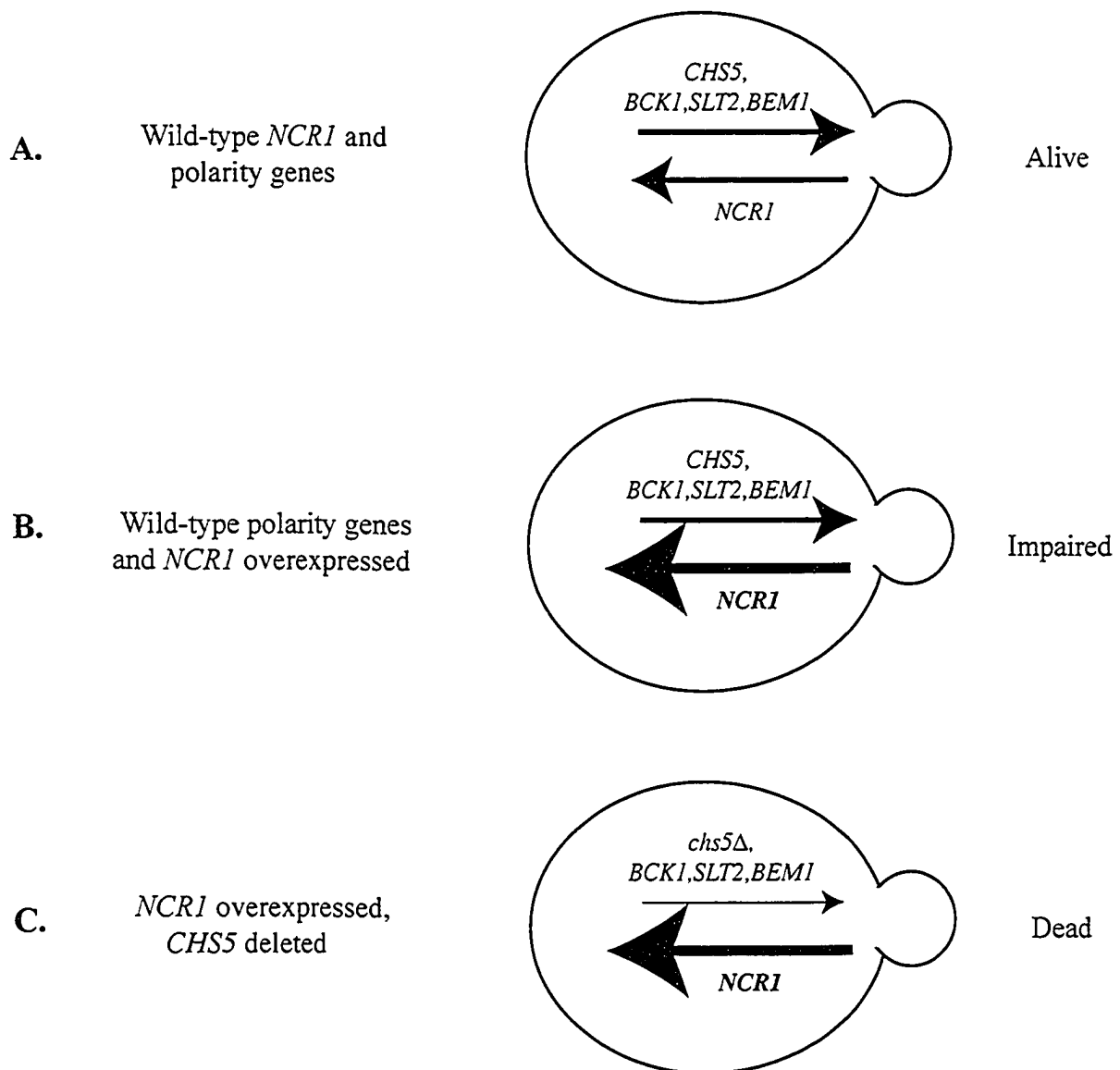


**Figure 27. Synthetic lethality of overexpressed *NCR1* in cell-polarity mutants suggests *Ncr1* participates in recycling from sites of polarized growth.** (A) Polarized secretion and recycling from the bud proceed normally when cells are wild-type for polarity genes and *NCR1*. Overexpression of *NCR1* (B) increases flux in the recycling pathway, impairing growth of yeast. (C) Deletion of a cell-polarity gene (i.e. *chs5Δ*) decreases polarized secretion, and when combined with increased flux away from the bud due to *NCR1* overexpression is lethal.

*Schizosaccharomyces pombe*, does not encode an NPC1 homologue. If NPC1 protein homologues are important in recycling from sites of polarized secretion, the absence of this protein may reflect a loss of a specialized recycling function, such as that required by budding yeast to form the bud or neurons to recover from firing. Whether other eukaryotes also lack NPC1 homologues will become apparent as genome sequencing projects are completed.

Other genes identified in the SGA screen whose deletion enhances toxicity of overexpressed *NCR1* include *GOT1*, *IRA2*, *MCK1*, *DAL81*, *HFA1*, *LIP2*, *SPT3*, *YLR021w* and *YML030w*. The cellular roles of the latter two genes are unknown. Spt3 and Dal81 are transcription activators (22, 47), and their modes of synthetic enhancement are unclear. *GOT1* encodes a protein that is required for ER to Golgi transport (33). *IRA2* (which encodes a GTPase-activating protein for Ras) (152) and *MCK1* (a protein kinase involved in the control of chromosome segregation and in regulating entry into meiosis) (89) may be indirectly involved in establishing cell polarity, since cells lacking these genes participate in synthetic lethal interactions with known polarity genes (156). *LIP2* encodes a protein that modifies mitochondrial enzymes by attaching lipoic acid groups (101). Surprisingly, the only gene involved in lipid metabolism that was identified in this screen is *HFA1*. Hfa1 is a mitochondrial acetyl-CoA carboxylase that catalyzes the production of malonyl-CoA, required for mitochondrial fatty acid biosynthesis (68). This may imply a role for

Ncr1 in transport of fatty acids from the mitochondrion, or degradation of mitochondrial fatty acids. This possibility remains to be tested but is intriguing in light of the observed genetic interaction between loss of *NCR1* and a putative mitochondrial DNA mutation.

My finding that *NHX1* allows cells to cope with excess Ncr1 suggests the cellular role of Ncr1 may be opposite to that of Nhxl. Nhxl is a sodium-proton antiporter localized to the PVC of yeast, that imports Na<sup>+</sup> ions into this compartment in exchange for protons (106, 107). The sensitivity of yeast lacking *NHX1* to the aminoglycoside antibiotic hygromycin B (53) suggested a way to test for functional overlap between *NCR1* and *NHX1*. I examined the sensitivity to hygromycin B of cells overexpressing or deficient in Ncr1. Consistent with *NCR1* overexpression being more deleterious in an *nhxlΔ* yeast, overexpression of *NCR1*, like deletion of *NHX1*, resulted in sensitivity to even very low levels of hygromycin B while, compared to *NCR1* yeast, *ncr1Δ* cells were slightly more resistant. By analogy with the *nhxlΔ* phenotype, *NCR1*-overexpressing yeast may be more sensitive to hygromycin B either because of increased uptake or because intracellular sequestration is decreased. The opposite would explain resistance of *ncr1Δ* yeast to hygromycin B. Alternatively, overexpression of *NCR1* may perturb PM sterol levels, altering the conformation of transporters in the PM and increasing uptake of

hygromycin B. However, since a sterol-related phenotype has yet to be observed in yeast lacking *NCR1* the former possibility is favoured. The hygromycin phenotypes of cells overexpressing or lacking Ncr1 suggest Ncr1 participates in a process that may counteract the cellular activity of Nhx1. Ncr1 could import protons into or efflux Na<sup>+</sup> ions from the PVC, either directly or by regulating other transporters, or Ncr1 may inhibit or negatively regulate Nhx1.

If Ncr1 negatively regulates Nhx1, it may do so by physical interaction with the antiporter. This possibility was tested in a yeast two-hybrid protein-interaction assay. The Ncr1 cysteine-rich loop was not found to interact with the C-terminal domain of Nhx1 in this genetic assay, despite the fact that each of these domains is predicted to lie within the PVC/vacuole lumen. This may imply that Ncr1 and Nhx1 do not physically interact. However, one caveat of the yeast two-hybrid assay is the fusion proteins must be delivered to the nucleus to be able to activate the reporter gene. Since the Nhx1 and Ncr1 domains that were tested are predicted to be in the PVC/vacuole lumen, where the pH is lower than in the nucleus, improper folding at the higher pH may have prevented their physical interaction in the nucleus. Improper folding of the carboxy-terminal domain of Nhx1 is unlikely since the same fusion protein has been shown to interact with Gyp6 in a two-hybrid assay and coimmunoprecipitation of the full-length proteins has confirmed this as a real interaction (1). It is possible that Nhx1 requires Gyp6 to bind to the Ncr1 cysteine-

rich loop and Gyp6 would not be present in the nucleus to facilitate this interaction in the two-hybrid assay. Alternatively, the Ncr1-binding site on Nhx1 may lie outside the C terminus or require other domains of Ncr1 that are not present in my two-hybrid fusion protein. Ncr1 and Gyp6 could co-regulate Nhx1 such that when one is bound, the other is physically occluded. Gyp6, like Ncr1, confers sensitivity to hygromycin B when overexpressed and results in resistance when absent (1). Further investigation of possible interaction of Nhx1 and Ncr1 awaits a test of whether the full-length native proteins coimmunoprecipitate, as would be expected if they physically interact *in vivo*.

Ncr1 may not physically interact with Nhx1 but could still directly inhibit the Na<sup>+</sup>-proton antiporter activity of Nhx1, or Ncr1 may indirectly oppose Nhx1 function by promoting trafficking into the PVC. Cells lacking Nhx1 have an acidified PVC, which promotes trafficking from the PVC to the vacuole and inhibits retrograde trafficking from the PVC to the Golgi (17). The impaired retrograde trafficking delays recycling of the CPY receptor, Vps10, to the Golgi, resulting in CPY secretion by *nhx1Δ* cells (17). Since cells overexpressing *NCRI*, like *nhx1Δ* cells, were found to be hygromycin B-sensitive, I next examined whether *NCRI*-overexpressing cells shared a CPY secretion phenotype with *nhx1Δ* cells. Wild-type yeast overexpressing *NCRI* did not secrete CPY, implying that Ncr1 is not an inhibitor of Nhx1 activity. Therefore, Ncr1 may oppose the function of Nhx1, but does not appear to act by

inhibiting Nhx1-mediated retrograde trafficking from the PVC to the Golgi. In addition, anterograde trafficking from the Golgi to the PVC is likely unaffected by overexpression of Ncr1 since these cells properly deliver CPY from the Golgi to the PVC. This suggests that if Ncr1 indirectly opposes Nhx1 function by promoting transport of cargo to the PVC, this cargo originates from the early endosome or the vacuole, but not from the Golgi. Furthermore, overexpression of *NCR1* did not exaggerate the CPY-secretion defect of *nhx1Δ* cells, suggesting that the loss of viability due to *NCR1* overexpression in these cells can not be attributed to a more severe impairment of retrograde trafficking from the PVC to the Golgi.

If Ncr1 directly opposes Nhx1 activity, it may efflux  $\text{Na}^+$  ions from the PVC or transport protons into this compartment. The ability of Nhx1 to sequester  $\text{Na}^+$  ions in the PVC is believed to be dependent on a pH gradient across the PVC membrane, established by the vacuolar  $\text{H}^+$ -ATPase (17). To determine if Ncr1 promotes the import of protons into the PVC, yeast were grown on media buffered to a range of different pHs. If Ncr1 participates in intracellular trafficking of protons, cells lacking *NCR1* might be expected to have diminished capacity to maintain pH balance at extremes in pH. However, cells lacking *NCR1* were able to grow as well as wild-type cells did at all pH values tested (Fig. 24), suggesting that Ncr1 does not significantly contribute to pH homeostasis in wild-type yeast, where the vacuolar  $\text{H}^+$ -ATPase can compensate for pH variations (3). If Ncr1 promoted movement of protons into the



PVC, a mutation in the PVC inward proton pump might be expected to be more deleterious in *ncr1Δ* yeast. Yeast lacking a gene encoding a subunit of the vacuolar H<sup>+</sup>-ATPase (*vma6Δ*) in combination with loss of *NCR1* were sensitive on media buffered below pH 3 and above pH 7.5. The sensitivity to extremes of pH due to the combined loss of *NCR1* and *VMA6* was more severe than that conferred by the *vma6Δ* mutation. This additive phenotype is indicative that Ncr1 and Vma6 share functional overlap, in this case pH homeostasis, but contribute distinctly to this process. Since loss of the *VMA6*-encoded subunit of the V-ATPase alone significantly decreases the viability of yeast at alkaline pH and deletion of *NCR1* on its own has no effect, the major contributor to pH homeostasis is the V-ATPase, while *NCR1* is a minor player. The ability of the V-ATPase to compensate may explain the lack of phenotype attributed to loss of Ncr1 under all conditions we previously examined.

The vacuolar H<sup>+</sup>-ATPase consists of an integral membrane proton-translocating pore domain (V<sub>0</sub>) and a peripherally associated complex (V<sub>1</sub>) that hydrolyzes ATP (11). Vma6 is a component of the V<sub>0</sub> sector and is required for its proper assembly (11). While the V-ATPase is involved in maintenance of endosomal/vacuolar acidification, the V<sub>0</sub> sector has also been implicated in vacuolar membrane fusion (124). To determine if Ncr1 functions in PVC/vacuolar acidification or vacuolar fusion, the genetic interaction between *NCR1* and the V-

ATPase must be dissected further. This could be accomplished by testing for a synthetic lethal interaction at extremes of pH when both *NCR1* and *VMA1*, a component of the  $V_1$  sector, which is not directly involved in vacuolar fusion (12), are deleted. Interestingly, fusion of vacuolar membranes triggers an efflux of  $\text{Ca}^{2+}$  from the vacuolar lumen, which promotes the binding of calmodulin to the membranes (12). If *Ncr1* is an ion transporter responsible for vacuolar storage of  $\text{Ca}^{2+}$ , impairment caused by overexpression of *NCR1* may be due to reduction of the cytosolic calcium concentration below a critical threshold, that may be compensated for by increasing the extracellular calcium concentration.

*Ncr1* or *NPC1* may transport protons or other acidic molecules into the PVC/late endosome. They could function as an antiporter or a symporter that transports a second molecule across the PVC/late endosome membrane. The second molecule may be the offending molecule that accumulates in the late endosome, precipitating NPC disease. The simultaneous loss of proton import and diminished egress of this second molecule may contribute to the pathogenesis of NPC disease. Regardless, the genetic interaction between *NCR1* and *NHX1* identified in this study has led us to propose that *Ncr1* may transport protons across the PVC/vacuole membrane. This contributes to the hypothesis presented by Davies *et al.* suggesting *NPC1* is a permease (41). A proton transport role for *Ncr1* accentuates the group of genes (11%) encoding transporters identified in the first SGA screen, which, when

deleted, suppress the toxicity of *NCR1* overexpression. All of these transporters are localized in the PM, with the exception of the vacuolar Smf3 (129) and Ydr061w, a putative mitochondrial ABC-transporter (70, 119). Loss of these transporters may suppress the toxicity of *NCR1* overexpression due to decreased transport of a molecule that accumulates to toxic levels when *NCR1* is overexpressed. The substances these proteins transport are candidates for transport by Ncr1 across the PVC/vacuolar membrane. *QDR1* and *PDR15* are believed to encode multidrug transporters (114, 177). *TNA1* and *DAL5* encode permeases for nicotinic acid (95) and allantoin (157), respectively. Smf1 is a proton-coupled divalent metal ion transporter that transfers  $Mn^{2+}$ ,  $Zn^{2+}$  and  $Cu^{2+}$  into the cytoplasm (29) and Smf3 is believed to mobilize iron ions from the vacuole (129). Therefore, by analogy with these transporters, I speculate that Ncr1 could directly or indirectly transport nicotinic acid, allantoin, divalent cations or some other molecule into or out of the PVC/vacuolar compartment.

In the absence of a V-ATPase, at extremes in pH, *NCR1* is essential. This suggests Ncr1 can transport protons into the PVC. If we assume this is the only role for Ncr1, two models might explain why loss of NPC1 in mammalian cells gives rise to trafficking defects. In the first model, loss of NPC1 may decrease the flux of protons into the late endosome, though this does not significantly impact most cells because the V-ATPase can compensate and balance pH levels. However, trafficking

away from the late endosome toward the lysosome may be less efficient in some cell types, specifically neurons. With time, sterols or other lipids that comprise the predominant molecules moved between these compartments by vesicular transport may accumulate in the late endosome. Because the V-ATPase is raft-associated (178), alterations in sterol levels could impact the function of the proton pump. Decreased efficiency of the V-ATPase would render the cell more reliant on NPC1 to maintain pH balance. However, when NPC1 is absent, the trafficking defect is amplified, causing more sterols or lipids to accumulate with time.

In the second model, the severe mitochondrial abnormalities resulting in decreased intracellular ATP, as has been observed in NPC1<sup>-/-</sup> neurons from mice, may affect the efficiency of the vacuolar or vesicular H<sup>+</sup>-ATPase, which requires ATP to transport protons against the pH gradient into the lumen of the endosome/lysosome. If the cell cannot acidify the vacuole due to a depletion in ATP, it becomes reliant on NPC1. However, in the absence of NPC1, in combination with limiting ATP levels, the cell is restricted in its ability to acidify the vacuole, leading to missorting of proteins and other trafficking defects. These competing hypotheses can be directly tested in the yeast model system by genetic screens that will identify either high-copy or deletion suppressors of the pH extreme lethality phenotype conferred by loss of *NCR1* in a *vma6* mutant strain.

My studies have allowed the cellular role of the NPC1 protein to be investigated using a yeast model system. This study has suggested a role for Ncr1 in pH homeostasis. The ability of Ncr1 to acidify the vacuole can be tested using pH-sensitive fluorescent probes. The involvement of Ncr1 in vacuole biogenesis can be investigated by performing homotypic vacuole fusion assays using vacuoles purified from yeast lacking *NCR1*. Vacuolar contents can be analysed to test the ability of Ncr1 to transport cations or nutrients across the membrane. Future genetic screens, in concert with biochemical assays, will further illuminate the role of Ncr1.

## References

1. Ali, R., C. L. Brett, S. Mukherjee, and R. Rao. 2004. Inhibition of sodium/proton exchange by a Rab-GTPase-activating protein regulates endosomal traffic in yeast. *J. Biol. Chem.* **279**:4498-4506.
2. Ames, B. N., and D. T. Dubin. 1960. The role of polyamines in the neutralization of bacteriophage deoxyribonucleic acid. *J. Biol. Chem.* **235**:769-775.
3. Anraku, Y., R. Hirata, Y. Wada, and Y. Ohya. 1992. Molecular genetics of the yeast vacuolar H<sup>+</sup>-ATPase. *J. Exp. Biol.* **172**:67-81.
4. Ashburner, M., C. A. Ball, J. A. Blake, H. Butler, J. M. Cherry, J. Corradi, K. Dolinski, J. T. Eppig, M. Harris, D. P. Hill, S. Lewis, B. Marshall, C. Mungall, L. Reiser, S. Rhee, J. E. Richardson, J. Richter, M. Ringwald, G. M. Rubin, G. Sherlock, and J. Yoon. 2001. Creating the gene ontology resource: design and implementation. *Genome Res.* **11**:1425-1433.
5. Bach, M. L., F. Lacroute, and D. Botstein. 1979. Evidence for transcriptional regulation of orotidine-5'-phosphate decarboxylase in yeast by hybridization of mRNA to the yeast structural gene cloned in *Escherichia coli*. *Proc. Natl. Acad. Sci. USA* **76**:386-390.

6. **Bagnat, M., A. Chang, and K. Simons.** 2000. Lipid rafts function in biosynthetic delivery of proteins to the cell surface in yeast. *Proc. Natl. Acad. Sci. USA* **97**:3254-3259.
7. **Ballou, L., R. A. Hitzeman, M. S. Lewis, and C. E. Ballou.** 1991. Vanadate-resistant yeast mutants are defective in protein glycosylation. *Proc. Natl. Acad. Sci. USA* **88**:3209-3212.
8. **Bankaitis, V. A., D. E. Malehorn, S. D. Emr, and R. Greene.** 1989. The *Saccharomyces cerevisiae* *SEC14* gene encodes a cytosolic factor that is required for transport of secretory proteins from the yeast Golgi complex. *J. Cell Biol.* **108**:1271-1281.
9. **Barbour, L., Y. Zhu, and W. Xiao.** 2000. Improving synthetic lethal screens by regulating the yeast centromere sequence. *Genome* **43**:910-917.
10. **Bartel, P., C. T. Chien, R. Sternglanz, and S. Fields.** 1993. Using the two-hybrid system to detect protein-protein interactions, p. 153-179. In D. A. Hartley (ed.), *Cellular Interactions in Development: A Practical Approach*. IRL Press, Oxford, United Kingdom.
11. **Bauerle, C., M. N. Ho, M. A. Lindorfer, and T. H. Stevens.** 1993. The *Saccharomyces cerevisiae* *VMA6* gene encodes the 36-kDa subunit of the vacuolar H<sup>+</sup>-ATPase membrane sector. *J. Biol. Chem.* **268**:12749-12757.

12. **Bayer, M. J., C. Reese, S. Buhler, C. Peters, and A. Mayer.** 2003. Vacuole membrane fusion:  $V_0$  functions after *trans*-SNARE pairing and is coupled to the  $Ca^{2+}$ -releasing channel. *J. Cell Biol.* **162**:211-222.
13. **Beh, C. T., L. Cool, J. Phillips, and J. Rine.** 2001. Overlapping functions of the yeast oxysterol-binding protein homologues. *Genetics* **157**:1117-1140.
14. **Bhuiyan, M. S., Y. Ito, A. Nakamura, N. Tanaka, H. Fujita, and K. Takegawa.** 1999. Nystatin effects on vacuolar function in *Saccharomyces cerevisiae*. *Biosci. Biotechnol. Biochem.* **63**:1075-1082.
15. **Blanchette-Mackie, E. J., N. K. Dwyer, L. M. Amende, H. S. Kruth, J. D. Butler, J. Sokol, M. E. Comly, M. T. Vanier, J. T. August, R. O. Brady, and P. G. Pentchev.** 1988. Type-C Niemann-Pick disease: Low density lipoprotein uptake is associated with premature cholesterol accumulation in the Golgi complex and excessive cholesterol storage in lysosomes. *Proc. Natl. Acad. Sci. USA* **85**:8022-8026.
16. **Botstein, D., S. C. Falco, S. E. Stewart, M. Brennan, S. Scherer, D. T. Stinchcomb, K. Struhl, and R. W. Davis.** 1979. Sterile host yeasts (SHY): a eukaryotic system of biological containment for recombinant DNA experiments. *Gene* **8**:17-24.



17. **Bowers, K., B. P. Levi, F. I. Patel, and T. H. Stevens.** 2000. The sodium/proton exchanger Nhx1p is required for endosomal protein trafficking in the yeast *Saccharomyces cerevisiae*. *Mol. Biol. Cell* **11**:4277-4294.
18. **Breitkreutz, B. J., C. Stark, and M. Tyers.** 2003. The GRID: the General Repository for Interaction Datasets. *Genome Biol.* **4**:R23.
19. **Breitkreutz, B. J., C. Stark, and M. Tyers.** 2003. Osprey: a network visualization system. *Genome Biol.* **4**:R22.
20. **Brett, C. L., D. N. Tukaye, S. Mukherjee, and R. Rao.** 2005. The yeast endosomal Na<sup>+</sup>(K<sup>+</sup>)/H<sup>+</sup> exchanger Nhx1 regulates cellular pH to control vesicle trafficking. *Mol. Biol. Cell* **16**:1396-1405.
21. **Brewster, J. L., T. de Valoir, N. D. Dwyer, E. Winter, and M. C. Gustin.** 1993. An osmosensing signal transduction pathway in yeast. *Science* **259**:1760-1763.
22. **Bricmont, P. A., J. R. Daugherty, and T. G. Cooper.** 1991. The *DAL81* gene product is required for induced expression of two differently regulated nitrogen catabolic genes in *Saccharomyces cerevisiae*. *Mol. Cell. Biol.* **11**:1161-1166.
23. **Calcott, P. H., and A. M. Gargett.** 1981. Mutagenicity of freezing and thawing. *FEMS Microbiol. Lett.* **10**:151-155.
24. **Carman, G. M., and M. C. Kersting.** 2004. Phospholipid synthesis in yeast: regulation by phosphorylation. *Biochem. Cell Biol.* **82**:62-70.

25. Carstea, E. D., J. A. Morris, K. G. Coleman, S. K. Loftus, D. Zhang, C. Cummings, J. Gu, M. A. Rosenfeld, W. J. Pavan, D. B. Krizman, J. Nagle, M. H. Polymeropoulos, S. L. Sturley, Y. A. Ioannou, M. E. Higgins, M. Comly, A. Cooney, A. Brown, C. R. Kaneski, E. J. Blanchette-Mackie, N. K. Dwyer, E. B. Neufeld, T. Y. Chang, L. Liscum, J. F. Strauss III, K. Ohno, M. Zeigler, R. Carmi, J. Sokol, D. Markie, R. R. O'Neill, O. P. van Diggelen, M. Elleder, M. C. Patterson, R. O. Brady, M. T. Vanier, P. G. Pentchev, and D. A. Tagle. 1997. Niemann-Pick C1 disease gene: homology to mediators of cholesterol homeostasis. *Science* **277**:228-231.
26. Cesareni, G., and J. Murray. 1987. Genetic Engineering, vol. 9, Plenum, New York.
27. Chaudhuri, B., S. Ingavale, and A. K. Bachhawat. 1996. *apd1+*, a gene required for red pigment formation in *ade6* mutants of *Schizosaccharomyces pombe*, encodes an enzyme required for glutathione biosynthesis: A role for glutathione and a glutathione-conjugate pump. *Genetics* **145**:75-83.
28. Chen, L., and N. Davis. 2000. Recycling of the yeast  $\alpha$ -factor receptor. *J. Cell Biol.* **151**:731-738.

29. **Chen, X. Z., J. B. Peng, A. Cohen, H. Nelson, N. Nelson, and M. A. Hediger.** 1999. Yeast *SMF1* mediates H<sup>+</sup>-coupled iron uptake with concomitant uncoupled cation currents. *J. Biol. Chem.* **274**:35089-35094.
30. **Chen, Y., and P. W. Piper.** 1995. Consequences of the overexpression of ubiquitin in yeast: elevated tolerances of osmostress, ethanol and canavanine, yet reduced tolerances of cadmium, arsenite and paromycin. *Biochim. Biophys. Acta* **1268**:59-64.
31. **Choudhury, A., M. Dominguez, V. Puri, D. K. Sharma, K. Narita, C. L. Wheatley, D. L. Marks, and R. E. Pagano.** 2002. Rab proteins mediate Golgi transport of caveola-internalized glycosphingolipids and correct lipid trafficking in Niemann-Pick C cells. *J. Clin. Invest.* **109**:1541-1550.
32. **Cleves, A. E., P. J. Novick, and V. A. Bankaitis.** 1989. Mutations in the *SAC1* gene suppress defects in yeast Golgi and yeast actin function. *J. Cell Biol.* **109**:2939-2950.
33. **Conchon, S., X. Cao, C. Barlowe, and H. R. B. Pelham.** 1999. Got1p and Sft2p: membrane proteins involved in traffic to the Golgi complex. *EMBO J.* **18**:3934-3946.

34. **Cooper, A. A., and T. H. Stevens.** 1996. Vps10p cycles between the late-Golgi and prevacuolar compartments in its function as the sorting receptor for multiple yeast vacuolar hydrolases. *J. Cell Biol.* **133**:529-541.
35. **Costigan, C., S. Gehrung, and M. Snyder.** 1992. A synthetic lethal screen identifies *SLK1*, a novel protein kinase homolog implicated in yeast cell morphogenesis and cell growth. *Mol. Cell. Biol.* **12**:1162-1178.
36. **Counillon, L., and J. Pouyssegur.** 2000. The expanding family of eucaryotic Na<sup>+</sup>/H<sup>+</sup> exchangers. *J. Biol. Chem.* **275**:1-4.
37. **Crocker, A. C.** 1961. The cerebral defect in Tay-Sachs disease and Niemann-Pick disease. *J. Neurochem.* **7**:69.
38. **Cross, F. R.** 1997. 'Marker swap' plasmids: convenient tools for budding yeast molecular genetics. *Yeast* **13**:647-653.
39. **Cruz, J. C., and T. Chang.** 2000. Fate of endogenously synthesized cholesterol in Niemann-Pick Type C1 cells. *J. Biol. Chem.* **275**:41309-41316.
40. **Cruz, J. C., S. Sugii, C. Yu, and T. Chang.** 2000. Role of Niemann-Pick Type C1 protein in intracellular trafficking of low density lipoprotein-derived cholesterol. *J. Biol. Chem.* **275**:4013-4021.
41. **Davies, J. P., F. W. Chen, and Y. A. Ioannou.** 2000. Transmembrane molecular pump activity of Niemann-Pick C1 protein. *Science* **290**:2295-2298.

42. **Davies, J. P., and Y. A. Ioannou.** 2000. Topological analysis of Niemann-Pick C1 protein reveals that the membrane orientation of the putative sterol-sensing domain is identical to those of 3-hydroxy-3-methylglutaryl-CoA reductase and sterol regulatory element binding protein cleavage-activating protein. *J. Biol. Chem.* **275**:24367-24374.
43. **Davies, J. P., B. Levy, and Y. A. Ioannou.** 2000. Evidence for a Niemann-Pick C (NPC) gene family: Identification and characterization of NPC1L1. *Genomics* **65**:137-145.
44. **Delley, P. A., and M. N. Hall.** 1999. Cell wall stress depolarizes cell growth via hyperactivation of *RHO1*. *J. Cell Biol.* **147**:163-174.
45. **Dickson, R. C., E. E. Nagiec, M. Skrzypek, P. Tillman, G. B. Wells, and R. L. Lester.** 1997. Sphingolipids are potential heat stress signals in *Saccharomyces*. *J. Biol. Chem.* **272**:30196-30200.
46. **Dobson, M. J., F. E. Yull, M. Molina, S. M. Kingsman, and A. J. Kingsman.** 1988. Reconstruction of the yeast 2 $\mu$ m plasmid partitioning mechanism. *Nucl. Acids Res.* **16**:7103-7117.
47. **Eisenmann, D. M., K. M. Arndt, S. L. Ricupero, J. W. Rooney, and F. Winston.** 1992. *SPT3* interacts with TFIID to allow normal transcription in *Saccharomyces cerevisiae*. *Genes Dev.* **6**:1319-1331.

48. **Eitzen, G. A., R. K. Szilard, and R. A. Rachubinski.** 1997. Enlarged peroxisomes are present in oleic acid-grown *Yarrowia lipolytica* overexpressing the *PEX16* gene encoding an intraperoxisomal peripheral membrane peroxin. *J. Cell Biol.* **137**:1265-1278.
49. **Erhart, E., and C. P. Hollenberg.** 1983. The presence of a defective *LEU2* gene on 2 $\mu$  DNA recombinant plasmids of *Saccharomyces cerevisiae* is responsible for curing and high copy number. *J. Bacteriol.* **156**:625-635.
50. **Evangelista, M., D. Pruyne, D. C. Amberg, C. Boone, and A. Bretscher.** 2002. Formins direct Arp2/3-independent actin filament assembly to polarize cell growth in yeast. *Nat. Cell Biol.* **4**:32-41.
51. **Feramisco, J. D., J. L. Goldstein, and M. S. Brown.** 2004. Membrane topology of human insig-1, a protein regulator of lipid synthesis. *J. Biol. Chem.* **279**:8487-8496.
52. **Freemont, P. S.** 1993. The RING finger - A novel protein sequence motif related to the zinc-finger. *Ann. N.Y. Acad. Sci.* **684**:174-192.
53. **Gaxiola, R. A., R. Rao, A. Sherman, P. Grisafi, S. L. Alper, and G. R. Fink.** 1999. The *Arabidopsis thaliana* proton transporters, AtNhx1 and Avp1, can function in cation detoxification in yeast. *Proc. Natl. Acad. Sci. USA* **96**:1480-1485.

54. **Gietz, R. D., R. H. Schiestl, A. R. Willems, and R. A. Woods.** 1995. Studies on the transformation of intact yeast cells by the LiAc/SS-DNA/PEG procedure. *Yeast* **11**:355-360.
55. **Goldring, E. S., L. I. Grossman, D. Krupnick, D. R. Cryer, and J. Marmur.** 1970. The petite mutation in yeast: Loss of mitochondrial deoxyribonucleic acid during induction of petites with ethidium bromide. *J. Mol. Biol.* **52**:323-335.
56. **Goldstein, A., and J. O. Lampen.** 1975. Beta-D-fructofuranoside fructohydrolase from yeast. *Methods Enzymol.* **42**:504-511.
57. **Gollub, E. G., P. Trocha, P. K. Liu, and D. B. Sprinson.** 1974. Yeast mutants requiring ergosterol as only lipid supplement. *Biochem. Biophys. Res. Commun.* **56**:471-477.
58. **Gondre-Lewis, M. C., R. McGlynn, and S. U. Walkley.** 2003. Cholesterol accumulation in NPC1-deficient neurons is ganglioside dependent. *Curr. Biol.* **13**:1324-1329.
59. **Greer, W. L., M. J. Dobson, G. S. Girouard, D. M. Byers, D. C. Riddell, and P. E. Neumann.** 1999. Mutations in NPC1 highlight a conserved Npc1-specific cysteine-rich domain. *Am. J. Hum. Genet.* **65**:1252-1260.
60. **Greer, W. L., D. C. Riddell, T. L. Gillan, G. S. Girouard, S. M. Sparrow, D. M. Byers, M. J. Dobson, and P. E. Neumann.** 1998. The Nova Scotia (type D)

form of Niemann-Pick disease is caused by a G3097 to T transversion in NPC1. .

*Am. J. Hum. Genet.* **63**:52-54.

61. **Guarente, L., and M. Ptashne.** 1981. Fusion of *Escherichia coli lacZ* to the cytochrome c gene of *Saccharomyces cerevisiae*. *Proc. Natl. Acad. Sci. USA* **78**:2199-2203.

62. **Hallstrom, T. C., L. Lambert, S. Schorling, E. Balzi, A. Goffeau, and W. S. Moye-Rowley.** 2001. Coordinate control of sphingolipid biosynthesis and multidrug resistance in *Saccharomyces cerevisiae*. *J. Biol. Chem.* **276**:23674-23680.

63. **Hampsey, M.** 1997. A review of phenotypes in *Saccharomyces cerevisiae*. *Yeast* **13**:1099-1133.

64. **Heinisch, J. J., A. Lorberg, H. P. Schmitz, and J. J. Jacoby.** 1999. The protein kinase C-mediated MAP kinase pathway is involved in the maintenance of cellular integrity in *Saccharomyces cerevisiae*. *Mol. Microbiol.* **32**:671-680.

65. **Heung, L. J., C. Luberto, A. Plowden, Y. Hannun, and M. Del Poeta.** 2004. The sphingolipid pathway regulates Pkc1 through the formation of diacylglycerol in *Cryptococcus neoformans*. *J. Biol. Chem.* **279**:21144-21153.

66. **Higgins, M. E., J. P. Davies, F. W. Chen, and Y. A. Ioannou.** 1999. Niemann-Pick C1 is a late endosome-resident protein that transiently associates with lysosomes and the *trans*-Golgi network. *Mol. Genet. Metab.* **68**:1-13.



67. **Hill, J. E., A. M. Myers, T. J. Koerner, and A. Tzagoloff.** 1986. *Yeast/E. coli* shuttle vectors with multiple unique restriction sites. *Yeast* **2**:163-7.
68. **Hoja, Y., S. Marthol, J. Hofmann, S. Stegner, R. Schulz, S. Meier, E. Greiner, and E. Schweizer.** 2004. *HFA1* encoding an organelle-specific acetyl-CoA carboxylase controls mitochondrial fatty acid synthesis in *Saccharomyces cerevisiae*. *J. Biol. Chem.* **279**:21779-21786.
69. **Hong, Z., P. Mann, N. H. Brown, L. E. Tran, K. J. Shaw, R. S. Hare, and B. DiDomenico.** 1994. Cloning and characterization of *KNR4*, a yeast gene involved in (1,3)-beta-glucan synthesis. *Mol. Cell. Biol.* **14**:1017-1025.
70. **Huh, W. K., J. V. Falvo, L. C. Gerke, A. S. Carroll, R. W. Howson, J. S. Weissman, and E. K. O'Shea.** 2003. Global analysis of protein localization in budding yeast. *Nature* **425**:686-691.
71. **Ioannou, Y. A.** 2001. Multidrug permeases and subcellular cholesterol transport. *Nat. Rev. Mol. Cell Biol.* **2**:657-668.
72. **Ito, T., T. Chiba, M. Yoshida, M. Hattori, and Y. Sakaki.** 2001. A comprehensive two-hybrid analysis to explore the yeast protein interactome. *Proc. Natl. Acad. Sci. USA* **98**:4569-4574.

73. **Jamsa, R., M. Simonen, and M. Makarow.** 1994. Selective retention of secretory proteins in the yeast endoplasmic reticulum by treatment of cells with a reducing agent. *Yeast* **10**:355-370.
74. **Jenkins, G. M., A. Richards, T. Wahl, C. Mao, L. Obeid, and Y. Hannun.** 1997. Involvement of yeast sphingolipids in the heat stress response of *Saccharomyces cerevisiae*. *J. Biol. Chem.* **272**:32566-32572.
75. **Jones, E. W., and G. R. Fink.** 1982. Regulation of amino acid and nucleotide biosynthesis in yeast., p. 181-299. In J. N. Strathern, E. W. Jones, and J. R. Broach (ed.), The molecular biology of the yeast *Saccharomyces*: metabolism and gene expression., 1st ed. Cold Spring Harbor Laboratory Press, Cold Spring Harbor, New York.
76. **Kamada, Y., U. S. Jung, J. Piotrowski, and D. E. Levin.** 1995. The protein kinase C-activated MAP kinase pathway of *Saccharomyces cerevisiae* mediates a novel aspect of the heat shock response. *Genes Dev.* **9**:1559-1571.
77. **Karten, B., D. E. Vance, R. B. Campenot, and J. E. Vance.** 2002. Cholesterol accumulates in cell bodies, but is decreased in distal axons of Niemann-Pick C1-deficient neurons. *J. Neurochem.* **83**:1154-1163.

78. **Kennedy, M. A., R. Barbuch, and M. Bard.** 1999. Transcriptional regulation of the squalene synthase gene (*ERG9*) in the yeast *Saccharomyces cerevisiae*. *Biochim. Biophys. Acta* **1445**:110-122.
79. **Kitamoto, K., K. Yoshizawa, Y. Ohsumi, and Y. Anraku.** 1988. Dynamic aspects of vacuolar and cytosolic amino acid pools of *Saccharomyces cerevisiae*. *J. Bacteriol.* **170**:2683-2686.
80. **Kobayashi, N., and K. McEntee.** 1993. Identification of *cis* and *trans* components of a novel heat shock stress regulatory pathway in *Saccharomyces cerevisiae*. *Mol. Cell. Biol.* **13**:248-256.
81. **Kobayashi, T., M. Beuchat, M. Lindsay, S. Frias, R. D. Palmiter, H. Sakuraba, R. G. Parton, and J. Gruenberg.** 1999. Late endosomal membranes rich in lysobisphosphatidic acid regulate cholesterol transport. *Nat. Cell Biol.* **1**:113-118.
82. **Koike, T., G. Ishida, M. Taniguchi, K. Higaki, Y. Ayaki, M. Saito, Y. Sakakihira, M. Iwamori, and K. Ohno.** 1998. Decreased membrane fluidity and unsaturated fatty acids in Niemann-Pick disease type C fibroblasts. *Biochim. Biophys. Acta* **1406**:327-335.
83. **Koning, A. J., L. L. Larson, E. J. Cadera, M. L. Parrish, and R. L. Wright.** 2002. Mutations that affect vacuole biogenesis inhibit proliferation of the endoplasmic reticulum in *Saccharomyces cerevisiae*. *Genetics* **160**:1335-1352.

84. **Koren, A., S. Ben-Aroya, R. Steinlauf, and M. Kupiec.** 2003. Pitfalls of the synthetic lethality screen in *Saccharomyces cerevisiae*: an improved design. *Curr. Genet.* **43**:62-69.
85. **Kruth, H. S., M. E. Comly, J. D. Butler, M. T. Vanier, J. K. Fink, D. A. Wenger, S. Patel, and P. G. Pentchev.** 1986. Type C Niemann-Pick disease: abnormal metabolism of low density lipoprotein in homozygous and heterozygous fibroblasts. *J. Biol. Chem.* **261**:16769-16774.
86. **Kuwabara, P. E., and M. Labouesse.** 2002. The sterol-sensing domain: multiple families, a unique role? *Trends Genet.* **18**:193-201.
87. **Laemmli, U. K.** 1970. Cleavage of structural proteins during the assembly of the head of bacteriophage T4. *Nature* **227**:680-685.
88. **Liao, X., and R. A. Butow.** 1993. *RTG1* and *RTG2*: Two yeast genes required for a novel path of communication from mitochondria to the nucleus. *Cell* **72**:61-71.
89. **Lim, M. Y., D. Dailey, G. S. Martin, and J. Thorner.** 1993. Yeast *MCK1* protein kinase autophosphorylates at tyrosine and serine but phosphorylates exogenous substrates at serine and threonine. *J. Biol. Chem.* **268**:21155-21164.
90. **Liscum, L., and J. R. Faust.** 1987. Low density lipoprotein (LDL)-mediated suppression of cholesterol synthesis and LDL uptake is defective in Niemann-Pick type C fibroblasts. *J. Biol. Chem.* **262**:17002-17008.

91. **Liscum, L., and J. J. Klansek.** 1998. Niemann-Pick disease type C. *Curr. Opin. Lipidol.* **9**:131-135.
92. **Liscum, L., and N. J. Munn.** 1999. Intracellular cholesterol transport. *Biochim. Biophys. Acta* **1438**:19-37.
93. **Liscum, L., R. M. Ruggiero, and J. R. Faust.** 1989. The intracellular transport of low density lipoprotein-derived cholesterol is defective in Niemann-Pick type C fibroblasts. *J. Cell Biol.* **108**:1625-1636.
94. **Liscum, L., and S. L. Sturley.** 2004. Introduction. *Biochim. Biophys. Acta* **1685**:1-2.
95. **Llorente, B., and H. Feldmann.** 2000. Transcriptional regulation of the *Saccharomyces cerevisiae* *DAL5* gene family and identification of the high affinity nicotinic acid permease *TNA1* (*YGR260w*). *FEBS Lett.* **475**:237-241.
96. **Loewith, R., E. Jacinto, S. Wullschleger, A. Lorber, J. L. Crespo, D. Bonenfant, W. Oppliger, P. Jenoe, and M. N. Hall.** 2002. Two *TOR* complexes, only one of which is rapamycin sensitive, have distinct roles in cell growth. *Mol. Cell* **10**:457-468.
97. **Madden, K., and M. Snyder.** 1998. Cell polarity and morphogenesis in budding yeast. *Annu. Rev. Microbiol.* **52**:687-744.

98. **Malathi, K., K. Higaki, H. Tinkelenberg, D. A. Balderes, D. Almanzar-Paramio, L. J. Wilcox, N. Erdeniz, F. Redican, M. Padamsee, Y. Liu, S. Khan, F. Alcantara, E. D. Carstea, J. A. Morris, and S. L. Sturley.** 2004. Mutagenesis of the putative sterol-sensing domain of yeast Niemann Pick C-related protein reveals a primordial role in subcellular sphingolipid distribution. *J. Cell. Biol.* **164**:547-556.
99. **Marcusson, E. G., B. F. Horazdovsky, J. L. Cereghino, E. Gharakhanian, and S. D. Emr.** 1994. The sorting receptor for yeast vacuolar carboxypeptidase Y is encoded by the *VPS10* gene. *Cell* **77**:579-586.
100. **Martin, V., G. Carrillo, C. Torroja, and I. Guerrero.** 2001. The sterol-sensing domain of Patched protein seems to control Smoothed activity through Patched vesicular trafficking. *Curr. Biol.* **11**:601-607.
101. **Marvin, M. E., P. H. Williams, and A. M. Cashmore.** 2001. The isolation and characterisation of a *Saccharomyces cerevisiae* gene (*LIP2*) involved in the attachment of lipoic acid groups to mitochondrial enzymes. *FEMS Microbiol. Lett.* **199**:131-136.
102. **Mazzoni, C., P. Zarzov, A. Rambourg, and C. Mann.** 1993. The *SLT2* (*MPK1*) MAP kinase homolog is involved in polarized cell growth in *Saccharomyces cerevisiae*. *J. Cell Biol.* **123**:1821-1833.

103. **Melcher, K., and H. E. Xu.** 2001. Gal80-Gal80 interaction on adjacent Gal4p binding sites is required for complete *GAL* gene repression. *EMBO J.* **20**:841-851.
104. **Millard, E. E., K. Srivastava, L. M. Traub, J. E. Schaffer, and D. S. Ory.** 2000. Niemann-Pick C1 (NPC1) overexpression alters cellular cholesterol homeostasis. *J. Biol. Chem.* **275**:38445-38451.
105. **Moreau, V., J. M. Galan, G. Devilliers, R. Haguenaue-Tsapis, and B. Winsor.** 1997. The yeast actin-related protein Arp2p is required for the internalization step of endocytosis. *Mol. Biol. Cell* **8**:1361-75.
106. **Nass, R., K. W. Cunningham, and R. Rao.** 1997. Intracellular sequestration of sodium by a novel Na<sup>+</sup>/H<sup>+</sup> exchanger in yeast is enhanced by mutations in the plasma membrane H<sup>+</sup>-ATPase. *J. Biol. Chem.* **272**:26145-26152.
107. **Nass, R., and R. Rao.** 1998. Novel localization of a Na<sup>+</sup>/H<sup>+</sup> exchanger in a late endosomal compartment of yeast. *J. Biol. Chem.* **273**:21054-21060.
108. **Naureckiene, S., D. E. Sleat, H. Lackland, A. Fensom, M. T. Vanier, R. Wattiaux, M. Jadot, and P. Lobel.** 2000. Identification of HE1 as the second gene of Neimann-Pick C disease. *Science* **290**:2298-2301.
109. **Nehlin, J. O., M. Carlberg, and H. Ronne.** 1989. Yeast galactose permease is related to yeast and mammalian glucose transporters. *Gene* **85**:313-319.

110. **Neufield, E. B., M. Wastney, S. Patel, S. Suresh, A. M. Cooney, N. K. Dwyer, C. F. Roff, K. Ohno, J. A. Morris, E. D. Carstea, J. P. Incardona, J. F. r. Strauss, M. T. Vanier, M. C. Patterson, R. O. Brady, P. G. Pentchev, and E. J. Blanchette-Mackie.** 1999. The Niemann-Pick C1 protein resides in a vesicular compartment linked to retrograde transport of multiple lysosomal cargo. *J. Biol. Chem.* **274**:9627-9635.
111. **Nickas, M. E., and M. P. Yaffe.** 1996. *BRO1*, a novel gene that interacts with components of the Pck1p-mitogen-activated protein kinase pathway in *Saccharomyces cerevisiae*. *Mol. Cell. Biol.* **16**:2585-2593.
112. **Novick, P., and D. Botstein.** 1985. Phenotypic analysis of temperature-sensitive yeast actin mutants. *Cell* **40**:405-416.
113. **Novick, P., C. Field, and R. Schekman.** 1980. Identification of 23 complementation groups required for post-translational events in the yeast secretory pathway. *Cell* **21**:205-215.
114. **Nunes, P. A., S. Tenreiro, and I. Sa-Correia.** 2001. Resistance and adaptation to quinidine in *Saccharomyces cerevisiae*: Role of *QDR1* (*YIL120w*), encoding a plasma membrane transporter of the major facilitator superfamily required for multidrug resistance. *Antimicrobial Agents Chemother.* **45**:1528-1534.



115. **Ogita, K., S. Miyamoto, H. Koide, T. Iwai, M. Oka, K. Ando, A. Kishimoto, K. Ikeda, Y. Fukami, and Y. Nishizuka.** 1990. Protein kinase C in *Saccharomyces cerevisiae*: comparison with the mammalian enzyme. *Proc. Natl. Acad. Sci. USA* **87**:5011-5015.
116. **Ohgami, N., D. C. Ko, M. Thomas, M. P. Scott, C. C. Y. Chang, and T. Chang.** 2004. Binding between the Niemann-Pick C1 protein and a photoactivatable cholesterol analog requires a functional sterol-sensing domain. *Proc. Natl. Acad. Sci. USA* **101**:12473-12478.
117. **Ohya, Y., S. Miyamoto, Y. Ohsumi, and Y. Anraku.** 1986. Calcium-sensitive *cls4* mutant of *Saccharomyces cerevisiae* with a defect in bud formation. *J. Bacteriol.* **165**:28-33.
118. **Passeggio, J., and L. Liscum.** 2005. Flux of fatty acids through NPC1 lysosomes. *J. Biol. Chem.* **280**:10333-10339.
119. **Paulsen, I. T., M. K. Sliwinski, B. Nelissen, A. Goffeau, and M. H. Saier.** 1998. Unified inventory of established and putative transporters encoded within the complete genome of *Saccharomyces cerevisiae*. *FEBS Lett.* **430**:116-125.
120. **Pentchev, P. G., M. E. Comly, H. S. Kruth, T. Tokoro, J. Butler, J. Sokol, M. Filling-Katz, J. M. Quirk, D. C. Marshall, S. Patel, M. T. Vanier, and R. O.**

- Brady.** 1987. Group C Niemann-Pick disease: faulty regulation of low-density lipoprotein uptake and cholesterol storage in cultured fibroblasts. *FASEB J.* **1**:40-45.
121. **Pentchev, P. G., M. E. Comly, H. S. Kruth, M. T. Vanier, D. A. Wenger, S. Patel, and R. O. Brady.** 1985. A defect in cholesterol esterification in Niemann-Pick disease (type C) patients. *Proc. Natl. Acad. Sci. USA* **82**:8247-8251.
122. **Pentchev, P. G., H. S. Kruth, M. E. Comly, J. D. Butler, M. T. Vanier, D. A. Wenger, and S. Patel.** 1986. Type C Niemann-Pick disease: a parallel loss of regulatory responses in both the uptake and esterification of low density lipoprotein-derived cholesterol in cultured fibroblasts. *J. Biol. Chem.* **261**:16775-16780.
123. **Pentchev, P. G., M. T. Vanier, K. Suzuki, and M. C. Patterson.** 1995. Niemann-Pick disease type C: A cellular cholesterol lipidosis, p. 2625-2639. In C. R. Scriver, A. L. Beaudet, W. S. Sly, and D. Valle (ed.), *Metabolic basis of inherited disease.*, vol. II. McGraw-Hill, New York.
124. **Peters, C., M. J. Bayer, S. Buhler, J. S. Andersen, M. Mann, and A. Mayer.** 2001. Trans-complex formation by proteolipid channels in the terminal phase of membrane fusion. *Nature* **409**:581-588.
125. **Peterson, J., Y. Zheng, L. Bender, A. Myers, R. Cerione, and A. Bender.** 1994. Interactions between the bud emergence proteins Bem1p and Bem2p and rho-type GTPases in yeast. *J. Cell Biol.* **127**:1395-1406.

126. **Pfeffer, S. R.** 2001. Rab GTPases: specifying and deciphering organelle identity and function. *Trends Cell Biol.* **11**:487-491.
127. **Pillus, L., and F. Solomon.** 1986. Components of microtubular structures in *Saccharomyces cerevisiae*. *Proc. Natl. Acad. Sci. USA* **83**:2468-2472.
128. **Popolo, L., and M. Vai.** 1999. The Gas1 glycoprotein, a putative wall polymer cross-linker. *Biochim. Biophys. Acta* **1426**:385-400.
129. **Portnoy, M. E., X. F. Liu, and V. C. Culotta.** 2000. *Saccharomyces cerevisiae* expresses three functionally distinct homologues of the Nramp family of metal transporters. *Mol. Cell. Biol.* **20**:7893-7902.
130. **Prinz, W.** 2002. Cholesterol trafficking in the secretory and endocytic systems. *Cell Dev. Biol.* **13**:197-203.
131. **Rodriguez-Pena, J. M., C. Rodriguez, A. Alvarez, C. Nombela, and J. Arroyo.** 2002. Mechanisms for targeting of the *Saccharomyces cerevisiae* GPI-anchored cell wall protein Crh2p to polarised growth sites. *J. Cell Sci.* **115**:2549-2558.
132. **Rogriguez-Navarro, A., and J. Ramos.** 1984. Dual system for potassium transport in *Saccharomyces cerevisiae*. *J. Bacteriol.* **159**:940-945.

133. **Roncero, C., M. H. Valdivieso, J. C. Ribas, and A. Duran.** 1988. Isolation and characterization of *Saccharomyces cerevisiae* mutants resistant to calcofluor white. *J. Bacteriol.* **170**:1950-1954.
134. **Ronne, H.** 1995. Glucose repression in fungi. *Trends Genet.* **11**:12-17.
135. **Rose, M. D., F. Winston, and P. Hieter.** 1990. Methods in Yeast Genetics. Cold Spring Harbor Press, Cold Spring Harbor, NY.
136. **Rothstein, R.** 1991. Targeting, disruption, replacement, and allele rescue: integrative DNA transformation in yeast. *Methods Enzymol.* **194**:281-301.
137. **Sambrook, J., E. F. Fritsch, and T. Maniatis.** 1989. Molecular cloning, a laboratory manual. Cold Spring Harbor Laboratory Press, Cold Spring Harbor, NY.
138. **Santos, B., A. Duran, and M. H. Valdivieso.** 1997. *CHS5*, a gene involved in chitin synthesis and mating in *Saccharomyces cerevisiae*. *Mol. Cell. Biol.* **17**:2485-2496.
139. **Santos, B., and M. Snyder.** 2003. Specific protein targeting during cell differentiation: polarized localization of Fus1p during mating depends on Chs5p in *Saccharomyces cerevisiae*. *Euk. Cell* **2**:821-825.
140. **Santos, B., and M. Snyder.** 1997. Targeting of chitin synthase 3 to polarized growth sites in yeast requires Chs5p and Myo2p. *J. Cell Biol.* **136**:95-110.

141. **Scheek, S., M. S. Brown, and J. L. Goldstein.** 1997. Sphingomyelin depletion in cultured cells blocks proteolysis of sterol regulatory element binding proteins at site 1. *Proc. Natl. Acad. Sci. USA* **94**:11179-11183.
142. **Sengupta, A., K. Blomqvist, A. J. Pickett, Y. Zhang, J. S. K. Chew, and M. J. Dobson.** 2001. Functional domains of yeast plasmid-encoded Rep proteins. *J. Bacteriol.* **183**:2306-2315.
143. **Sikorski, R. S., and P. Hieter.** 1989. A system of shuttle vectors and yeast host strains designed for efficient manipulation of DNA in *Saccharomyces cerevisiae*. *Genetics* **122**:19-27.
144. **Simons, K., and E. Ikonen.** 1997. Functional rafts in cell membranes. *Nature* **387**:569-572.
145. **Simons, K., and E. Ikonen.** 2000. How cells handle cholesterol. *Science* **290**:1721-1726.
146. **Soccio, R. E., and J. L. Breslow.** 2004. Intracellular cholesterol transport. *Arterioscler. Thromb. Vasc. Biol.* **24**:1150-1160.
147. **Stearns, T., M. A. Hoyt, and D. Botstein.** 1990. Yeast mutants sensitive to antimicrobial drugs define three genes that affect microtubule function. *Genetics* **124**:251-262.

148. **Stevens, T., B. Esmon, and R. Schekman.** 1982. Early stages in the yeast secretory pathway are required for transport of carboxypeptidase Y to the vacuole. *Cell* **30**:439-448.
149. **Sturley, S., L.** 2000. Conservation of eukaryotic sterol homeostasis: new insights from studies in budding yeast. *Biochim. Biophys. Acta* **1529**:155-163.
150. **Sugimoto, Y., H. Ninomiya, Y. Ohsaki, K. Higaki, J. P. Davies, Y. A. Ioannou, and K. Ohno.** 2001. Accumulation of cholera toxin and GM1 ganglioside in the early endosome of Niemann-Pick C1-deficient cells. *Proc. Natl. Acad. Sci. USA* **98**:12391-12396.
151. **Sutterlin, C., T. L. Doeiring, F. Schimoller, S. Schroder, and H. Reizman.** 1997. Specific requirements for the ER to Golgi transport of GPI-anchored proteins in yeast. *J. Cell Sci.* **110**:2703-2714.
152. **Tanaka, K., M. Nakafuku, F. Tamanai, Y. Kaziro, K. Matsumoto, and A. Toh-e.** 1990. *IRA2*, a second gene of *Saccharomyces cerevisiae* that encodes a protein with a domain homologous to mammalian ras GTPase-activating protein. *Mol. Cell. Biol.* **10**:4303-4313.
153. **Taniguchi, M., Y. Shinoda, H. Ninomiya, M. T. Vanier, and K. Ohno.** 2001. Sites and temporal changes of gangliosides GM1/GM2 storage in the Niemann-Pick disease type C mouse brain. *Brain Dev.* **23**:414-421.

154. **Taussig, R., and M. Carlson.** 1983. Nucleotide sequence of the yeast *SUC2* gene for invertase. *Nucl. Acids Res.* **11**:1943-1954.
155. **Tong, A. H. Y., M. Evangelista, A. B. Parsons, H. Xu, G. D. Bader, N. Page, M. Robinson, S. Raghbizadeh, C. W. V. Hogue, H. Bussey, B. Andrews, M. Tyers, and C. Boone.** 2001. Systematic genetic analysis with ordered arrays of yeast deletion mutants. *Science* **294**:2364-2368.
156. **Tong, A. H. Y., G. Lesage, G. D. Bader, H. Ding, H. Xu, X. Xin, J. Young, G. F. Berriz, R. L. Brost, and M. Chang.** 2004. Global mapping of the yeast genetic interaction network. *Science* **203**:808-813.
157. **Turoscy, V., and T. G. Cooper.** 1987. Ureidosuccinate is transported by the allantate transport system in *Saccharomyces cerevisiae*. *J. Bacteriol.* **169**:2598-2600.
158. **Ugolini, S., and C. V. Bruschi.** 1996. The red/white colony color assay in the yeast *Saccharomyces cerevisiae*: epistatic growth advantage of white *ade8-18, ade2* cells over red *ade2* cells. *Curr. Genet.* **30**:485-492.
159. **Uh, M., D. Jones, and D. M. Mueller.** 1990. The gene coding for the yeast oligomycin sensitivity-conferring protein. *J. Biol. Chem.* **265**:19047-19052.
160. **Vallejo, C. G., and R. Serrano.** 1989. Physiology of mutants with reduced expression of plasma membrane H<sup>+</sup>-ATPase. *Yeast* **5**:307-319.

161. **van der Hoeven, D.** 2004. Endocytic trafficking defects conferred by mutations in the yeast Niemann-Pick Type C related gene (NCR1). Master of Science Thesis, Dalhousie University .
162. **Vance, J. E., H. Hayashi, and B. Karten.** 2005. Cholesterol homeostasis in neurons and glial cells. *Sem. Cell Dev. Biol.* **16**:193-212.
163. **Vanier, M. T.** 1999. Lipid changes in Niemann-Pick disease type C brain: personal experience and review of the literature. *Neurochem. Res.* **24**:481-489.
164. **Vanier, M. T., S. Duthel, C. Rodriguez-Lafrasse, P. G. Pentchev, and E. D. Carstea.** 1996. Genetic heterogeneity in Niemann-Pick C disease: a study using cell hybridization and linkage analysis. *Am. J. Hum. Genet.* **58**:118-125.
165. **Vida, T. M., and S. D. Emr.** 1995. A new vital stain for visualizing vacuolar membrane dynamics and endocytosis in yeast. *J. Cell Biol.* **128**:779-792.
166. **Wach, A., A. Brachat, R. Pohlmann, and P. Philippsen.** 1994. New heterologous modules for classical or PCR-based disruptions in *Saccharomyces cerevisiae*. *Yeast* **10**:1793-1808.
167. **Watanabe, R., K. Funato, K. Venkararaman, A. H. Futerman, and H. Riezman.** 2002. Sphingolipids are required for the stable membrane association of glycosylphosphatidylinositol-anchored proteins in yeast. *J. Biol. Chem.* **277**:49538-49544.



168. **Watari, H., E. J. Blanchette-Mackie, N. K. Dwyer, J. M. Glick, S. Patel, E. B. Neufeld, R. O. Brady, P. G. Pentchev, and J. F. Strauss.** 1999. Niemann-Pick C1 protein: obligatory roles for N-terminal domains and lysosomal targeting in cholesterol mobilization. *Proc. Natl. Acad. Sci. USA* **96**:805-810.
169. **Watari, H., E. J. Blanchette-Mackie, N. K. Dwyer, M. Watari, C. G. Burd, S. Patel, P. G. Pentchev, and J. F. Strauss.** 2000. Determinants of NPC1 expression and action: key promoter regions, posttranscriptional control, and the importance of a "cysteine-rich" loop. *Exp. Cell Res.* **259**:247-256.
170. **Watari, H., E. J. Blanchette-Mackie, N. K. Dwyer, M. Watari, E. B. Neufeld, S. Patel, P. G. Pentchev, and J. F. r. Strauss.** 1999. Mutations in the leucine zipper motif and sterol-sensing domain inactivate the Niemann-Pick C1 glycoprotein. *J. Biol. Chem.* **274**:21861-21866.
171. **Watzel, G., and W. Tanner.** 1989. Cloning of the glutamine:fructose-6-phosphate amidotransferase gene from yeast. *J. Biol. Chem.* **264**:8753-8758.
172. **Wells, G. B., R. C. Dickson, and R. L. Lester.** 1998. Heat-induced elevation of ceramide in *Saccharomyces cerevisiae* via *de novo* synthesis. *J. Biol. Chem.* **273**:7235-7243.
173. **Wells, K. M., and R. Rao.** 2001. The yeast Na<sup>+</sup>/H<sup>+</sup> exchanger Nhx1 is an N-linked glycoprotein. *J. Biol. Chem.* **276**:3401-3407.

174. **Whelan, W. L., and C. E. Ballou.** 1975. Sporulation in D-glucosamine auxotrophs of *Saccharomyces cerevisiae*: Meiosis with defective ascospore wall formation. *J. Bacteriol.* **124**:1545-1557.
175. **Winters, M. J., and P. M. Pryciak.** 2005. Interaction with the SH3 domain protein Bem1 regulates signaling by the *Saccharomyces cerevisiae* p21-activated kinase Ste20. *Mol. Cell. Biol.* **25**:2177-2190.
176. **Winzeler, E. A., D. D. Shoemaker, A. Astromoff, H. Liang, K. Anderson, B. Andre, R. Bangham, R. Benito, J. D. Boeke, and H. Bussey.** 1999. Functional characterization of the *S. cerevisiae* genome by gene deletion and parallel analysis. *Science* **285**:901-906.
177. **Wolfger, H., Y. M. Mamnun, and K. Kuchler.** 2004. The yeast Pdr15p ATP-binding cassette (ABC) protein is a general stress response factor implicated in cellular detoxification. *J. Biol. Chem.* **279**:11593-11599.
178. **Yoshinaka, K., H. Kumanogoh, S. Nakamura, and S. Maekawa.** 2004. Identification of V-ATPase as a major component in the raft fraction prepared from the synaptic plasma membrane and the synaptic vesicle of rat brain. *Neurosci. Lett.* **363**:168-172.

179. **Yu, W., J. S. Gong, M. Ko, W. S. Garver, K. Yanagisawa, and M. Michikawa.** 2005. Altered cholesterol metabolism in Niemann-Pick C1 mouse brains affects mitochondrial function. *J. Biol. Chem.* **280**:11731-11739.
180. **Zaremborg, V., and C. R. McMaster.** 2002. Differential partitioning of lipids metabolized by separate yeast glycerol-3-phosphate acyltransferases reveals that phospholipase D generation of phosphatidic acid mediates sensitivity to choline-containing lysolipids and drugs. *J. Biol. Chem.* **277**:39035-39044.
181. **Zhang, M., N. K. Dwyer, D. C. Love, A. Cooney, M. Comly, E. Neufeld, P. G. Pentchev, E. J. Blanchette-Mackie, and J. A. Hanover.** 2001. Cessation of rapid late endosomal tubulovesicular trafficking in Niemann-Pick type C1 disease. *Proc. Natl. Acad. Sci. USA* **98**:4466-4471.
182. **Zhang, M., N. K. Dwyer, E. B. Neufeld, D. C. Love, A. Cooney, M. Comly, S. Patel, H. Watari, J. F. Strauss III, P. G. Pentchev, J. A. Hanover, and E. J. Blanchette-Mackie.** 2001. Sterol-modulated glycolipid sorting occurs in Niemann-Pick C1 late endosomes. *J. Biol. Chem.* **276**:3417-3425.
183. **Zhang, S., J. Ren, H. Li, Q. Zhang, J. S. Armstrong, A. L. Munn, and H. Yang.** 2004. Ncr1p, the yeast ortholog of mammalian Niemann Pick C1 protein, is dispensable for endocytic transport. *Traffic* **5**:1017-1030.

184. **Zheng, J., M. Khalil, and J. F. Cannon.** 2000. Glc7p protein phosphatase inhibits expression of glutamine-fructose-6-phosphate transaminase from *GFA1*. *J. Biol. Chem.* **275**:18070-18078.
185. **Zhou, Z., and S. J. Elledge.** 1992. Isolation of *crt* mutants constitutive for transcription of the DNA damage inducible gene *RNR3* in *Saccharomyces cerevisiae*. *Genetics* **131**:851-866.